

# The $\mathcal{N} = 1$ supersymmetric Pati-Salam models with extra $SU(2)_{L_2/R_2}$ gauge symmetry from intersecting D6-branes

Haotian Huangfu<sup>a,b,1</sup> Tianjun Li<sup>c,2</sup> Qi Sun<sup>a,b,3</sup> Rui Sun<sup>d,4</sup> Lina Wu<sup>e,5</sup>

<sup>a</sup>CAS Key Laboratory of Theoretical Physics, Institute of Theoretical Physics, Chinese Academy of Sciences, Beijing 100190, P. R. China

<sup>b</sup>School of Physical Sciences, University of Chinese Academy of Sciences, No.19A Yuquan Road, Beijing 100049, P. R. China

<sup>c</sup>School of Physics, Henan Normal University, Xinxiang 453007, P. R. China

<sup>d</sup>School of Mathematical Sciences, University of Chinese Academy of Sciences, No.19A Yuquan Road, Beijing 100049, P. R. China

<sup>e</sup>School of Sciences, Xi'an Technological University, Xi'an 710021, P. R. China

*E-mail:* [huangfuhao@itp.ac.cn](mailto:huangfuhao@itp.ac.cn), [tli@itp.ac.cn](mailto:tli@itp.ac.cn), [sunqi@itp.ac.cn](mailto:sunqi@itp.ac.cn), [sunrui24@ucas.ac.cn](mailto:sunrui24@ucas.ac.cn), [wulina@xatu.edu.cn](mailto:wulina@xatu.edu.cn)

ABSTRACT:

By introducing an extra stack of D6-branes to standard  $\mathcal{N} = 1$  supersymmetric Pati-Salam models, we extend the landscape of its complete search. In this construction, the  $d$ -stack of D6-branes is introduced besides the standard  $a$ ,  $b$ ,  $c$ -stacks. More intersections from the extra stacks of D6-branes appear, and thus Higgs/Higgs-like particles arise from more origins. Among these models, we find eight new classes of  $\mathcal{N} = 1$  supersymmetric Pati-Salam models with gauge symmetries  $SU(4)_C \times SU(2)_L \times SU(2)_{R_1} \times SU(2)_{R_2}$  and  $SU(4)_C \times SU(2)_{L_1} \times SU(2)_R \times SU(2)_{L_2}$ , where  $d$ -stack of D6-branes carries the gauge symmetries  $SU(2)_{R_2}$  and  $SU(2)_{L_2}$ , respectively. The  $SU(2)_{L_1/R_1} \times SU(2)_{L_2/R_2}$  can be broken down to the diagonal  $SU(2)_{L/R}$  gauge symmetry via bifundamental Higgs fields. In such a way, we for the first time successfully constructed three-family supersymmetric Pati-Salam models from non-rigid D6-branes with extra  $d$ -stacks of D6-branes as visible sectors. Interestingly, by introducing extra stack of D6-branes to the standard supersymmetric Pati-Salam models, the number of filler brane reduces in general, and eventually the models without any  $USp(N)$  gauge symmetry present. This reduces the exotic particles from filler brane intersection yet provides more vector-like particles from  $\mathcal{N} = 2$  subsector that are useful in renormalization group equation evolution as an advantage. Moreover, interesting degeneracy behavior with the same gauge coupling ratio exists in certain class of models.

---

## Contents

|          |  |           |
|----------|--|-----------|
| <b>1</b> | <b>Introduction</b>  | <b>1</b>  |
| <b>2</b> | <b>Basics on <math>\mathbb{T}^6/(\mathbb{Z}_2 \times \mathbb{Z}_2)</math> orientifolds with intersecting D6-branes</b>         | <b>3</b>  |
| <b>3</b> | <b>Three-family supersymmetric Pati-Salam configuration</b>  | <b>5</b>  |
| 3.1      | Generalized configurations with extra stack of D6-branes   | 6         |
| 3.2      | Gauge coupling relation with extra $d$ -stack of branes  | 9         |
| <b>4</b> | <b>Extended supersymmetric Pati-Salam models with <math>d</math>-stack of branes</b>   | <b>10</b> |
| 4.1      | $SU(2)_R$ gauge from extra symmetry breaking   | 11        |
| 4.1.1    | $SU(2)_R$ gauge from $c/d$ -stack of D6-branes   | 12        |
| 4.1.2    | Phenomenological studies   | 13        |
| 4.2      | $SU(2)_L$ gauge from extra symmetry breaking   | 18        |
| 4.2.1    | Phenomenological studies   | 19        |
| <b>5</b> | <b>Landscape of <math>\mathcal{N} = 1</math> supersymmetric Pati-Salam models with extra <math>d</math>-stack of D6-branes</b> | <b>25</b> |
| <b>6</b> | <b>String and GUT scale gauge coupling relation</b>  | <b>27</b> |
| <b>7</b> | <b>Conclusions and outlook</b>   | <b>33</b> |
| <b>A</b> | <b>Representative dual supersymmetric Pati-Salam models of Model 1</b>   | <b>39</b> |
| <b>B</b> | <b>RGE evolution for Model 1,2,3,7,8,9</b>   | <b>42</b> |

---

## 1 Introduction

Brane intersection theory has been extensively explored, bridging the theoretical work of model building and phenomenological analysis, as one of the most crucial topics in string phenomenology [1–11]. One of the main goals of string phenomenology is to realize  $\mathcal{N} = 1$  Minimal Supersymmetric Standard Models (MSSM) and Standard Models (SM), from Type I, Type IIA and Type IIB string theories. In particular, in order to acquire these quasi-realistic and realistic models, chiral fermions are required to arise from either singularities of worldvolumes on D-branes or intersections between distinct D-brane stacks in the internal space.

Moreover, Grand Unified Theories (GUTs) propose that all gauge couplings from MSSM are unified at GUT scale  $M_{GUT} \sim 2 \times 10^{16}$  GeV, as given in [12–14], while in weakly coupled heterotic string theories, the typical string scale is  $M_{string} \approx g_{string} \times 5.27 \times 10^{17}$

GeV [15, 16]. Considering the fact that  $g_{string} \sim \mathcal{O}(1)$ , we apply  $M_{string} \sim 5 \times 10^{17}$  GeV. In the internal space, the intersecting D6-branes are not transversal, and thus the typical string scale is close to the reduced Planck scale  $M_{\text{Pl}} \simeq 2.43 \times 10^{18}$  GeV [17]. It brings the gauge hierarchy problem considering large reduced Planck scale corrections at the loop level and was later solved with numerous MSSM models and GUTs constructed in [17–32]. Among these models,  $\mathcal{N} = 1$  supersymmetric three-family SU(5) models from Type IIA orientifolds on  $\mathbb{T}^6/(\mathbb{Z}_2 \times \mathbb{Z}_2)$  with intersecting D6-branes were systematically investigated [19]. Later in [17], three-family supersymmetric Pati-Salam models were systematically studied. The Pati-Salam gauge symmetry  $SU(4)_C \times SU(2)_L \times SU(2)_R$  breaks down to  $SU(3)_C \times SU(2)_L \times U(1)_{B-L} \times U(1)_{I_{3R}}$  via branes splitting, and continues to break down to the SM gauge symmetry  $SU(3)_C \times SU(2)_L \times U(1)_Y$  via Higgs mechanism.

The search for supersymmetric Pati-Salam models was carried out in many following works such as in [33], and later generalized in [34] that  $\mathcal{N} = 1$  supersymmetric  $SU(12)_C \times SU(2)_L \times SU(2)_R$  models,  $SU(4)_C \times SU(6)_L \times SU(2)_R$  models and  $SU(4)_C \times SU(2)_L \times SU(6)_R$  models were constructed from Type IIA orientifolds on  $\mathbb{T}^6/(\mathbb{Z}_2 \times \mathbb{Z}_2)$  with intersecting D6-branes. In which these generalized gauge symmetries can be further broken into the standard Pati-Salam gauge symmetry via Higgs mechanism. Along this way, powerful machine learning methods were also utilized with realistic intersecting D-brane models constructed in [35] and [36]. The Yukawa couplings are discussed in [37–47], and the masses and mixings of SM fermions from intersecting D6-branes were also studied in [48, 49]. As a milestone in the study of supersymmetric Pati-Salam models, a systematic method was developed in [50] with the landscape of supersymmetric Pati-Salam models completed. This is investigated under the three-generation condition  $I_{ab} + I_{ab'} = 3$ , and  $I_{ac} = -3, I_{ac'} = 0$  or  $I_{ac} = 0, I_{ac'} = -3$ . In this complete search of three-generation supersymmetric Pati-Salam models, a total of 202752 models were discovered, classified into 33 types from the perspective of gauge coupling relations. Besides, string-scale gauge coupling unification for the 33 classes of models can be achieved, and one can refer to [51, 52] for details. In recent work, by generalizing the three-generation condition to  $I_{ac} = -(3 + h)$  and  $I_{ac'} = h$  where  $h$  is a positive integer, another 4 types of supersymmetric Pati-Salam models were found in [53]. This extended the landscape of supersymmetric Pati-Salam models to the general framework proposed in [17], which was expected to be difficult to construct.

An intriguing question was raised in [19]: is it possible to exclude the situation where there are more than three stacks (noted as  $a$ -,  $b$ - and  $c$ -stacks) of branes not parallel to the orientifold planes, with each moduli equation satisfied. And the answer to this question appears to be negative. In [54], such  $d$ -stacks of D6-branes were first introduced in hidden sectors in three-family supersymmetric Pati-Salam models. More details are shown in Section III of [54]. The gauge couplings remain the same as those in [50] since the visible sectors are fixed the same. However, a class of consistent three-family supersymmetric Pati-Salam models was constructed from rigid intersecting D6-branes on the factorizable  $\mathbb{T}^6/(\mathbb{Z}_2 \times \mathbb{Z}'_2)$  orientifold with discrete torsion in [55]. Among all these models, additional  $d$ -stacks of rigid branes were introduced in visible sectors to yield right-handed chiral fermions by intersecting with  $a$ -stacks of branes as well as the intersection of  $a$ - and  $c$ -

stacks of branes. Therefore, the three-generation condition was modified to  $I_{ab} + I_{ab'} = -(I_{ac} + I_{ac'} + I_{ad} + I_{ad'}) = \pm 3$ , and the extended Pati-Salam gauge symmetry was written as  $SU(4)_C \times SU(2)_L \times SU(2)_{R_1} \times SU(2)_{R_2}$  accordingly. In which, the  $c$ - and  $d$ -stacks of the branes represent the  $SU(2)_{R_1}$  and  $SU(2)_{R_2}$  gauge symmetries, respectively.

Inspired by [55], we for the first time successfully construct three-family supersymmetric Pati-Salam models from non-rigid D6-branes with extra  $d$ -stacks of D6-branes as visible sectors. There are four classes of extended Pati-Salam models with  $d$ -stacks of branes that yield right-handed chiral fermions by intersecting with  $a$ -stacks of branes, as well as four classes of extended Pati-Salam models with  $d$ -stacks of branes that yield left-handed chiral fermions by intersecting with  $a$ -stacks of branes in our investigation. These eight new classes of models are distinct from the 37 models aforementioned from [50] and [53]. Considering the equal positions of certain stacks of branes, D6-brane Sign Equivalence Principle (DSEP), T-duality and other symmetries, there are 98304 equivalent models with the same gauge coupling relation for each class of models, greatly extending the landscape of Pati-Salam models.

From such construction, both the extended Pati-Salam gauge symmetries  $SU(4)_C \times SU(2)_L \times SU(2)_{R_1} \times SU(2)_{R_2}$  and  $SU(4)_C \times SU(2)_{L_1} \times SU(2)_R \times SU(2)_{L_2}$  can be broken down to the standard Pati-Salam gauge symmetry  $SU(4)_C \times SU(2)_L \times SU(2)_R$  via  $SU(2)_{R_1} \times SU(2)_{R_2} \rightarrow SU(2)_R$  and  $SU(2)_{L_1} \times SU(2)_{L_2} \rightarrow SU(2)_L$ , respectively, at first, and then yield to the SM gauge symmetry  $SU(3)_C \times SU(2)_L \times U(1)_Y$  via D6-branes splitting and Higgs mechanism, while the massless vector-like Higgs fields are allowed. Moreover, we find their gauge coupling relation can be realized at string and GUT scales via two-loop Renormalization Group Equation (RGE) running by introducing additional vector-like particles from the  $\mathcal{N} = 2$  subsector and/or adjoint chiral multiplets from  $SU(4)_C$  and  $SU(2)_L$  gauge symmetries.

This paper is organized as follows. In Section 2, we first review the basics of model building on Type IIA  $\mathbb{T}^6/(\mathbb{Z}_2 \times \mathbb{Z}_2)$  orientifolds with intersecting D6-branes. In Section 3, the basic tadpole cancellation conditions, supersymmetry constraints and three-generation conditions for three-family supersymmetric Pati-Salam models in our construction are given. In Section 4, we present the representative models of four classes with gauge symmetry  $SU(4)_C \times SU(2)_L \times SU(2)_{R_1} \times SU(2)_{R_2}$  and their spectra explicitly. In Section 5, we present the landscape of the other extended Pati-Salam models by generalizing the gauge symmetry to  $SU(4)_C \times SU(2)_{L_1} \times SU(2)_R \times SU(2)_{L_2}$ . In Section 6, we perform two-loop RGEs, and realize the gauge coupling relations at string scale for representative models. In Section 7, we eventually arrive at the conclusion of our study with the outlook given.

## 2 Basics on $\mathbb{T}^6/(\mathbb{Z}_2 \times \mathbb{Z}_2)$ orientifolds with intersecting D6-branes

In brane intersection theory, D6-branes are set to intersect at generic angles on Type IIA  $\mathbb{T}^6/(\mathbb{Z}_2 \times \mathbb{Z}_2)$  orientifolds, to obtain supersymmetric models. The six-torus  $\mathbb{T}^6$  can be considered as the direct product of three two-tori, namely  $\mathbb{T}^6 = \mathbb{T}^2 \times \mathbb{T}^2 \times \mathbb{T}^2$ . Each two-torus can be described with the real coordinates  $(x_i, y_i)$  or the complex coordinate  $z_i$ ,  $i = 1, 2, 3$ , respectively. The two generators  $\theta$  and  $\omega$  of the orbifold group  $\mathbb{Z}_2 \times \mathbb{Z}_2$ ,

corresponding to the twist vectors  $(1/2, -1/2, 0)$  and  $(0, 1/2, -1/2)$  respectively, acting on the complex coordinates  $z_i$ , such that

$$\begin{aligned}\theta &: (z_1, z_2, z_3) \mapsto (-z_1, -z_2, z_3) , \\ \omega &: (z_1, z_2, z_3) \mapsto (z_1, -z_2, -z_3) .\end{aligned}\tag{2.1}$$

The orientifold projection is introduced by gauging the  $\Omega R$  symmetry. Here,  $\Omega$  is the world-sheet parity and  $R$  is the inversion on each real axis, which acts as

$$R : (z_1, z_2, z_3) \mapsto (\bar{z}_1, \bar{z}_2, \bar{z}_3) ,\tag{2.2}$$

or  $(x_i, y_i) \mapsto (x_i, -y_i)$  on each two-torus. Hence we acquire four types of orientifold 6-planes (O6-planes) and result in four types of actions  $\Omega R$ ,  $\Omega R\theta$ ,  $\Omega R\omega$ , and  $\Omega R\theta\omega$ , respectively. Here, the O6-planes carry negative Ramond-Ramond (RR) charges. In order to cancel them and conserve the RR field flux in the compact  $\mathbb{T}^6/(\mathbb{Z}_2 \times \mathbb{Z}_2)$  without boundary, stacks of D6-branes wrapping on factorized three-cycles are introduced. There are two possible complex structures consistent on each two-torus under orientifold projection: rectangular or tilted [18, 19, 27, 56]. The homology classes of the three cycles wrapped by D6-brane stacks can be denoted by  $n_a^i[a_i] + m_a^i[b_i]$  for rectangular tori, and  $n_a^i[a_i'] + m_a^i[b_i]$  for the tilted tori, which are related by the fact  $[a_i'] = [a_i] + \frac{1}{2}[b_i]$ . Two wrapping numbers  $(n_a^i, l_a^i)$  regarding the different wrapping directions on the tori are used to label a generic one cycle on both tilted and untilted tori. Note that in the rectangular case  $l_a^i \equiv m_a^i$ , while one has  $l_a^i \equiv 2\tilde{m}_a^i = 2m_a^i + n_a^i$  for the tilted tori. Thus, it is important to remind that  $l_a^i - n_a^i$  must be even for the tilted two-torus. It is also often required that  $m_a^i$  and  $n_a^i$  be relatively co-prime to avoid multiply wrapped branes [19], which can be represented by

$$l_a^i \equiv 2^{\beta_i} (m_a^i + \frac{\beta_i}{2} n_a^i), \quad \beta_i = \begin{cases} 0, & \text{rectangular,} \\ 1, & \text{tilted.} \end{cases}\tag{2.3}$$

The  $a$ -stack of  $N_a$  D6-branes along the cycle  $(n_a^i, l_a^i)$  will be mapped to  $a'$ -stack of  $N_a$  D6-branes as images with wrapping numbers  $(n_a^i, -l_a^i)$ , under the action of  $\Omega R$ . The homology three-cycles can be denoted as

$$[\Pi_a] = \prod_{i=1}^3 \left( n_a^i [a_i] + 2^{-\beta_i} l_a^i [b_i] \right) \quad \text{and} \quad [\Pi_{a'}] = \prod_{i=1}^3 \left( n_a^i [a_i] - 2^{-\beta_i} l_a^i [b_i] \right) ,\tag{2.4}$$

where  $\beta_i = 0$  while the  $i$ -th torus is rectangular and while the  $i$ -th torus is tilted  $\beta_i = 1$ , as mentioned above. The homology three-cycles wrapped by the four orientifold planes are denoted as follows

$$\Omega R : [\Pi_1] = 2^3 [a_1] \times [a_2] \times [a_3] ,\tag{2.5}$$

$$\Omega R\omega : [\Pi_2] = -2^{3-\beta_2-\beta_3} [a_1] \times [b_2] \times [b_3] ,\tag{2.6}$$

$$\Omega R\theta\omega : [\Pi_3] = -2^{3-\beta_1-\beta_3} [b_1] \times [a_2] \times [b_3] ,\tag{2.7}$$

$$\Omega R\theta : [\Pi_4] = -2^{3-\beta_1-\beta_2} [b_1] \times [b_2] \times [a_3] . \quad (2.8)$$

In addition,  $[\Pi_{O6}] = [\Pi_{\Omega R}] + [\Pi_{\Omega R\omega}] + [\Pi_{\Omega R\theta\omega}] + [\Pi_{\Omega R\theta}]$  represents the sum of the four O6-plane homology three-cycles. And the intersection numbers between different stacks can be introduced with  $k = \beta_1 + \beta_2 + \beta_3$  denoting the total number of tilted two-tori. Recall the rules of Grassmann algebra, we have

$$[a_i][b_j] = -[b_j][a_i] = \delta_{ij}, \quad [a_i][a_j] = [b_i][b_j] = 0 . \quad (2.9)$$

Therefore, the intersection numbers between different stacks of D6-branes can be written in terms of wrapping numbers, such that

$$I_{ab} = [\Pi_a][\Pi_b] = \prod_{i=1}^3 [2^{-\beta_i} (n_a^i l_b^i - n_b^i l_a^i)] = 2^{-k} \prod_{i=1}^3 (n_a^i l_b^i - n_b^i l_a^i) , \quad (2.10)$$

$$I_{ab'} = [\Pi_a][\Pi_{b'}] = \prod_{i=1}^3 [-2^{-\beta_i} (n_a^i l_b^i + n_b^i l_a^i)] = -2^{-k} \prod_{i=1}^3 (n_a^i l_b^i + n_b^i l_a^i) , \quad (2.11)$$

$$I_{aa'} = [\Pi_a][\Pi_{a'}] = \prod_{i=1}^3 (-2^{1-\beta_i} n_a^i l_a^i) = -2^{3-k} \prod_{i=1}^3 (n_a^i l_a^i) , \quad (2.12)$$

$$I_{aO6} = [\Pi_a][\Pi_{O6}] = 2^{3-k} (-l_a^1 l_a^2 l_a^3 + l_a^1 n_a^2 n_a^3 + n_a^1 l_a^2 n_a^3 + n_a^1 n_a^2 l_a^3) , \quad (2.13)$$

In terms of intersection numbers, we acquire the generic massless particle spectrum for the intersecting D6-branes at generic angles, as shown in Table 1. It is suitable for both the case of all rectangular tori and the case when a tilted tori is present.

| Sector      | Representation  |
|-------------|---|
| $aa$        | $U(N_a/2)$ vector multiplet<br>3 adjoint chiral multiplets  |
| $ab + ba$   | $I_{ab} (\square_a, \bar{\square}_b)$ fermions  |
| $ab' + b'a$ | $I_{ab'} (\square_a, \square_b)$ fermions   |
| $aa' + a'a$ | $\frac{1}{2}(I_{aa'} - \frac{1}{2}I_{a,O6}) \square\square$ fermions<br>$\frac{1}{2}(I_{aa'} + \frac{1}{2}I_{a,O6}) \square$ fermions |

**Table 1.** The general massless particle spectrum arising from intersecting D6-branes at generic angles. The second column specifies the representations of the gauge group  $U(N_a/2)$  under the  $\mathbb{Z}_2 \times \mathbb{Z}_2$  orbifold projections.

### 3 Three-family supersymmetric Pati-Salam configuration

In this section, we will focus on the principle conditions in the model building of three-family supersymmetric Pati-Salam models: three generation condition, RR tadpole cancellation

conditions, and supersymmetry constraints.

### 3.1 Generalized configurations with extra stack of D6-branes

#### Extended three-generation conditions

Firstly, supersymmetric Pati-Salam models with three families of chiral fermions will be obtained through the D6-branes intersection. Instead of the previous studied three-generation condition  $I_{ab} + I_{ab'} = 3$  and  $I_{ac} + I_{ac'} = -3$  in [53], here we introduce the  $d$ -stack to the supersymmetric Pati-Salam models. The three generations of chiral fermions arise from the intersection of  $a$  and  $c/d$ -stacks, such that the three-generation conditions can be instead represented by [55]

$$I_{ab} + I_{ab'} = 3, \quad I_{ac} + I_{ac'} + I_{ad} + I_{ad'} = -3. \quad (3.1)$$

In our convention, the first and second equations in (3.1) refers to the left-handed and right-handed chiral fermions, respectively, which are expressed in terms of the intersection numbers.

#### Generalized RR tadpole cancellation conditions

For convenience of subsequent discussion, the products of wrapping numbers are introduced as follows. Consider the  $a$ -stack as an example

$$\begin{aligned} A_a &\equiv -n_a^1 n_a^2 n_a^3, & B_a &\equiv n_a^1 l_a^2 l_a^3, & C_a &\equiv l_a^1 n_a^2 l_a^3, & D_a &\equiv l_a^1 l_a^2 n_a^3, \\ \tilde{A}_a &\equiv -l_a^1 l_a^2 l_a^3, & \tilde{B}_a &\equiv l_a^1 n_a^2 n_a^3, & \tilde{C}_a &\equiv n_a^1 l_a^2 n_a^3, & \tilde{D}_a &\equiv n_a^1 n_a^2 l_a^3. \end{aligned} \quad (3.2)$$

The same expression applies to the other stack's products of wrapping numbers as well, denoted by subscripts  $b$ ,  $c$ , and  $d$ .

As we discussed above in the last section, negatively charged O6-planes are introduced in the spacetime, to be precise, carrying  $-4$  RR charges each. Such that the total amount of RR charges results in zero in a compact space to cancel the anomalies. In total, this contributes with

$$-4 [\Pi_{O6}] = -4([\Pi_1] + [\Pi_2] + [\Pi_3] + [\Pi_4]). \quad (3.3)$$

Taking the  $a$ -stack of D6-branes as an example, the  $a$ -stack and its  $\omega R$  images together provide charges of  $N_a[\Pi_a] + N_a[\Pi_{a'}]$  totally. Therefore, the RR tadpole cancellation conditions read

$$\sum_a N_a[\Pi_a] + \sum_a N_a[\Pi_{a'}] - 4[\Pi_{O6}] = 0, \quad (3.4)$$

where  $a$  stands for the contributions from all stacks of D6-branes. This can be reformulated with the product of wrapping number (3.2) in

$$16 + \sum_a N_a A_a = 16 + \sum_a N_a B_a = 16 + \sum_a N_a C_a = 16 + \sum_a N_a D_a = 0 \quad (3.5)$$

Moreover, considering the  $2N^{(i)}$  filler branes wrapping along the  $i$ -th O6-planes especially, the tadpole cancellation conditions read

$$\begin{aligned}
2^k N^{(1)} &= 16 + \sum_a N_a A_a , \\
2^k N^{(2)} &= 16 + \sum_a N_a B_a , \\
2^k N^{(3)} &= 16 + \sum_a N_a C_a , \\
2^k N^{(4)} &= 16 + \sum_a N_a D_a ,
\end{aligned} \tag{3.6}$$

while the possible configurations of the filler branes are shown in Table 2.

| Orientifold Action     | O6-Plane | $(n^1, l^1) \times (n^2, l^2) \times (n^3, l^3)$                    |
|------------------------|----------|---|
| $\Omega R$             | 1        | $(2^{\beta_1}, 0) \times (2^{\beta_2}, 0) \times (2^{\beta_3}, 0)$  |
| $\Omega R\omega$       | 2        | $(2^{\beta_1}, 0) \times (0, -2^{\beta_2}) \times (0, 2^{\beta_3})$ |
| $\Omega R\theta\omega$ | 3        | $(0, -2^{\beta_1}) \times (2^{\beta_2}, 0) \times (0, 2^{\beta_3})$ |
| $\Omega R\theta$       | 4        | $(0, -2^{\beta_1}) \times (0, 2^{\beta_2}) \times (2^{\beta_3}, 0)$ |

**Table 2.** Possible wrapping numbers of the four O6-planes.

### Supersymmetry condition with extra stack of D6-brane

In order to preserve  $\mathcal{N} = 1$  supersymmetry, the relative angles to the orientifold plane of any D6-branes on the three two-tori,  $\theta_1$ ,  $\theta_2$  and  $\theta_3$ , should be the group elements of  $SU(3)$ . This requires that the rotation matrix acting on the complexified compact coordinates must be unimodular [19], leading to

$$\theta_1 + \theta_2 + \theta_3 = 0 \pmod{2\pi} , \tag{3.7}$$

which is equivalent to  $\sin(\theta_1 + \theta_2 + \theta_3) = 0$  and  $\cos(\theta_1 + \theta_2 + \theta_3) > 0$ . Denoting  $L^i(n^i, l^i) = \sqrt{(2^{-\beta_i} l^i R^i)^2 + (n^i R^i)^2}$  as the length of the  $i$ -th torus, we obtain

$$\sin \theta_i = \frac{2^{-\beta_i} l^i R^i}{L^i(n^i, l^i)} , \quad \cos \theta_i = \frac{n^i R^i}{L^i(n^i, l^i)} , \quad \tan \theta_i = \frac{l^i R^i}{2^{\beta_i} n^i R^i} . \tag{3.8}$$

Applying the products defined in (3.2), for all stacks of D6-branes the supersymmetry condition can be represented by

$$\begin{aligned}
x_A \tilde{A}_a + x_B \tilde{B}_a + x_C \tilde{C}_a + x_D \tilde{D}_a &= 0 , \\
\frac{A_a}{x_A} + \frac{B_a}{x_B} + \frac{C_a}{x_C} + \frac{D_a}{x_D} &< 0 ,
\end{aligned} \tag{3.9}$$

where  $x_A = \lambda$  is constant,  $x_B = \lambda 2^{\beta_2 + \beta_3} / \chi_2 \chi_3$ ,  $x_C = \lambda 2^{\beta_1 + \beta_3} / \chi_1 \chi_3$ , and  $x_D = \lambda 2^{\beta_1 + \beta_2} / \chi_1 \chi_2$  denoting a set of non-trivial solutions to the equation in (3.9), and  $\chi_i = R_i^2 / R_i^1$  represents the complex structure modulus for the  $i$ -th torus. It is obvious that  $\chi_i$  should be real and positive, which directly leads  $x_A$ ,  $x_B$ ,  $x_C$  and  $x_D$  to share the same sign.

In our work, we consider intersecting branes of four stacks of D6-branes, corresponding to  $a$ -,  $b$ -,  $c$ - and  $d$ -stacks respectively. In this case, different with the construction from three stacks of D6-branes, the rank of the matrix of wrapping numbers products

$$M = \begin{bmatrix} \tilde{A}_a & \tilde{B}_a & \tilde{C}_a & \tilde{D}_a \\ \tilde{A}_b & \tilde{B}_b & \tilde{C}_b & \tilde{D}_b \\ \tilde{A}_c & \tilde{B}_c & \tilde{C}_c & \tilde{D}_c \\ \tilde{A}_d & \tilde{B}_d & \tilde{C}_d & \tilde{D}_d \end{bmatrix} \quad (3.10)$$

shall be three instead. This is due to that if the rank of matrix  $M$  is four, equation  $M\vec{x} = \vec{0}$  (Eq. 3.9) admits only the trivial solution  $x_A = x_B = x_C = x_D = 0$ , and if the rank of  $M$  is less than three, the complex modulus for the tori will not be determined. Cramer's rule indicates that equation  $M\vec{x} = \vec{0}$  has infinitely many solutions with only one fundamental set of solutions. Therefore, we must first identify a row in matrix  $M$  where all cofactors are nonzeros, then assign its four corresponding algebraic cofactors as  $y_A$ ,  $y_B$ ,  $y_C$ , and  $y_D$ . Without loss of generality, we can take the second row as example and have

$$y_A = \begin{vmatrix} \tilde{B}_a & \tilde{C}_a & \tilde{D}_a \\ \tilde{B}_c & \tilde{C}_c & \tilde{D}_c \\ \tilde{B}_d & \tilde{C}_d & \tilde{D}_d \end{vmatrix}, \quad y_B = - \begin{vmatrix} \tilde{A}_a & \tilde{C}_a & \tilde{D}_a \\ \tilde{A}_c & \tilde{C}_c & \tilde{D}_c \\ \tilde{A}_d & \tilde{C}_d & \tilde{D}_d \end{vmatrix}, \quad y_C = \begin{vmatrix} \tilde{A}_a & \tilde{B}_a & \tilde{D}_a \\ \tilde{A}_c & \tilde{B}_c & \tilde{D}_c \\ \tilde{A}_d & \tilde{B}_d & \tilde{D}_d \end{vmatrix}, \quad y_D = - \begin{vmatrix} \tilde{A}_a & \tilde{B}_a & \tilde{C}_a \\ \tilde{A}_c & \tilde{B}_c & \tilde{C}_c \\ \tilde{A}_d & \tilde{B}_d & \tilde{C}_d \end{vmatrix}, \quad (3.11)$$

which are all non-zeros. Such that, the set of solutions to the equations in (3.9) can be rewritten as  $x_A = \lambda$ ,  $x_B = \lambda y_B / y_A$ ,  $x_C = \lambda y_C / y_A$  and  $x_D = \lambda y_D / y_A$ . When the algebraic cofactors of the first, third, and fourth row are nonzeros, analogous calculations can be performed. The D6-branes configurations preserving 4-dimensional  $\mathcal{N} = 1$  supersymmetry can be classified into three categories.

First, there are D6-branes whose wrapping numbers are the same as O6-planes (shown in Table 2). Among  $A_a$ ,  $B_a$ ,  $C_a$  and  $D_a$ , where the subscript  $a$  denotes any stack, there are one negative and three zeros, represented as  $(-, 0, 0, 0)$ . This type of D6-branes carrying  $USp(n)$  gauge symmetry can be identified with  $USp(n)_1$ ,  $USp(n)_2$ ,  $USp(n)_3$  and  $USp(n)_4$  groups according to which one of  $A_a$ ,  $B_a$ ,  $C_a$  and  $D_a$  takes zero value, respectively.

Second, this case corresponds to wrapping numbers that are all non-zero, leading to one positive number and three negative numbers  $(+, -, -, -)$  in  $A_a$ ,  $B_a$ ,  $C_a$  and  $D_a$ , which is called NZ-type D6-branes in [17].

Third, if there is one and only one zero wrapping number, there will be two negative numbers and two zeros in  $A_a$ ,  $B_a$ ,  $C_a$  and  $D_a$   $(0, 0, -, -)$  and this case is called Z-type D6-branes in [17]. Since both Z- and NZ-type branes carry  $U(n)$  gauge symmetry, they are sometimes called U-branes. The combinations of wrapping numbers of NZ-type D6-branes can be classified into

$$A1 : (-, -) \times (+, +) \times (+, +), \quad A2 : (-, +) \times (-, +) \times (-, +); \quad (3.12)$$

$$B1 : (+, -) \times (+, +) \times (+, +), \quad B2 : (+, +) \times (-, +) \times (-, +); \quad (3.13)$$

$$C1 : (+, +) \times (+, -) \times (+, +), \quad C2 : (-, +) \times (+, +) \times (-, +); \quad (3.14)$$

$$D1 : (+, +) \times (+, +) \times (+, -), \quad D2 : (-, +) \times (-, +) \times (+, +). \quad (3.15)$$

To conclude,  $A_a$ ,  $B_a$ ,  $C_a$  and  $D_a$  in (3.6) each corresponds to one of the types of U-branes.

### 3.2 Gauge coupling relation with extra $d$ -stack of branes

Recall that the Kähler potential of the Pati-Salam models is represented by [57]

$$K = -\ln(S + \bar{S}) - \sum_{i=1}^3 \ln(U^i + \bar{U}^i), \quad (3.16)$$

where  $S$  and  $U^i$  stand for dilaton and complex structure moduli, and the relations of their real parts are as follows

$$\text{Re}(S) = \frac{M_s^3 R_1^1 R_2^1 R_3^1}{2\pi g_s}, \quad \text{Re}(U^i) = \text{Re}(S) \chi_j \chi_k. \quad (3.17)$$

We have already mentioned in Section 3.1 that  $R_i^1$  and  $R_i^2$  are geometric parameters, together with the ratio  $\chi_i = R_i^2/R_i^1$ , describing the  $i$ -th two-torus, where  $g_s$  is the string coupling.

For the  $x$ -stacks of D6-branes ( $x$  is  $a$ ,  $b$ ,  $c$  or  $d$ ), carrying a gauge symmetry of  $U(n)$ , we have the following holomorphic gauge kinetic function represented by

$$f_x = \frac{1}{4\kappa_x} (n_x^1 n_x^2 n_x^3 S - \sum_{i=1}^3 2^{-\beta_j - \beta_k} n_x^i n_x^j n_x^k U^i) \quad (i \neq j \neq k). \quad (3.18)$$

Here, we take  $\kappa_x = 1$  with respect to  $SU(n)$  symmetry. Meanwhile, we have the relation between the gauge coupling constant and the kinetic function of  $x$ -stack of D6-branes as

$$g_{D6_x}^{-2} = |\text{Re}(f_x)|. \quad (3.19)$$

In the case of model building from symmetry breaking to the diagonal subgroup with  $SU(2)_{R_1} \times SU(2)_{R_2} \rightarrow SU(2)_R$ , then  $g_R^{-2}$  can be written in terms of  $g_c^{-2}$  and  $g_d^{-2}$  as [55]

$$g_R^{-2} = g_c^{-2} + g_d^{-2} = |\text{Re}(f_c)| + |\text{Re}(f_d)|, \quad (3.20)$$

Alternatively, this can be represented by the gauge kinetic function:

$$f_R = f_c + f_d. \quad (3.21)$$

The holomorphic gauge kinetic function of the  $U(1)_Y$  gauge symmetry can be expressed as a linear combination of the kinetic function related to  $SU(4)_C$  and  $SU(2)_R$  as [27, 56]

$$f_Y = \frac{3}{5} \left( \frac{2}{3} f_a + f_R \right) = \frac{3}{5} \left( \frac{2}{3} f_a + f_c + f_d \right). \quad (3.22)$$

Then the tree-level MSSM gauge couplings of the Pati-Salam models can be expressed as

$$g_a^2 = \alpha g_b^2 = \beta \frac{5}{3} g_Y^2 = \gamma [\pi e^{\phi_4}], \quad (3.23)$$

where  $g_a^2$ ,  $g_b^2$  and  $\frac{5}{3}g_Y^2$  are strong, weak and hypercharge gauge couplings, respectively, while the ratios  $\alpha$ ,  $\beta$  and  $\gamma$  are different for each independent class of models.

In addition, according to the supersymmetry conditions we discussed above, the complex structure moduli  $\chi_1$ ,  $\chi_2$  and  $\chi_3$  are completely determined by the gauge symmetry, while there remains the dilation degree of freedom to be stabilized. In order to complete the stabilization, the beta functions of  $2N^{(i)}$  filler branes shall be calculated such that

$$\begin{aligned}\beta_i^g &= -3 \left( \frac{N^{(i)}}{2} + 1 \right) + 2|I_{ai}| + |I_{bi}| + |I_{ci}| + |I_{di}| + 3 \left( \frac{N^{(i)}}{2} - 1 \right) \\ &= -6 + 2|I_{ai}| + |I_{bi}| + |I_{ci}| + |I_{di}| \quad (i = 1, 2, 3, 4) .\end{aligned}\tag{3.24}$$

We demand that the beta functions for the  $USp(n)_i$  groups at the one-loop level be negative, which provides an approach to achieve gaugino condensations as shown in [58–60].

#### 4 Extended supersymmetric Pati-Salam models with $d$ -stack of branes

To build a standard model or standard model-like theories from the D6-brane intersection, besides the  $U(3)_C$  and  $U(2)_L$  gauge symmetries, there are at least two additional  $U(1)$  gauge groups present. One  $U(1)_{I_{3R}}$  is analogous to the third component of the right-handed weak isospin, while the other  $U(1)_L$  is the lepton symmetry.  $Q_B$  is introduced as the charge of  $U(1)_B$  in  $U(3)_C \cong SU(3)_C \times U(1)_B$ , and then the hypercharge should be

$$Q_Y = Q_{I_{3R}} + \frac{Q_B - Q_L}{2} .\tag{4.1}$$

From branes splitting,  $U(1)_{B-L}$  comes from  $SU(4)_C$ , and  $U(1)_{I_{3R}}$  originates from  $SU(2)_R$ . And no anomalies arise during the symmetry breaking from the Pati-Salam model to SM. In this work, the  $a$ -,  $b$ -,  $c$ - and  $d$ -stack of D6-branes corresponds to the  $U(4)_C$ ,  $U(2)_L$ ,  $U(2)_{R_1}$  and  $U(2)_{R_2}$  gauge symmetries, respectively. This leads to the total gauge symmetries  $SU(4)_C \times SU(2)_L \times SU(2)_{R_1} \times SU(2)_{R_2}$ . The right-handed  $SU(2)_R$  is then obtained from the diagonal subgroup of  $SU(2)_{R_1} \times SU(2)_{R_2}$  via the bifundamental Higgs fields. Finally, a conventional gauge symmetry  $SU(4)_C \times SU(2)_L \times SU(2)_R$  of the Pati-Salam model is achieved. And the SM gauge symmetry can then be obtained by branes splitting and Higgs mechanism as before [17]. The complete chain of symmetry breaking can be written as

$$\begin{aligned}SU(4) \times SU(2)_L \times SU(2)_{R_1} \times SU(2)_{R_2} &\xrightarrow{\text{bifundamental Higgs}} SU(4) \times SU(2)_L \times SU(2)_R \\ &\xrightarrow{a \rightarrow a_1 + a_2} SU(3)_C \times SU(2)_L \times SU(2)_R \times U(1)_{B-L} \\ &\xrightarrow{c \rightarrow c_1 + c_2} SU(3)_C \times SU(2)_L \times U(1)_{I_{3R}} \times U(1)_{B-L} \\ &\xrightarrow{\text{Higgs mechanism}} SU(3)_C \times SU(2)_L \times U(1)_Y .\end{aligned}\tag{4.2}$$

#### 4.1 $SU(2)_R$ gauge from extra symmetry breaking

Based on the extended construction of supersymmetric Pati-Salam models with extra  $d$ -stack of branes, the  $SU(2)_R$  gauge is realized from symmetry breaking of  $SU(2)_{R_1} \times SU(2)_{R_2} \rightarrow SU(2)_R$ . In the D6-brane configuration, we find four classes of independent models with representative Model 1-4 shown in Table 3, 4, 5, 6. They are independent of each other from the perspective of gauge coupling relation. In particular, the three-family of right-handed chiral fermions arises from the combined contribution of the intersections including  $a$ - and  $c$ -stacks and  $a$ - and  $d$ -stacks.

**Table 3.** D6-brane configurations and intersection numbers of Model 1, and its MSSM gauge coupling relation is  $g_a^2 = g_b^2 = \frac{1}{2}g_R^2 = \frac{5}{8}(\frac{5}{3}g_Y^2) = 2\sqrt{2} 3^{1/4} \pi e^{\phi_4}$ , for which the second torus is tilted.

| Model 1 | $U(4) \times U(2)_L \times U(2)_{R_1} \times U(2)_{R_2} \times USp(2)^2$ |  |  |               |     |      |     |      |     |      |    |    |
|---------|--|--|--|---------------|-----|------|-----|------|-----|------|----|----|
| stack   | $N$  | $(n^1, l^1) \times (n^2, l^2) \times (n^3, l^3)$ | $n_{\square\square}$   | $n_{\square}$ | $b$ | $b'$ | $c$ | $c'$ | $d$ | $d'$ | 1  | 4  |
| $a$     | 8  | $(1, -1) \times (1, 1) \times (1, 0)$            | 0  | 0             | 3   | 0    | -1  | 0    | -2  | 0    | 0  | 0  |
| $b$     | 4  | $(0, -1) \times (1, -1) \times (-1, 3)$          | 2  | -2            | -   | -    | 0   | -2   | 2   | 1    | -3 | 0  |
| $c$     | 4  | $(-1, 0) \times (-1, 1) \times (1, 1)$           | 0  | 0             | -   | -    | -   | -    | -2  | 1    | 0  | 1  |
| $d$     | 4  | $(-1, -1) \times (-1, -3) \times (0, -1)$        | -2   | 2             | -   | -    | -   | -    | -   | -    | 3  | -1 |
| 1       | 2  | $(1, 0) \times (2, 0) \times (1, 0)$             | $x_A = \frac{1}{3}x_B = \frac{1}{3}x_C = \frac{1}{3}x_D$<br>$\beta_1^g = 0, \quad \beta_4^g = -4$<br>$\chi_1 = \frac{1}{\sqrt{3}}, \chi_2 = \frac{2}{\sqrt{3}}, \chi_3 = \frac{1}{\sqrt{3}}$ |               |     |      |     |      |     |      |    |    |
| 4       | 2  | $(0, -1) \times (0, 2) \times (1, 0)$            |  |               |     |      |     |      |     |      |    |    |

**Table 4.** D6-brane configurations and intersection numbers of Model 2, and its MSSM gauge coupling relation is  $g_a^2 = 3g_b^2 = \frac{3}{4}g_R^2 = \frac{5}{6}(\frac{5}{3}g_Y^2) = 2\sqrt{2} 3^{3/4} \pi e^{\phi_4}$ , for which the third torus is tilted.

| Model 2 | $U(4) \times U(2)_L \times U(2)_{R_1} \times U(2)_{R_2} \times USp(2)^2$ |  |   |               |     |      |     |      |     |      |   |    |
|---------|--|--|---|---------------|-----|------|-----|------|-----|------|---|----|
| stack   | $N$  | $(n^1, l^1) \times (n^2, l^2) \times (n^3, l^3)$ | $n_{\square\square}$  | $n_{\square}$ | $b$ | $b'$ | $c$ | $c'$ | $d$ | $d'$ | 2 | 4  |
| $a$     | 8  | $(-1, 1) \times (0, -1) \times (1, -1)$          | 0   | 0             | 1   | 2    | -1  | 0    | 0   | -2   | 0 | 0  |
| $b$     | 4  | $(0, 1) \times (-1, 1) \times (-1, 3)$           | 2   | -2            | -   | -    | 0   | -2   | -3  | -6   | 1 | 0  |
| $c$     | 4  | $(1, 0) \times (1, -1) \times (1, 1)$            | 0   | 0             | -   | -    | -   | -    | -1  | 0    | 0 | 1  |
| $d$     | 4  | $(-3, -1) \times (-1, 0) \times (1, -1)$         | 2   | -2            | -   | -    | -   | -    | -   | -    | 1 | -3 |
| 2       | 2  | $(1, 0) \times (0, -1) \times (0, 2)$            | $x_A = \frac{1}{3}x_B = x_C = x_D$<br>$\beta_2^g = -4, \quad \beta_4^g = -2$<br>$\chi_1 = \sqrt{3}, \chi_2 = \frac{1}{\sqrt{3}}, \chi_3 = \frac{2}{\sqrt{3}}$ |               |     |      |     |      |     |      |   |    |
| 4       | 2  | $(0, -1) \times (0, 1) \times (2, 0)$            |   |               |     |      |     |      |     |      |   |    |

In Model 1 and 2, the supersymmetric Pati-Salam models are realized similar with the ones presented in [50] while with extra gauge coupling relations appear. In Model 3 and 4, the tadpole cancellation condition can be satisfied without filler brane from the  $USp(N)$  gauge symmetry. This is distinct with the usual supersymmetric Pati-Salam models found in [50]. It shows to us that by introducing extra  $d$ -stack of branes opens a new scenario in filler brane configuration. In particular, we observe that the ratio itself of gauge couplings  $g_a^2 : g_b^2 : g_R^2 : (\frac{5}{3}g_Y^2)$  of Model 4 is the same as that of Model 10 from [50], yet with different value of  $g_a^2 = 4 \times 3^{3/4} \pi e^{\phi_4}$  with  $d$ -stack and  $g_a^2 = \frac{16 \times 2^{1/4}}{3\sqrt{3}} \pi e^{\phi_4}$  while without  $d$ -stack.

**Table 5.** D6-brane configurations and intersection numbers of Model 3, and its MSSM gauge coupling relation is  $g_a^2 = 6g_b^2 = \frac{3}{2}g_R^2 = \frac{5}{4}(\frac{5}{3}g_Y^2) = 4 \times 3^{3/4}\pi e^{\phi_4}$ , for which the first torus is tilted.

| Model 3 |     | $U(4) \times U(2)_L \times U(2)_{R_1} \times U(2)_{R_2}$ |   |               |     |      |     |      |     |      |  |
|---------|-----|--|---|---------------|-----|------|-----|------|-----|------|--|
| stack   | $N$ | $(n^1, l^1) \times (n^2, l^2) \times (n^3, l^3)$         | $n_{\square\square}$  | $n_{\square}$ | $b$ | $b'$ | $c$ | $c'$ | $d$ | $d'$ |  |
| $a$     | 8   | $(1, -1) \times (0, -1) \times (-1, 1)$                  | 0   | 0             | 2   | 1    | -1  | 0    | -2  | 0    |  |
| $b$     | 4   | $(-1, -3) \times (-1, -2) \times (0, -1)$                | -5  | 5             | -   | -    | 4   | 0    | 6   | 12   |  |
| $c$     | 4   | $(-1, -1) \times (-1, 2) \times (1, 0)$                  | 1   | -1            | -   | -    | -   | -    | 0   | -2   |  |
| $d$     | 4   | $(-1, -1) \times (-1, 0) \times (3, -1)$                 | -2  | 2             | -   | -    | -   | -    | -   | -    |  |
|         |     |  | $x_A = \frac{1}{2}x_B = x_C = \frac{1}{6}x_D$<br>$\chi_1 = \frac{2}{\sqrt{3}}, \chi_2 = \frac{1}{2\sqrt{3}}, \chi_3 = \sqrt{3}$ |               |     |      |     |      |     |      |  |

**Table 6.** D6-brane configurations and intersection numbers of Model 4, and its MSSM gauge coupling relation is  $g_a^2 = 2g_b^2 = g_R^2 = (\frac{5}{3}g_Y^2) = 4 \times 3^{1/4}\pi e^{\phi_4}$ , for which the first torus is tilted.

| Model 4 |     | $U(4) \times U(2)_L \times U(2)_{R_1} \times U(2)_{R_2}$ |   |               |     |      |     |      |     |      |  |
|---------|-----|--|---|---------------|-----|------|-----|------|-----|------|--|
| stack   | $N$ | $(n^1, l^1) \times (n^2, l^2) \times (n^3, l^3)$         | $n_{\square\square}$  | $n_{\square}$ | $b$ | $b'$ | $c$ | $c'$ | $d$ | $d'$ |  |
| $a$     | 8   | $(1, -1) \times (0, -1) \times (-1, 1)$                  | 0   | 0             | 3   | 0    | -1  | 0    | 0   | -2   |  |
| $b$     | 4   | $(-1, -1) \times (-3, -2) \times (0, -1)$                | 1   | -1            | -   | -    | 0   | -4   | 2   | 4    |  |
| $c$     | 4   | $(-1, -1) \times (-1, 2) \times (1, 0)$                  | 1   | -1            | -   | -    | -   | -    | 2   | -4   |  |
| $d$     | 4   | $(3, 1) \times (1, 0) \times (1, -1)$                    | 2   | -2            | -   | -    | -   | -    | -   | -    |  |
|         |     |  | $x_A = \frac{1}{2}x_B = x_C = \frac{3}{2}x_D$<br>$\chi_1 = 2\sqrt{3}, \chi_2 = \frac{\sqrt{3}}{2}, \chi_3 = \frac{1}{\sqrt{3}}$ |               |     |      |     |      |     |      |  |

Note that while tree-level MSSM gauge couplings of Pati-Salam models  $g_a^2 = \alpha g_b^2 = \beta \frac{5}{3}g_Y^2 = \gamma[\pi e^{\phi_4}]$  with the same gauge coupling ratio yet with different  $\gamma$  in their value, (3.23) can be related by scaling of the dilaton. Therefore, we propose a new phenomenological relation between the models with filler branes and  $d$ -stack of D6-branes.

#### 4.1.1 $SU(2)_R$ gauge from $c/d$ -stack of D6-branes

In addition to Models 1-4, special models with either  $I_{ac} + I_{ac'} = 0, I_{ad} + I_{ad'} = -3$  or  $I_{ac} + I_{ac'} = -3, I_{ad} + I_{ad'} = 0$  also appear, such as Model 5.

**Table 7.** D6-brane configurations and intersection numbers of Model 5, and its MSSM gauge coupling relation is  $g_a^2 = g_b^2 = \frac{1}{2}g_R^2 = \frac{5}{8}(\frac{5}{3}g_Y^2) = 4\sqrt{\frac{2}{3}}\pi e^{\phi_4}$ , for which the third torus is tilted.

| Model 5 |     | $U(4) \times U(2)_L \times U(2)_{R_1} \times U(2)_{R_2} \times USp(2)^2$ |   |               |     |      |     |      |     |      |    |    |
|---------|-----|--|---|---------------|-----|------|-----|------|-----|------|----|----|
| stack   | $N$ | $(n^1, l^1) \times (n^2, l^2) \times (n^3, l^3)$                         | $n_{\square\square}$  | $n_{\square}$ | $b$ | $b'$ | $c$ | $c'$ | $d$ | $d'$ | 1  | 3  |
| $a$     | 8   | $(1, -1) \times (0, -1) \times (-1, 1)$                                  | 0   | 0             | 3   | 0    | -3  | 0    | 0   | 0    | -1 | 1  |
| $b$     | 4   | $(0, 1) \times (3, 1) \times (-1, -1)$                                   | 2   | -2            | -   | -    | 0   | 0    | 0   | -3   | 1  | 0  |
| $c$     | 4   | $(1, 0) \times (-3, 1) \times (-1, -1)$                                  | -2  | 2             | -   | -    | -   | -    | 0   | 3    | 0  | -1 |
| $d$     | 4   | $(-1, -1) \times (0, -1) \times (-1, -1)$                                | 0   | 0             | -   | -    | -   | -    | -   | -    | 1  | -1 |
| 1       | 2   | $(1, 0) \times (1, 0) \times (2, 0)$                                     | $x_A = 3x_B = x_C = 3x_D$<br>$\beta_1^g = -2, \beta_3^g = -2$<br>$\chi_1 = 1, \chi_2 = 3, \chi_3 = 2$ |               |     |      |     |      |     |      |    |    |
| 3       | 2   | $(0, -1) \times (1, 0) \times (0, 2)$                                    |   |               |     |      |     |      |     |      |    |    |

**Table 8.** D6-brane configurations and intersection numbers of Model 6 (dual to Model 5 in [50]), and its MSSM gauge coupling relation is  $g_a^2 = g_b^2 = g_c^2 = (\frac{5}{3}g_Y^2) = 4\sqrt{\frac{2}{3}}\pi e^{\phi_4}$ . for which the third torus is tilted.

| Model 6 |     | $U(4) \times U(2)_L \times U(2)_R \times USp(2)^4$ |   |               |     |      |     |      |    |    |    |   |
|---------|-----|--|---|---------------|-----|------|-----|------|----|----|----|---|
| stack   | $N$ | $(n^1, l^1) \times (n^2, l^2) \times (n^3, l^3)$   | $n_{\square\square}$  | $n_{\square}$ | $b$ | $b'$ | $c$ | $c'$ | 1  | 2  | 3  | 4 |
| $a$     | 8   | $(1, -1) \times (0, -1) \times (-1, 1)$            | 0   | 0             | 3   | 0    | -3  | 0    | -1 | 0  | 1  | 0 |
| $b$     | 4   | $(0, 1) \times (3, 1) \times (-1, -1)$             | 2   | -2            | -   | -    | 0   | 0    | 1  | -3 | 0  | 0 |
| $c$     | 4   | $(1, 0) \times (-3, 1) \times (-1, -1)$            | -2  | 2             | -   | -    | -   | -    | 0  | 0  | -1 | 3 |
| 1       | 2   | $(1, 0) \times (1, 0) \times (2, 0)$               | $x_A = 3x_B = x_C = 3x_D$<br>$\beta_1^g = -3, \beta_2^g = -3, \beta_3^g = -3, \beta_4^g = -3$<br>$\chi_1 = 1, \chi_2 = 3, \chi_3 = 2$ |               |     |      |     |      |    |    |    |   |
| 2       | 2   | $(1, 0) \times (0, -1) \times (0, 2)$              |   |               |     |      |     |      |    |    |    |   |
| 3       | 2   | $(0, -1) \times (1, 0) \times (0, 2)$              |   |               |     |      |     |      |    |    |    |   |
| 4       | 2   | $(0, -1) \times (0, 1) \times (2, 0)$              |   |               |     |      |     |      |    |    |    |   |

Similar as we observed for Model 4 and Model 10 in [50] that there is a hidden relation between the filler brane and the extra  $d$ -stack of brane introduced, we find that Model 5 and Model 6 (dual to Model 5 in [50]) share the same intersection numbers. Different with the former case, Model 5 and Model 6 share the same gauge coupling value  $g_a^2 = 4\sqrt{\frac{2}{3}}\pi e^{\phi_4}$  yet do *not* share the same gauge coupling ratio, that opposite to the former interesting case between Model 4 and Model 10.

From the perspective of gauge couplings unification study, they share the same  $g_a$  value while exhibiting completely different ratios of  $g_a^2 : g_R^2 : g_Y^2$ . Therefore, from the perspective of gauge couplings, these models are distinct and will exhibit different behaviors in the gauge coupling unification. Their gauge coupling unification at string and GUT scales will be shown latter in Section 6.

#### 4.1.2 Phenomenological studies

In this section, we present the full spectra of Model 1 to 4 explicitly and discuss the outcome with the extra  $d$ -stack of D6-branes introduced.

In particular, different with the standard supersymmetric Pati-Salam models, here Higgs multiplets not just arise from both the intersection of  $b$ - and  $c$ -stacks of branes (or its image) but also arise from the intersection of  $b$ - and  $d$ -stacks of branes (or its image) simultaneously. This can be read from Table 9-14. In which,  $Q_L$  and  $L_L$  represent left-handed quarks and leptons,  $Q_R$  and  $L_R$  represent right-handed quarks and leptons, respectively. Besides,  $H$  stands for the Higgs particle,  $H'$  stands for the Higgs-like particle, and  $\Phi$  stands for the bifundamental Higgs.

Firstly, the chiral spectrum of Model 1 is shown in Table 9. From its spectrum, 4 Higgs doublets arise from the  $\mathcal{N} = 2$  subsector of the intersection of  $b$ - and  $c$ -stacks of D6-branes. Besides, there is one  $USp(2)$  group with  $\beta$  function to be zero and one  $USp$  group with negative  $\beta$  function from Table 3.

Note that a composite particle spectrum also appears for Model 1 as shown in Table 10. The  $USp(2)_1$  group has two charged intersections, giving rise to three exotic particles  $(1, \bar{2}, 1, 1, 2, 1)$  and three exotic particles  $(1, 1, 1, 2, \bar{2}, 1)$ . The mixing of these two types of exotic particles yields 9 chiral multiplets  $(1, \bar{2}, 1, 2, 1, 1)$ . Besides, their self-confinement results

**Table 9.** The chiral spectrum in the open string sector of Model 1

| Model 1   | $SU(4) \times SU(2)_L \times SU(2)_{R1} \times SU(2)_{R2} \times USp(2)^2$ | $Q_4$ | $Q_{2L}$ | $Q_{2R1}$ | $Q_{2R2}$ | $Q_{em}$                           | $B - L$           | Field        |
|---|--|-------|----------|-----------|-----------|------------------------------------|-------------------|--------------|
| $ab$  | $3 \times (4, \bar{2}, 1, 1, 1, 1)$  | 1     | -1       | 0         | 0         | $-\frac{1}{3}, \frac{2}{3}, -1, 0$ | $\frac{1}{3}, -1$ | $Q_L, L_L$   |
| $ac$  | $1 \times (\bar{4}, 1, 2, 1, 1, 1)$  | -1    | 0        | 1         | 0         | $\frac{1}{3}, -\frac{2}{3}, 1, 0$  | $-\frac{1}{3}, 1$ | $Q_R, L_R$   |
| $ad$  | $2 \times (\bar{4}, 1, 1, 2, 1, 1)$  | -1    | 0        | 0         | 1         | $\frac{1}{3}, -\frac{2}{3}, 1, 0$  | $-\frac{1}{3}, 1$ | $Q_R, L_R$   |
| $bc'$   | $2 \times (1, \bar{2}, \bar{2}, 1, 1, 1)$                                  | 0     | -1       | -1        | 0         | 0, $\mp 1$                         | 0                 | $H'$         |
| $bd$  | $2 \times (1, 2, 1, \bar{2}, 1, 1)$  | 0     | 1        | 0         | -1        | 0, $\pm 1$                         | 0                 | $H$          |
| $bd'$   | $1 \times (1, 2, 1, 2, 1, 1)$  | 0     | 1        | 0         | 1         | 0, $\pm 1$                         | 0                 | $H'$         |
| $cd$  | $2 \times (1, 1, \bar{2}, 2, 1, 1)$  | 0     | 0        | -1        | 1         | 0, $\mp 1$                         | 0                 | $\Phi$       |
| $cd'$   | $1 \times (1, 1, 2, 2, 1, 1)$  | 0     | 0        | 1         | 1         | 0, $\pm 1$                         | 0                 | $\Phi$       |
| $b1$  | $3 \times (1, \bar{2}, 1, 1, 2, 1)$  | 0     | -1       | 0         | 0         | $\pm \frac{1}{2}$                  | 0                 |              |
| $c4$  | $1 \times (1, 1, 2, 1, 1, \bar{2})$  | 0     | 0        | 1         | 0         | $\pm \frac{1}{2}$                  | 0                 |              |
| $d1$  | $3 \times (1, 1, 1, 2, \bar{2}, 1)$  | 0     | 0        | 0         | 1         | $\pm \frac{1}{2}$                  | 0                 |              |
| $d4$  | $1 \times (1, 1, 1, \bar{2}, 1, 2)$  | 0     | 0        | 0         | -1        | $\mp \frac{1}{2}$                  | 0                 |              |
| $b \begin{array}{ c } \hline \square \\ \hline \end{array}$                   | $2 \times (1, 3, 1, 1, 1, 1)$  | 0     | 2        | 0         | 0         | 0, $\pm 1$                         | 0                 |              |
| $b \begin{array}{ c } \hline \square \\ \hline \square \\ \hline \end{array}$ | $2 \times (1, \bar{1}, 1, 1, 1, 1)$  | 0     | -2       | 0         | 0         | 0                                  | 0                 |              |
| $d \begin{array}{ c } \hline \square \\ \hline \end{array}$                   | $2 \times (1, 1, 1, \bar{3}, 1, 1)$  | 0     | 0        | 0         | -2        | 0, $\mp 1$                         | 0                 |              |
| $d \begin{array}{ c } \hline \square \\ \hline \square \\ \hline \end{array}$ | $2 \times (1, 1, 1, 1, 1, 1)$  | 0     | 0        | 0         | 2         | 0                                  | 0                 |              |
| $bc$  | $4 \times (1, 2, \bar{2}, 1, 1, 1)$  | 0     | 1        | -1        | 0         | 0, $\pm 1$                         | 0                 | $H_u, H_d^i$ |
|   | $4 \times (1, \bar{2}, 2, 1, 1, 1)$  | 0     | -1       | 1         | 0         |                                    |                   |              |

**Table 10.** The composite particle spectrum for Model 1

| Model 1         |              | $U(4) \times U(2)_L \times U(2)_{R1} \times U(2)_{R2} \times USp(2)^2$ |  |
|-----------------|--------------|--|--|
| Confining Force | Intersection | Exotic particle Spectrum   | Confined Particle Spectrum   |
| $USp(2)_1$      | b1           | $3 \times (1, \bar{2}, 1, 1, 2, 1)$                                    | $6 \times (1, \bar{2}^2, 1, 1, 1, 1), 9 \times (1, \bar{2}, 1, 2, 1, 1),$<br>$6 \times (1, 1, 1, 2^2, 1, 1)$ |
|                 | d1           | $3 \times (1, 1, 1, 2, \bar{2}, 1)$                                    |  |
| $USp(2)_4$      | c4           | $1 \times (1, 1, 2, 1, 1, \bar{2})$                                    | $1 \times (1, 1, 2^2, 1, 1, 1), 1 \times (1, 1, 2, \bar{2}, 1, 1),$<br>$1 \times (1, 1, 1, \bar{2}^2, 1, 1)$ |
|                 | d4           | $1 \times (1, 1, 1, \bar{2}, 1, 2)$                                    |  |

in 6 tensor representations  $(1, \bar{2}^2, 1, 1, 1, 1)$  and 6 tensor representations  $(1, 1, 1, 2^2, 1, 1)$ , which can be further decomposed so that

$$\begin{aligned}
 6 \times (1, \bar{2}^2, 1, 1, 1, 1) &\rightarrow 6 \times (1, \bar{3}, 1, 1, 1, 1) + 6 \times (1, \bar{1}, 1, 1, 1, 1), \\
 6 \times (1, 1, 1, 2^2, 1, 1) &\rightarrow 6 \times (1, 1, 1, 3, 1, 1) + 6 \times (1, 1, 1, 1, 1, 1),
 \end{aligned} \tag{4.3}$$

leading to chiral multiplets  $(1, \bar{3}, 1, 1, 1, 1)$  and  $(1, 1, 1, 3, 1, 1)$ . Meanwhile, the  $USp(2)_4$  group also has two charged intersections, which give rise to one exotic particle  $(1, 1, 2, 1, 1, \bar{2})$  and one exotic particle  $(1, 1, 1, \bar{2}, 1, 2)$ . The mixing of these two types of exotic particles yields one chiral multiplet  $(1, 1, 2, 2, 1, 1)$ . Besides, their self-confinement results in a tensor representation  $(1, 1, 2^2, 1, 1, 1)$  and a tensor representation  $(1, 1, 1, \bar{2}^2, 1, 1)$ , which can be

further decomposed into

$$\begin{aligned}
1 \times (1, 1, 2^2, 1, 1, 1) &\rightarrow 1 \times (1, 1, 3, 1, 1, 1) + 1 \times (1, 1, 1, 1, 1, 1), \\
1 \times (1, 1, 1, \bar{2}^2, 1, 1) &\rightarrow 1 \times (1, 1, 1, \bar{3}, 1, 1) + 1 \times (1, 1, 1, \bar{1}, 1, 1),
\end{aligned} \tag{4.4}$$

leading to chiral multiplets  $(1, 1, 3, 1, 1, 1)$  and  $(1, 1, 1, \bar{3}, 1, 1)$ .

Secondly, the chiral spectrum of Model 2 is shown in Table 11, where a bifundamental Higgs doublet arises from the  $\mathcal{N} = 2$  subsector of the intersection of the  $c$ -stack and the  $\mathbb{Z}_2$  image of the  $d$ -stack of D6-branes. Besides, there are two  $USp$  groups with negative  $\beta$  functions from Table 4, where two confining groups could lead to a stable minimum and dynamical supersymmetry breaking.

**Table 11.** The chiral spectrum in the open string sector of Model 2

| Model 2   | $SU(4) \times SU(2)_L \times SU(2)_{R1} \times SU(2)_{R2} \times USp(2)^2$ | $Q_4$ | $Q_{2L}$ | $Q_{2R1}$ | $Q_{2R2}$ | $Q_{em}$                           | $B - L$           | Field                |
|---|--|-------|----------|-----------|-----------|------------------------------------|-------------------|----------------------|
| $ab$  | $1 \times (4, \bar{2}, 1, 1, 1, 1)$  | 1     | -1       | 0         | 0         | $-\frac{1}{3}, \frac{2}{3}, -1, 0$ | $\frac{1}{3}, -1$ | $Q_L, L_L$           |
| $ab'$   | $2 \times (4, 2, 1, 1, 1, 1)$  | 1     | 1        | 0         | 0         | $-\frac{1}{3}, \frac{2}{3}, -1, 0$ | $\frac{1}{3}, -1$ | $Q_L, L_L$           |
| $ac$  | $1 \times (\bar{4}, 1, 2, 1, 1, 1)$  | -1    | 0        | 1         | 0         | $\frac{1}{3}, -\frac{2}{3}, 1, 0$  | $-\frac{1}{3}, 1$ | $Q_R, L_R$           |
| $ad'$   | $2 \times (\bar{4}, 1, 1, \bar{2}, 1, 1)$                                  | -1    | 0        | 0         | -1        | $\frac{1}{3}, -\frac{2}{3}, 1, 0$  | $-\frac{1}{3}, 1$ | $Q_R, L_R$           |
| $bc'$   | $2 \times (1, \bar{2}, \bar{2}, 1, 1, 1)$                                  | 0     | -1       | -1        | 0         | 0, $\mp 1$                         | 0                 | $H$                  |
| $bd$  | $3 \times (1, \bar{2}, 1, 2, 1, 1)$  | 0     | -1       | 0         | 1         | 0, $\mp 1$                         | 0                 | $H$                  |
| $bd'$   | $6 \times (1, \bar{2}, 1, \bar{2}, 1, 1)$                                  | 0     | -1       | 0         | -1        | 0, $\mp 1$                         | 0                 | $H'$                 |
| $cd$  | $1 \times (1, 1, \bar{2}, 2, 1, 1)$  | 0     | 0        | -1        | 1         | 0, $\mp 1$                         | 0                 | $\Phi$               |
| $b2$  | $1 \times (1, 2, 1, 1, \bar{2}, 1)$  | 0     | 1        | 0         | 0         | $\pm \frac{1}{2}$                  | 0                 |                      |
| $c4$  | $1 \times (1, 1, 2, 1, 1, \bar{2})$  | 0     | 0        | 1         | 0         | $\pm \frac{1}{2}$                  | 0                 |                      |
| $d2$  | $1 \times (1, 1, 1, 2, \bar{2}, 1)$  | 0     | 0        | 0         | 1         | $\pm \frac{1}{2}$                  | 0                 |                      |
| $d4$  | $3 \times (1, 1, 1, \bar{2}, 1, 2)$  | 0     | 0        | 0         | -1        | $\mp \frac{1}{2}$                  | 0                 |                      |
| $b \begin{array}{ c } \hline \square \\ \hline \end{array}$                   | $2 \times (1, 3, 1, 1, 1, 1)$  | 0     | 2        | 0         | 0         | 0, $\pm 1$                         | 0                 |                      |
| $b \begin{array}{ c } \hline \square \\ \hline \square \\ \hline \end{array}$ | $2 \times (1, \bar{1}, 1, 1, 1, 1)$  | 0     | -2       | 0         | 0         | 0                                  | 0                 |                      |
| $d \begin{array}{ c } \hline \square \\ \hline \end{array}$                   | $2 \times (1, 1, 1, 3, 1, 1)$  | 0     | 0        | 0         | 2         | 0, $\pm 1$                         | 0                 |                      |
| $d \begin{array}{ c } \hline \square \\ \hline \square \\ \hline \end{array}$ | $2 \times (1, 1, 1, \bar{1}, 1, 1)$  | 0     | 0        | 0         | -2        | 0                                  | 0                 |                      |
| $cd'$   | $1 \times (1, 1, 2, 2, 1, 1)$  | 0     | 0        | 1         | 1         | 0, $\pm 1$                         | 0                 | $\Phi_u^i, \Phi_d^i$ |
|   | $1 \times (1, 1, \bar{2}, \bar{2}, 1, 1)$                                  | 0     | 0        | -1        | -1        |                                    |                   |                      |

**Table 12.** The composite particle spectrum for Model 2

| Model 2         |              | $U(4) \times U(2)_L \times U(2)_{R1} \times U(2)_{R2} \times USp(2)^2$ |  |
|-----------------|--------------|--|--|
| Confining Force | Intersection | Exotic particle Spectrum   | Confined Particle Spectrum   |
| $USp(2)_2$      | b2           | $1 \times (1, 2, 1, 1, \bar{2}, 1)$                                    | $1 \times (1, 2^2, 1, 1, 1, 1), 1 \times (1, 2, 1, 2, 1, 1),$<br>$1 \times (1, 1, 1, 2^2, 1, 1)$             |
|                 | d2           | $1 \times (1, 1, 1, 2, \bar{2}, 1)$                                    |  |
| $USp(2)_4$      | c4           | $1 \times (1, 1, 2, 1, 1, \bar{2})$                                    | $1 \times (1, 1, 2^2, 1, 1, 1), 3 \times (1, 1, 2, \bar{2}, 1, 1),$<br>$6 \times (1, 1, 1, \bar{2}^2, 1, 1)$ |
|                 | d4           | $3 \times (1, 1, 1, \bar{2}, 1, 2)$                                    |  |

The composite particle spectrum for Model 2 is given in Table 12. The  $USp(2)_2$  group has two charged intersections, which give rise to an exotic particle  $(1, 2, 1, 1, \bar{2}, 1)$

and an exotic particle  $(1, 1, 1, 2, \bar{2}, 1)$ . The mixing of these two types of exotic particles yields a chiral multiplet  $(1, 2, 1, 2, 1, 1)$ . Besides, their self-confinement results in tensor representations  $(1, 2^2, 1, 1, 1, 1)$  and tensor representations  $(1, 1, 1, 2^2, 1, 1)$ , which can be further decomposed

$$\begin{aligned} 1 \times (1, 2^2, 1, 1, 1, 1) &\rightarrow 1 \times (1, 3, 1, 1, 1, 1) + 1 \times (1, 1, 1, 1, 1, 1) , \\ 1 \times (1, 1, 1, 2^2, 1, 1) &\rightarrow 1 \times (1, 1, 1, 3, 1, 1) + 1 \times (1, 1, 1, 1, 1, 1) , \end{aligned} \quad (4.5)$$

leading to chiral multiplets  $(1, 3, 1, 1, 1, 1)$  and  $(1, 1, 1, 3, 1, 1)$ . Meanwhile, the  $USp(2)_4$  group also has two charged intersections, which give rise to one exotic particle  $(1, 1, 2, 1, 1, \bar{2})$  and three exotic particles  $(1, 1, 1, \bar{2}, 1, 2)$ . The mixing of these two types of exotic particles yields 3 chiral multiplets  $(1, 1, 2, \bar{2}, 1, 1)$ . Besides, their self-confinement results in a tensor representation  $(1, 1, 2^2, 1, 1, 1)$  and 6 tensor representation  $(1, 1, 1, \bar{2}^2, 1, 1)$ , which can be further decomposed,

$$\begin{aligned} 1 \times (1, 1, 2^2, 1, 1, 1) &\rightarrow 1 \times (1, 1, 3, 1, 1, 1) + 1 \times (1, 1, 1, 1, 1, 1) , \\ 6 \times (1, 1, 1, \bar{2}^2, 1, 1) &\rightarrow 6 \times (1, 1, 1, \bar{3}, 1, 1) + 6 \times (1, 1, 1, \bar{1}, 1, 1) , \end{aligned} \quad (4.6)$$

leading to chiral multiplets  $(1, 1, 3, 1, 1, 1)$  and  $(1, 1, 1, \bar{3}, 1, 1)$ .

**Table 13.** The chiral spectrum in the open string sector of Model 3

| Model 3  | $SU(4) \times SU(2)_L \times SU(2)_{R1} \times SU(2)_{R2}$ | $Q_4$ | $Q_{2L}$ | $Q_{2R_1}$ | $Q_{2R_2}$ | $Q_{em}$                           | $B-L$             | Field                |
|--|--|-------|----------|------------|------------|------------------------------------|-------------------|----------------------|
| $ab$   | $2 \times (4, \bar{2}, 1, 1)$                              | 1     | -1       | 0          | 0          | $-\frac{1}{3}, \frac{2}{3}, -1, 0$ | $\frac{1}{3}, -1$ | $Q_L, L_L$           |
| $ab'$  | $1 \times (4, 2, 1, 1)$                                    | 1     | 1        | 0          | 0          | $-\frac{1}{3}, \frac{2}{3}, -1, 0$ | $\frac{1}{3}, -1$ | $Q_L, L_L$           |
| $ac$   | $1 \times (\bar{4}, 1, 2, 1)$                              | -1    | 0        | 1          | 0          | $\frac{1}{3}, -\frac{2}{3}, 1, 0$  | $-\frac{1}{3}, 1$ | $Q_R, L_R$           |
| $ad$   | $2 \times (\bar{4}, 1, 1, 2)$                              | -1    | 0        | 0          | 1          | $\frac{1}{3}, -\frac{2}{3}, 1, 0$  | $-\frac{1}{3}, 1$ | $Q_R, L_R$           |
| $bc$   | $4 \times (1, 2, \bar{2}, 1)$                              | 0     | 1        | -1         | 0          | $0, \pm 1$                         | 0                 | $H$                  |
| $bd$   | $6 \times (1, 2, 1, \bar{2})$                              | 0     | 1        | 0          | -1         | $0, \pm 1$                         | 0                 | $H$                  |
| $bd'$  | $12 \times (1, 2, 1, 2)$                                   | 0     | 1        | 0          | 1          | $0, \mp 1$                         | 0                 | $H'$                 |
| $cd'$  | $2 \times (1, 1, \bar{2}, \bar{2})$                        | 0     | 0        | -1         | -1         | $0, \mp 1$                         | 0                 | $\Phi$               |
| $b$<br> | $5 \times (1, \bar{3}, 1, 1)$                              | 0     | -2       | 0          | 0          | $0, \mp 1$                         | 0                 |                      |
| $b$<br> | $5 \times (1, 1, 1, 1)$                                    | 0     | 2        | 0          | 0          | 0                                  | 0                 |                      |
| $c$<br> | $1 \times (1, 1, 3, 1)$                                    | 0     | 0        | 2          | 0          | $0, \pm 1$                         | 0                 |                      |
| $c$<br> | $1 \times (1, 1, \bar{1}, 1)$                              | 0     | 0        | -2         | 0          | 0                                  | 0                 |                      |
| $d$<br> | $2 \times (1, 1, 1, \bar{3})$                              | 0     | 0        | 0          | -2         | $0, \mp 1$                         | 0                 |                      |
| $d$<br> | $2 \times (1, 1, 1, 1)$                                    | 0     | 0        | 0          | 2          | 0                                  | 0                 |                      |
| $cd$   | $2 \times (1, 1, 2, \bar{2})$                              | 0     | 0        | 1          | -1         | $0, \pm 1$                         | 0                 | $\Phi_u^i, \Phi_d^i$ |
|  | $2 \times (1, 1, \bar{2}, 2)$                              | 0     | 0        | -1         | 1          |                                    |                   |                      |

Third, the chiral spectrum of Models 3 and 4 is shown in Table 13 and 14, respectively. Different with the standard Pati-Salam models found in [50], there is no  $USp$  group in Models 3 and 4. In Model 3, there are 2 bifundamental Higgs doublets arising from the  $\mathcal{N} = 2$  subsector of the intersection of the  $c$ - and  $d$ -stacks of the D6-branes. In Model 4,

there are 8 Higgs doublets arising from the  $\mathcal{N} = 2$  subsector of the intersection of the  $b$ - and  $c$ -stacks of the D6-branes.

**Table 14.** The chiral spectrum in the open string sector of Model 4

| Model 4   | $SU(4) \times SU(2)_L \times SU(2)_{R1} \times SU(2)_{R2}$ | $Q_4$ | $Q_{2L}$ | $Q_{2R_1}$ | $Q_{2R_2}$ | $Q_{em}$                           | $B - L$           | Field          |
|---|--|-------|----------|------------|------------|------------------------------------|-------------------|----------------|
| $ab$  | $3 \times (4, \bar{2}, 1, 1)$                              | 1     | -1       | 0          | 0          | $-\frac{1}{3}, \frac{2}{3}, -1, 0$ | $\frac{1}{3}, -1$ | $Q_L, L_L$     |
| $ac$  | $1 \times (\bar{4}, 1, 2, 1)$                              | -1    | 0        | 1          | 0          | $\frac{1}{3}, -\frac{2}{3}, 1, 0$  | $-\frac{1}{3}, 1$ | $Q_R, L_R$     |
| $ad'$   | $2 \times (\bar{4}, 1, 1, \bar{2})$                        | -1    | 0        | 0          | -1         | $\frac{1}{3}, -\frac{2}{3}, 1, 0$  | $-\frac{1}{3}, 1$ | $Q_R, L_R$     |
| $bc'$   | $4 \times (1, \bar{2}, \bar{2}, 1)$                        | 0     | -1       | -1         | 0          | $0, \pm 1$                         | 0                 | $H'$           |
| $bd$  | $2 \times (1, 2, 1, \bar{2})$                              | 0     | 1        | 0          | -1         | $0, \pm 1$                         | 0                 | $H'$           |
| $bd'$   | $4 \times (1, 2, 1, 2)$                                    | 0     | 1        | 0          | 1          | $0, \mp 1$                         | 0                 | $H$            |
| $cd$  | $2 \times (1, 1, 2, \bar{2})$                              | 0     | 0        | 1          | -1         | $0, \pm 1$                         | 0                 | $\Phi$         |
| $cd'$   | $4 \times (1, 1, \bar{2}, \bar{2})$                        | 0     | 0        | -1         | -1         | $0, \mp 1$                         | 0                 | $\Phi$         |
| $b \begin{array}{ c } \hline \square \\ \hline \end{array}$                   | $1 \times (1, 3, 1, 1)$                                    | 0     | 2        | 0          | 0          | $0, \pm 1$                         | 0                 |                |
| $b \begin{array}{ c } \hline \square \\ \hline \square \\ \hline \end{array}$ | $1 \times (1, \bar{1}, 1, 1)$                              | 0     | -2       | 0          | 0          | 0                                  | 0                 |                |
| $c \begin{array}{ c } \hline \square \\ \hline \end{array}$                   | $1 \times (1, 1, 3, 1)$                                    | 0     | 0        | 2          | 0          | $0, \pm 1$                         | 0                 |                |
| $c \begin{array}{ c } \hline \square \\ \hline \square \\ \hline \end{array}$ | $1 \times (1, 1, \bar{1}, 1)$                              | 0     | 0        | -2         | 0          | 0                                  | 0                 |                |
| $d \begin{array}{ c } \hline \square \\ \hline \end{array}$                   | $2 \times (1, 1, 1, 3)$                                    | 0     | 0        | 0          | 2          | $0, \pm 1$                         | 0                 |                |
| $d \begin{array}{ c } \hline \square \\ \hline \square \\ \hline \end{array}$ | $2 \times (1, 1, \bar{1}, 1)$                              | 0     | 0        | 0          | -2         | 0                                  | 0                 |                |
| $bc$  | $8 \times (1, 2, \bar{2}, 1)$                              | 0     | 1        | -1         | 0          | $0, \pm 1$                         | 0                 | $H_u^i, H_d^i$ |
|   | $8 \times (1, \bar{2}, 2, 1)$                              | 0     | -1       | 1          | 0          |                                    |                   |                |

These four classes of extended Pati-Salam models are constructed with two confining groups (see Model 1 and 2) and without confining group (see Model 3 and 4). The supersymmetry breaking can be realized via gaugino condensation when there are four confining gauge groups in the hidden sector, which means all  $\beta$  functions are negative. However, as discussed in [57–59], there should be at least two confining  $USp$  groups with negative  $\beta$  functions for gaugino condensation in order to stabilize the complex structure moduli. For this reason, among these four classes of models, models in the same class of Model 2 with two negative  $\beta$  functions are the most likely to break the supersymmetry via gaugino condensation <sup>1</sup>.

Recall that Model 4 and Model 10 in [50] share the same gauge coupling ratio  $g_a^2 : g_b^2 : g_R^2 : (\frac{5}{3}g_Y^2)$  with different  $g_a$  value and  $\gamma$  in (3.23). It is obvious that with an extra  $d$ -stack of D6-branes, the number of filler branes turns to be “replaced” by the additional stack of branes that carry  $SU(2)$  gauge symmetry. From the spectra shown in Table 14 and 15, it is obvious that with an extra  $d$ -stack of brane introduced, the Higgs multiplets have two sources:  $bd'$ -brane and  $bc$ -brane intersections. although without extra  $d$ -stack of branes there is only one source for Higgs doublets to appear from  $bc'$ -brane intersection.

The chiral spectrum of Model 10 from [50] is shown in Table 15. This spectrum is quite different from the chiral spectrum of Model 4 with  $d$ -stack of  $SU(2)$  gauge, although they

<sup>1</sup>Note that only when the moduli stabilization is achieved at the stable extremum supersymmetry breaking appears, while at the saddle points, such supersymmetry breaking cannot be staggered that alternative mechanism need to be searched for.

**Table 15.** The chiral spectrum in the open string sector of Model 10 from [50]

| Model 10 [50]     | $SU(4) \times SU(2)_L \times SU(2)_R \times USp(2)^3$ | $Q_4$ | $Q_{2L}$ | $Q_{2R}$ | $Q_{em}$                           | $B - L$           | Field          |
|-------------------|---|-------|----------|----------|------------------------------------|-------------------|----------------|
| $ab$              | $3 \times (4, \bar{2}, 1, 1, 1, 1)$                   | 1     | -1       | 0        | $-\frac{1}{3}, \frac{2}{3}, -1, 0$ | $\frac{1}{3}, -1$ | $Q_L, L_L$     |
| $ac'$             | $3 \times (\bar{4}, 1, \bar{2}, 1, 1, 1)$             | -1    | 0        | -1       | $\frac{1}{3}, -\frac{2}{3}, 1, 0$  | $-\frac{1}{3}, 1$ | $Q_R, L_R$     |
| $bc$              | $3 \times (1, 2, \bar{2}, 1, 1, 1)$                   | 0     | 1        | -1       | $0, \pm 1$                         | 0                 | $H'$           |
| $a2$              | $1 \times (4, 1, 1, 1, \bar{2}, 1)$                   | 1     | 0        | 0        | $\frac{1}{6}, -\frac{1}{2}$        | $\frac{1}{3}, -1$ |                |
| $a4$              | $1 \times (\bar{4}, 1, 1, 1, 1, 2)$                   | -1    | 0        | 0        | $-\frac{1}{6}, \frac{1}{2}$        | $-\frac{1}{3}, 1$ |                |
| $b3$              | $3 \times (1, \bar{2}, 1, 1, 2, 1)$                   | 0     | -1       | 0        | $\mp \frac{1}{2}$                  | 0                 |                |
| $b4$              | $2 \times (1, 2, 1, 1, 1, \bar{2})$                   | 0     | 1        | 0        | $\pm \frac{1}{2}$                  | 0                 |                |
| $c2$              | $1 \times (1, 1, 2, \bar{2}, 1, 1)$                   | 0     | 0        | 1        | $\pm \frac{1}{2}$                  | 0                 |                |
| $b \square$       | $1 \times (1, 3, 1, 1, 1, 1)$                         | 0     | 2        | 0        | $0, \pm 1$                         | 0                 |                |
| $\bar{b} \square$ | $1 \times (1, \bar{1}, 1, 1, 1, 1)$                   | 0     | -2       | 0        | 0                                  | 0                 |                |
| $c \square$       | $2 \times (1, 1, 3, 1, 1, 1)$                         | 0     | 0        | 2        | $0, \pm 1$                         | 0                 |                |
| $\bar{c} \square$ | $2 \times (1, 1, \bar{1}, 1, 1, 1)$                   | 0     | 0        | -2       | 0                                  | 0                 |                |
| $bc'$             | $9 \times (1, 2, 2, 1, 1, 1)$                         | 0     | 1        | 1        | $0, \pm 1$                         | 0                 | $H_u^2, H_d^2$ |
|                   | $9 \times (1, \bar{2}, \bar{2}, 1, 1, 1)$             | 0     | -1       | -1       |                                    |                   |                |

have the same gauge coupling ration. In Model 10 from [50], there are 9 Higgs doublets arising from the  $\mathcal{N} = 2$  subsector of the intersection of the  $b$ -stack and the  $\mathbb{Z}_2$  image of  $c$ -stack of D6-branes only, while with  $d$ -stack, Model 4 has 8 Higgs multiplets from  $bc$ -brane intersections, and 4 Higgs multiplets from  $bd'$ -brane intersections. Besides, there are three  $USp$  groups in Model 10 from [50], yielding charged exotic particles by intersecting with branes in the visible sector, while there is no  $USp$  group in Model 4 with  $d$ -stack of  $SU(2)$  gauge branes.

From the perspective that they share the same gauge coupling ratio (and therefore behave similarly in the RGE rolling), it indicates that by introducing an extra stack of D6-branes carrying  $SU(2)$  gauge will provide more possibilities/origins for Higgs particles.

#### 4.2 $SU(2)_L$ gauge from extra symmetry breaking

Analogously to the configuration with an extra  $d$ -stack of D6-branes introduced to the right-handed  $SU(2)_R$ , we can also introduce the extra  $d$ -stack of D6-branes to the left-handed  $SU(2)_L$  symmetry, with  $SU(2)_{L_1} \times SU(2)_{L_2} \rightarrow SU(2)_L$ . Hence, the  $SU(2)_L$  gauge coupling  $g_L^{-2}$  can be expressed in terms of  $g_b^{-2}$  and  $g_d^{-2}$  as

$$g_L^{-2} = g_b^{-2} + g_d^{-2} = |\text{Re}(f_b)| + |\text{Re}(f_d)|. \quad (4.7)$$

The gauge kinetic function related to  $SU(2)_L$  is then written in

$$f_L = f_b + f_d, \quad (4.8)$$

while the kinetic function of  $U(1)_Y$  gauge symmetry remains the same as that in [50], simply

$$f_Y = \frac{3}{5} \left( \frac{2}{3} f_a + f_c \right). \quad (4.9)$$

The corresponding gauge coupling relations are read as follows

$$g_a^2 = \alpha g_L^2 = \beta \frac{5}{3} g_Y^2 = \gamma [\pi e^{\phi_4}], \quad (4.10)$$

with  $g_L$  replacing  $g_b$  as the new weak gauge coupling.

The three-family of chiral fermions is then obtained through (3.1) as

$$I_{ab} + I_{ab'} + I_{ad} + I_{ad'} = 3, \quad I_{ac} + I_{ac'} = -3. \quad (4.11)$$

In this construction, we constructed four classes of independent models with representative Models 7-10 shown in Table 16-19. Especially in Models 9 and 10, the tadpole cancellation condition is satisfied without a filler brane as in Models 3 and 4.

In Model 10, the ratio of gauge couplings  $g_a^2 : g_b^2 : g_R^2 : (\frac{5}{3} g_Y^2)$  is the same as that of Model 18 in the previous complete search for supersymmetric three-family Pati-Salam models with only  $a$ -,  $b$ - and  $c$ -stacks [50]. The difference in gauge couplings is that with extra  $d$ -stack of  $SU(2)_L$  we have  $g_a^2 = 4 \times 3^{1/4} \pi e^{\phi_4}$  while in [50]  $g_a^2 = \frac{16 \times 2^{1/4}}{3\sqrt{3}} \pi e^{\phi_4}$ . Again, these two different values of  $\gamma$  in (4.10) are supposed to be related by the scaling of dilaton.

Moreover, the gauge coupling relations of Models 1 and 7, Models 2 and 8, Model 3 and 9, and Models 4 and 10, respectively, share the same values of  $\gamma$  from (3.23) and (4.10), which shows a left-right symmetry in Pati-Salam models.

**Table 16.** D6-brane configurations and intersection numbers of Model 7, and its MSSM gauge coupling relation is  $g_a^2 = \frac{1}{2} g_L^2 = g_c^2 = (\frac{5}{3} g_Y^2) = 2\sqrt{2} 3^{1/4} \pi e^{\phi_4}$ , for which the first torus is tilted.

| Model 7 |     | $U(4) \times U(2)_{L_1} \times U(2)_R \times U(2)_{L_2} \times USp(2)^2$ |  |               |     |      |     |      |     |      |   |    |
|---------|-----|--|--|---------------|-----|------|-----|------|-----|------|---|----|
| stack   | $N$ | $(n^1, l^1) \times (n^2, l^2) \times (n^3, l^3)$                         | $n_{\square\square}$   | $n_{\square}$ | $b$ | $b'$ | $c$ | $c'$ | $d$ | $d'$ | 2 | 4  |
| $a$     | 8   | $(1, -1) \times (0, -1) \times (-1, 1)$                                  | 0  | 0             | 1   | 0    | -3  | 0    | 0   | 2    | 0 | 0  |
| $b$     | 4   | $(-1, -1) \times (-1, -1) \times (0, -1)$                                | 0  | 0             | -   | -    | 0   | 2    | -1  | 2    | 0 | -1 |
| $c$     | 4   | $(-1, -1) \times (-3, 1) \times (1, 0)$                                  | -2   | 2             | -   | -    | -   | -    | -1  | -2   | 3 | 0  |
| $d$     | 4   | $(1, 3) \times (1, 0) \times (1, -1)$                                    | -2   | 2             | -   | -    | -   | -    | -   | -    | 3 | -1 |
| 2       | 2   | $(2, 0) \times (0, -1) \times (0, 1)$                                    | $x_A = 3x_B = x_C = x_D$<br>$\beta_2^g = 0, \quad \beta_4^g = -4$<br>$\chi_1 = \frac{2}{\sqrt{3}}, \chi_2 = \sqrt{3}, \chi_3 = \sqrt{3}$ |               |     |      |     |      |     |      |   |    |
| 4       | 2   | $(0, -2) \times (0, 1) \times (1, 0)$                                    |  |               |     |      |     |      |     |      |   |    |

#### 4.2.1 Phenomenological studies

The particle spectra of Models 7-10, are shown in Table 20, 22, 24, and 25 respectively. From the spectrum of Model 7, 4 Higgs doublets arise from the  $\mathcal{N} = 2$  subsector of the intersection of  $b$ - and  $c$ -stacks of D6-branes. Besides, there is one  $USp$  group with negative  $\beta$  function and one  $USp(2)$  group with  $\beta$  function to be zero from Table 16. This  $\beta$  with zero value might result in difficulty in dynamical supersymmetry breaking.

**Table 17.** D6-brane configurations and intersection numbers of Model 8, and its MSSM gauge coupling relation is  $g_a^2 = \frac{3}{4}g_L^2 = 3g_c^2 = \frac{5}{3}(\frac{5}{3}g_Y^2) = 2\sqrt{2} 3^{3/4} \pi e^{\phi_4}$ , for which the first torus is tilted.

| Model 8 |     | $U(4) \times U(2)_{L_1} \times U(2)_R \times U(2)_{L_2} \times USp(2)^2$ |  |               |     |      |     |      |     |      |    |    |
|---------|-----|--|--|---------------|-----|------|-----|------|-----|------|----|----|
| stack   | $N$ | $(n^1, l^1) \times (n^2, l^2) \times (n^3, l^3)$                         | $n_{\square\square}$   | $n_{\square}$ | $b$ | $b'$ | $c$ | $c'$ | $d$ | $d'$ | 2  | 4  |
| $a$     | 8   | $(1, -1) \times (0, -1) \times (-1, 1)$                                  | 0  | 0             | 1   | 0    | -1  | -2   | 2   | 0    | 0  | 0  |
| $b$     | 4   | $(-1, -1) \times (-1, -1) \times (0, -1)$                                | 0  | 0             | -   | -    | 0   | 2    | 0   | 1    | 0  | -1 |
| $c$     | 4   | $(-3, 1) \times (-1, -1) \times (1, 0)$                                  | -2   | 2             | -   | -    | -   | -    | 6   | 3    | -1 | 0  |
| $d$     | 4   | $(1, 1) \times (1, 0) \times (1, -3)$                                    | 2  | -2            | -   | -    | -   | -    | -   | -    | 1  | -3 |
| 2       | 2   | $(2, 0) \times (0, -1) \times (0, 1)$                                    | $x_A = \frac{1}{3}x_B = x_C = x_D$<br>$\beta_2^g = -4, \beta_4^g = -2$<br>$\chi_1 = 2\sqrt{3}, \chi_2 = \frac{1}{\sqrt{3}}, \chi_3 = \frac{1}{\sqrt{3}}$ |               |     |      |     |      |     |      |    |    |
| 4       | 2   | $(0, -2) \times (0, 1) \times (1, 0)$                                    |  |               |     |      |     |      |     |      |    |    |

**Table 18.** D6-brane configurations and intersection numbers of Model 9, and its MSSM gauge coupling relation is  $g_a^2 = \frac{3}{2}g_L^2 = 6g_c^2 = 2(\frac{5}{3}g_Y^2) = 4 \times 3^{3/4} \pi e^{\phi_4}$ , for which the first torus is tilted.

| Model 9 |     | $U(4) \times U(2)_{L_1} \times U(2)_R \times U(2)_{L_2}$ |  |               |     |      |     |      |     |      |  |  |
|---------|-----|--|--|---------------|-----|------|-----|------|-----|------|--|--|
| stack   | $N$ | $(n^1, l^1) \times (n^2, l^2) \times (n^3, l^3)$         | $n_{\square\square}$   | $n_{\square}$ | $b$ | $b'$ | $c$ | $c'$ | $d$ | $d'$ |  |  |
| $a$     | 8   | $(1, -1) \times (0, -1) \times (-1, 1)$                  | 0  | 0             | 1   | 0    | -2  | -1   | 2   | 0    |  |  |
| $b$     | 4   | $(-1, -1) \times (-1, -2) \times (0, -1)$                | -1   | 1             | -   | -    | 4   | 0    | 0   | 2    |  |  |
| $c$     | 4   | $(-3, -1) \times (-1, 2) \times (1, 0)$                  | 5  | -5            | -   | -    | -   | -    | -6  | -12  |  |  |
| $d$     | 4   | $(1, 1) \times (1, 0) \times (1, -3)$                    | 2  | -2            | -   | -    | -   | -    | -   | -    |  |  |
|         |     |  | $x_A = \frac{1}{6}x_B = x_C = \frac{1}{2}x_D$<br>$\chi_1 = 2\sqrt{3}, \chi_2 = \frac{1}{2\sqrt{3}}, \chi_3 = \frac{1}{\sqrt{3}}$ |               |     |      |     |      |     |      |  |  |

**Table 19.** D6-brane configurations and intersection numbers of Model 10, and its MSSM gauge coupling relation is  $g_a^2 = g_L^2 = 2g_c^2 = \frac{10}{7}(\frac{5}{3}g_Y^2) = 4 \times 3^{1/4} \pi e^{\phi_4}$ , for which the first torus is tilted.

| Model 10 |     | $U(4) \times U(2)_{L_1} \times U(2)_R \times U(2)_{L_2}$ |  |               |     |      |     |      |     |      |  |  |
|----------|-----|--|--|---------------|-----|------|-----|------|-----|------|--|--|
| stack    | $N$ | $(n^1, l^1) \times (n^2, l^2) \times (n^3, l^3)$         | $n_{\square\square}$   | $n_{\square}$ | $b$ | $b'$ | $c$ | $c'$ | $d$ | $d'$ |  |  |
| $a$      | 8   | $(1, -1) \times (0, -1) \times (-1, 1)$                  | 0  | 0             | 1   | 0    | -3  | 0    | 0   | 2    |  |  |
| $b$      | 4   | $(-1, -1) \times (-1, -2) \times (0, -1)$                | -1   | 1             | -   | -    | 0   | 4    | -2  | 4    |  |  |
| $c$      | 4   | $(-1, -1) \times (-3, 2) \times (1, 0)$                  | -1   | 1             | -   | -    | -   | -    | -2  | -4   |  |  |
| $d$      | 4   | $(1, 3) \times (1, 0) \times (1, -1)$                    | -2   | 2             | -   | -    | -   | -    | -   | -    |  |  |
|          |     |  | $x_A = \frac{3}{2}x_B = x_C = \frac{1}{2}x_D$<br>$\chi_1 = \frac{2}{\sqrt{3}}, \chi_2 = \frac{\sqrt{3}}{2}, \chi_3 = \sqrt{3}$ |               |     |      |     |      |     |      |  |  |

The composite particle spectrum for Model 7 is given in Table 21. The  $USp(2)_2$  group has two charged intersections, which give rise to three exotic particles with quantum number  $(1, 1, 2, 1, \bar{2}, 1)$  and three exotic particles with quantum number  $(1, 1, 1, 2, \bar{2}, 1)$ . The mixing of these two kinds of exotic particles yields 9 chiral multiplets  $(1, 1, 2, 2, 1, 1)$ . Their self-confinement results in 6 tensor representations  $(1, 2^2, 1, 1, 1, 1)$  and 6 tensor representations

**Table 20.** The chiral spectrum in the open string sector of Model 7

| Model 7  | $SU(4) \times SU(2)_{L1} \times SU(2)_R$<br>$\times SU(2)_{L2} \times USp(2)^2$ | $Q_4$ | $Q_{2L1}$ | $Q_{2R}$ | $Q_{2L2}$ | $Q_{em}$                           | $B - L$           | Field          |
|--|---|-------|-----------|----------|-----------|------------------------------------|-------------------|----------------|
| $ab$   | $1 \times (4, \bar{2}, 1, 1, 1, 1)$   | 1     | -1        | 0        | 0         | $-\frac{1}{3}, \frac{2}{3}, -1, 0$ | $\frac{1}{3}, -1$ | $Q_L, L_L$     |
| $ac$   | $3 \times (\bar{4}, 1, 2, 1, 1, 1)$   | -1    | 0         | 1        | 0         | $\frac{1}{3}, -\frac{2}{3}, 1, 0$  | $-\frac{1}{3}, 1$ | $Q_R, L_R$     |
| $ad'$  | $2 \times (4, 1, 1, 2, 1, 1)$   | 1     | 0         | 0        | 1         | $-\frac{1}{3}, \frac{2}{3}, -1, 0$ | $\frac{1}{3}, -1$ | $Q_L, L_L$     |
| $bc'$  | $2 \times (1, 2, 2, 1, 1, 1)$   | 0     | 1         | 1        | 0         | $0, \pm 1$                         | 0                 | $H'$           |
| $bd$   | $1 \times (1, \bar{2}, 1, 2, 1, 1)$   | 0     | -1        | 0        | 1         | $0, \mp 1$                         | 0                 | $\Phi$         |
| $bd'$  | $2 \times (1, 2, 1, 2, 1, 1)$   | 0     | 1         | 0        | 1         | $0, \pm 1$                         | 0                 | $\Phi$         |
| $cd$   | $1 \times (1, 1, \bar{2}, 2, 1, 1)$   | 0     | 0         | -1       | 1         | $0, \mp 1$                         | 0                 | $H'$           |
| $cd'$  | $2 \times (1, 1, \bar{2}, \bar{2}, 1, 1)$                                       | 0     | 0         | -1       | -1        | $0, \mp 1$                         | 0                 | $H$            |
| $b4$   | $1 \times (1, \bar{2}, 1, 1, 1, 2)$   | 0     | -1        | 0        | 0         | $\mp \frac{1}{2}$                  | 0                 |                |
| $c2$   | $3 \times (1, 1, 2, 1, \bar{2}, 1)$   | 0     | 0         | 1        | 0         | $\pm \frac{1}{2}$                  | 0                 |                |
| $d2$   | $3 \times (1, 1, 1, 2, \bar{2}, 1)$   | 0     | 0         | 0        | 1         | $\pm \frac{1}{2}$                  | 0                 |                |
| $d4$   | $1 \times (1, 1, 1, \bar{2}, 1, 2)$   | 0     | 0         | 0        | -1        | $\mp \frac{1}{2}$                  | 0                 |                |
| $c$<br> | $2 \times (1, 1, \bar{3}, 1, 1, 1)$   | 0     | 0         | -2       | 0         | $0, \mp 1$                         | 0                 |                |
| $c$<br> | $2 \times (1, 1, 1, 1, 1, 1)$   | 0     | 0         | 2        | 0         | 0                                  | 0                 |                |
| $d$<br> | $2 \times (1, 1, 1, \bar{3}, 1, 1)$   | 0     | 0         | 0        | -2        | $0, \mp 1$                         | 0                 |                |
| $d$<br> | $2 \times (1, 1, 1, 1, 1, 1)$   | 0     | 0         | 0        | 2         | 0                                  | 0                 |                |
| $bc$   | $4 \times (1, 2, \bar{2}, 1, 1, 1)$   | 0     | 1         | -1       | 0         | $0, \pm 1$                         | 0                 | $H_u^i, H_d^i$ |
|  | $4 \times (1, \bar{2}, 2, 1, 1, 1)$   | 0     | -1        | 1        | 0         |                                    |                   |                |

**Table 21.** The composite particle spectrum for Model 7

| Model 7         |              | $U(4) \times U(2)_{L1} \times U(2)_R \times U(2)_{L2} \times USp(2)^2$ |   |
|-----------------|--------------|--|---|
| Confining Force | Intersection | Exotic particle Spectrum   | Confined Particle Spectrum  |
| $USp(2)_2$      | c2           | $3 \times (1, 1, 2, 1, \bar{2}, 1)$                                    | $6 \times (1, 1, 2^2, 1, 1, 1), 9 \times (1, 1, 2, 2, 1, 1),$                   |
|                 | d2           | $3 \times (1, 1, 1, 2, \bar{2}, 1)$                                    | $6 \times (1, 1, 1, 2^2, 1, 1)$   |
| $USp(2)_4$      | b4           | $1 \times (1, \bar{2}, 1, 1, 1, 2)$                                    | $1 \times (1, \bar{2}^2, 1, 1, 1, 1), 1 \times (1, \bar{2}, 1, \bar{2}, 1, 1),$ |
|                 | d4           | $1 \times (1, 1, 1, \bar{2}, 1, 2)$                                    | $1 \times (1, 1, 1, \bar{2}^2, 1, 1)$   |

$(1, 1, 1, 2^2, 1, 1)$ , which can be further decomposed into

$$\begin{aligned}
 6 \times (1, 1, 2^2, 1, 1, 1) &\rightarrow 6 \times (1, 1, 3, 1, 1, 1) + 6 \times (1, 1, 1, 1, 1, 1) , \\
 6 \times (1, 1, 1, 2^2, 1, 1) &\rightarrow 6 \times (1, 1, 1, 3, 1, 1) + 6 \times (1, 1, 1, 1, 1, 1) ,
 \end{aligned} \tag{4.12}$$

leading to chiral multiplets  $(1, 1, 3, 1, 1, 1)$  and  $(1, 1, 1, 3, 1, 1)$ . Meanwhile, the  $USp(2)_4$  group also has two charged intersections, which give rise to one exotic particle  $(1, \bar{2}, 1, 1, 1, 2)$  and one exotic particle  $(1, 1, 1, \bar{2}, 1, 2)$ . The mixing of these two kinds of exotic particles yields one chiral multiplet  $(1, \bar{2}, 1, \bar{2}, 1, 1)$ . Besides, their self-confinement results in a tensor representation  $(1, \bar{2}^2, 1, 1, 1, 1)$  and a tensor representation  $(1, 1, 1, \bar{2}^2, 1, 1)$ , which can be further decomposed

$$\begin{aligned}
 1 \times (1, \bar{2}^2, 1, 1, 1, 1) &\rightarrow 1 \times (1, \bar{3}, 1, 1, 1, 1) + 1 \times (1, \bar{1}, 1, 1, 1, 1) , \\
 1 \times (1, 1, 1, \bar{2}^2, 1, 1) &\rightarrow 1 \times (1, 1, 1, \bar{3}, 1, 1) + 1 \times (1, 1, 1, \bar{1}, 1, 1) ,
 \end{aligned} \tag{4.13}$$

leading to chiral multiplets  $(1, \bar{3}, 1, 1, 1, 1)$  and  $(1, 1, 1, \bar{3}, 1, 1)$ .

The chiral spectrum of Model 8 is shown in Table 22, where a bifundamental Higgs doublet arises from the  $\mathcal{N} = 2$  subsector of the intersection of  $b$ -stack and  $d$ -stack of D6-branes. Besides, there are two  $USp$  groups with negative  $\beta$  functions from Table 17. These two possible confining groups may lead to stable minimum and dynamical supersymmetry breaking.

**Table 22.** The chiral spectrum in the open string sector of Model 8

| Model 8  | $SU(4) \times SU(2)_{L1} \times SU(2)_R$<br>$\times SU(2)_{L2} \times USp(2)^2$ | $Q_4$ | $Q_{2L1}$ | $Q_{2R}$ | $Q_{2L2}$ | $Q_{em}$                           | $B - L$           | Field                |
|--|---|-------|-----------|----------|-----------|------------------------------------|-------------------|----------------------|
| $ab$   | $1 \times (4, \bar{2}, 1, 1, 1, 1)$   | 1     | -1        | 0        | 0         | $-\frac{1}{3}, \frac{2}{3}, -1, 0$ | $\frac{1}{3}, -1$ | $Q_L, L_L$           |
| $ac$   | $1 \times (4, 1, 2, 1, 1, 1)$   | -1    | 0         | 1        | 0         | $\frac{1}{3}, -\frac{2}{3}, 1, 0$  | $-\frac{1}{3}, 1$ | $Q_R, L_R$           |
| $ac'$  | $2 \times (4, 1, \bar{2}, 1, 1, 1)$   | -1    | 0         | -1       | 0         | $\frac{1}{3}, -\frac{2}{3}, 1, 0$  | $-\frac{1}{3}, 1$ | $Q_R, L_R$           |
| $ad$   | $2 \times (4, 1, 1, \bar{2}, 1, 1)$   | 1     | 0         | 0        | -1        | $-\frac{1}{3}, \frac{2}{3}, -1, 0$ | $\frac{1}{3}, -1$ | $Q_L, L_L$           |
| $bc'$  | $2 \times (1, 2, 2, 1, 1, 1)$   | 0     | 1         | 1        | 0         | $0, \pm 1$                         | 0                 | $H$                  |
| $bd'$  | $1 \times (1, 2, 1, 2, 1, 1)$   | 0     | 1         | 0        | 1         | $0, \pm 1$                         | 0                 | $\Phi$               |
| $cd$   | $6 \times (1, 1, 2, \bar{2}, 1, 1)$   | 0     | 0         | 1        | -1        | $0, \pm 1$                         | 0                 | $H'$                 |
| $cd'$  | $3 \times (1, 1, 2, 2, 1, 1)$   | 0     | 0         | 1        | 1         | $0, \pm 1$                         | 0                 | $H$                  |
| $b4$   | $1 \times (1, \bar{2}, 1, 1, 1, 2)$   | 0     | -1        | 0        | 0         | $\mp \frac{1}{2}$                  | 0                 |                      |
| $c2$   | $1 \times (1, 1, \bar{2}, 1, 2, 1)$   | 0     | 0         | -1       | 0         | $\mp \frac{1}{2}$                  | 0                 |                      |
| $d2$   | $1 \times (1, 1, 1, 2, \bar{2}, 1)$   | 0     | 0         | 0        | 1         | $\pm \frac{1}{2}$                  | 0                 |                      |
| $d4$   | $3 \times (1, 1, 1, \bar{2}, 1, 2)$   | 0     | 0         | 0        | -1        | $\mp \frac{1}{2}$                  | 0                 |                      |
| $c$<br> | $2 \times (1, 1, \bar{3}, 1, 1, 1)$   | 0     | 0         | -2       | 0         | $0, \mp 1$                         | 0                 |                      |
| $c$<br> | $2 \times (1, 1, 1, 1, 1, 1)$   | 0     | 0         | 2        | 0         | 0                                  | 0                 |                      |
| $d$<br> | $2 \times (1, 1, 1, 3, 1, 1)$   | 0     | 0         | 0        | 2         | $0, \pm 1$                         | 0                 |                      |
| $d$<br> | $2 \times (1, 1, 1, \bar{1}, 1, 1)$   | 0     | 0         | 0        | -2        | 0                                  | 0                 |                      |
| $bd$   | $1 \times (1, 2, 1, \bar{2}, 1, 1)$   | 0     | 1         | 0        | -1        | $0, \pm 1$                         | 0                 | $\Phi_u^i, \Phi_d^i$ |
|  | $1 \times (1, \bar{2}, 1, 2, 1, 1)$   | 0     | -1        | 0        | 1         |                                    |                   |                      |

**Table 23.** The composite particle spectrum for Model 8

| Model 8         |              | $U(4) \times U(2)_{L1} \times U(2)_R \times U(2)_{L2} \times USp(2)^2$ |  |
|-----------------|--------------|--|--|
| Confining Force | Intersection | Exotic particle Spectrum   | Confined Particle Spectrum   |
| $USp(2)_2$      | $c2$         | $1 \times (1, 1, \bar{2}, 1, 2, 1)$                                    | $1 \times (1, 1, \bar{2}^2, 1, 1, 1), 1 \times (1, 1, \bar{2}, 2, 1, 1),$<br>$1 \times (1, 1, 1, 2^2, 1, 1)$             |
|                 | $d2$         | $1 \times (1, 1, 1, 2, \bar{2}, 1)$                                    |  |
| $USp(2)_4$      | $b4$         | $1 \times (1, \bar{2}, 1, 1, 1, 2)$                                    | $1 \times (1, \bar{2}^2, 1, 1, 1, 1), 3 \times (1, \bar{2}, 1, \bar{2}, 1, 1),$<br>$6 \times (1, 1, 1, \bar{2}^2, 1, 1)$ |
|                 | $d4$         | $3 \times (1, 1, 1, \bar{2}, 1, 2)$                                    |  |

The composite particle spectrum for Model 8 is given in Table 23. The  $USp(2)_2$  group has two charged intersections, which give rise to an exotic particle  $(1, 1, \bar{2}, 1, 2, 1)$  and an exotic particle  $(1, 1, 1, 2, \bar{2}, 1)$ . The mixing of these two kinds of exotic particles yields a chiral multiplet  $(1, 1, \bar{2}, 2, 1, 1)$ . Besides, their self-confinement results in tensor representations  $(1, 1, \bar{2}^2, 1, 1, 1)$  and tensor representations  $(1, 1, 1, 2^2, 1, 1)$ , which can be

further decomposed

$$\begin{aligned}
1 \times (1, 1, \bar{2}^2, 1, 1, 1) &\rightarrow 1 \times (1, 1, \bar{3}, 1, 1, 1) + 1 \times (1, 1, \bar{1}, 1, 1, 1) , \\
1 \times (1, 1, 1, 2^2, 1, 1) &\rightarrow 1 \times (1, 1, 1, 3, 1, 1) + 1 \times (1, 1, 1, 1, 1, 1) ,
\end{aligned} \tag{4.14}$$

leading to chiral multiplets  $(1, 1, \bar{3}, 1, 1, 1)$  and  $(1, 1, 1, 3, 1, 1)$ . Meanwhile, the  $USp(2)_4$  group also has two charged intersections that give rise to one exotic particle  $(1, \bar{2}, 1, 1, 1, 2)$  and three exotic particles  $(1, 1, 1, \bar{2}, 1, 2)$ . The mixing of these two kinds of exotic particles yields 3 chiral multiplets  $(1, \bar{2}, 1, \bar{2}, 1, 1)$ . Besides, their self-confinement results in a tensor representation  $(1, \bar{2}^2, 1, 1, 1, 1)$  and a 6 tensor representation  $(1, 1, 1, \bar{2}^2, 1, 1)$ , which can be further decomposed, with

$$\begin{aligned}
1 \times (1, \bar{2}^2, 1, 1, 1, 1) &\rightarrow 1 \times (1, \bar{3}, 1, 1, 1, 1) + 1 \times (1, \bar{1}, 1, 1, 1, 1) , \\
6 \times (1, 1, 1, \bar{2}^2, 1, 1) &\rightarrow 6 \times (1, 1, 1, \bar{3}, 1, 1) + 6 \times (1, 1, 1, \bar{1}, 1, 1) ,
\end{aligned} \tag{4.15}$$

leading to chiral multiplets  $(1, \bar{3}, 1, 1, 1, 1)$  and  $(1, 1, 1, \bar{3}, 1, 1)$ .

**Table 24.** The chiral spectrum in the open string sector of Model 9

| Model 9  | $SU(4) \times SU(2)_{L_1} \times SU(2)_R \times SU(2)_{L_2}$ | $Q_4$ | $Q_{2L_1}$ | $Q_{2R}$ | $Q_{2L_2}$ | $Q_{em}$                           | $B - L$           | Field                |
|--|--|-------|------------|----------|------------|------------------------------------|-------------------|----------------------|
| $ab$   | $1 \times (4, \bar{2}, 1, 1)$                                | 1     | -1         | 0        | 0          | $-\frac{1}{3}, \frac{2}{3}, -1, 0$ | $\frac{1}{3}, -1$ | $Q_L, L_L$           |
| $ac$   | $2 \times (4, 1, 2, 1)$                                      | -1    | 0          | 1        | 0          | $\frac{1}{3}, -\frac{2}{3}, 1, 0$  | $-\frac{1}{3}, 1$ | $Q_R, L_R$           |
| $ac'$  | $1 \times (4, 1, \bar{2}, 1)$                                | -1    | 0          | -1       | 0          | $\frac{1}{3}, -\frac{2}{3}, 1, 0$  | $-\frac{1}{3}, 1$ | $Q_R, L_R$           |
| $ad$   | $2 \times (4, 1, 1, \bar{2})$                                | 1     | 0          | 0        | -1         | $-\frac{1}{3}, \frac{2}{3}, -1, 0$ | $\frac{1}{3}, -1$ | $Q_L, L_L$           |
| $bc$   | $4 \times (1, 2, \bar{2}, 1)$                                | 0     | 1          | -1       | 0          | $0, \pm 1$                         | 0                 | $H$                  |
| $bd'$  | $2 \times (1, 2, 1, 2)$                                      | 0     | 1          | 0        | 1          | $0, \pm 1$                         | 0                 | $\Phi$               |
| $cd$   | $6 \times (1, 1, \bar{2}, 2)$                                | 0     | 0          | -1       | 1          | $0, \mp 1$                         | 0                 | $H$                  |
| $cd'$  | $12 \times (1, 1, \bar{2}, \bar{2})$                         | 0     | 0          | -1       | -1         | $0, \mp 1$                         | 0                 | $H'$                 |
| $b$<br> | $1 \times (1, \bar{3}, 1, 1)$                                | 0     | -2         | 0        | 0          | $0, \mp 1$                         | 0                 |                      |
| $b$<br> | $1 \times (1, 1, 1, 1)$                                      | 0     | 2          | 0        | 0          | 0                                  | 0                 |                      |
| $c$<br> | $5 \times (1, 1, 3, 1)$                                      | 0     | 0          | 2        | 0          | $0, \pm 1$                         | 0                 |                      |
| $c$<br> | $5 \times (1, 1, \bar{1}, 1)$                                | 0     | 0          | -2       | 0          | 0                                  | 0                 |                      |
| $d$<br> | $2 \times (1, 1, 1, 3)$                                      | 0     | 0          | 0        | 2          | $0, \pm 1$                         | 0                 |                      |
| $d$<br> | $2 \times (1, 1, 1, \bar{1})$                                | 0     | 0          | 0        | -2         | 0                                  | 0                 |                      |
| $bd$   | $2 \times (1, 2, 1, \bar{2})$                                | 0     | 1          | 0        | -1         | $0, \pm 1$                         | 0                 | $\Phi_u^i, \Phi_d^i$ |
|  | $2 \times (1, \bar{2}, 1, 2)$                                | 0     | -1         | 0        | 1          |                                    |                   |                      |

The full spectrum of Model 9 and 10 are shown in Table 24 and 25, respectively. In Model 9, there are 2 bifundamental Higgs doublets arising from the  $\mathcal{N} = 2$  subsector of the intersection of the  $b$ - and  $d$ -stacks of the D6-branes. In Model 10, there are 8 Higgs doublets arising from the  $\mathcal{N} = 2$  subsector of the intersection of the  $b$ - and  $c$ -stacks of the D6-branes. In addition, since Models 9 and 10 has no  $USp$  group, one cannot break the supersymmetry through gaugino condensation.

**Table 25.** The chiral spectrum in the open string sector of Model 10

| Model 10  | $SU(4) \times SU(2)_{L_1} \times SU(2)_R \times SU(2)_{L_2}$ | $Q_4$ | $Q_{2L_1}$ | $Q_{2R}$ | $Q_{2L_2}$ | $Q_{em}$                           | $B-L$             | Field          |
|---|--|-------|------------|----------|------------|------------------------------------|-------------------|----------------|
| $ab$  | $1 \times (4, \bar{2}, 1, 1)$                                | 1     | -1         | 0        | 0          | $-\frac{1}{3}, \frac{2}{3}, -1, 0$ | $\frac{1}{3}, -1$ | $Q_L, L_L$     |
| $ac$  | $3 \times (\bar{4}, 1, 2, 1)$                                | -1    | 0          | 1        | 0          | $\frac{1}{3}, -\frac{2}{3}, 1, 0$  | $-\frac{1}{3}, 1$ | $Q_R, L_R$     |
| $ad'$   | $2 \times (4, 1, 1, 2)$                                      | 1     | 0          | 0        | 1          | $-\frac{1}{3}, \frac{2}{3}, -1, 0$ | $\frac{1}{3}, -1$ | $Q_L, L_L$     |
| $bc'$   | $4 \times (1, 2, 2, 1)$                                      | 0     | 1          | 1        | 0          | $0, \pm 1$                         | 0                 | $H'$           |
| $bd$  | $2 \times (1, \bar{2}, 1, 2)$                                | 0     | -1         | 0        | 1          | $0, \mp 1$                         | 0                 | $\Phi$         |
| $bd'$   | $4 \times (1, 2, 1, 2)$                                      | 0     | 1          | 0        | 1          | $0, \pm 1$                         | 0                 | $\Phi$         |
| $cd$  | $2 \times (1, 1, \bar{2}, 2)$                                | 0     | 0          | -1       | 1          | $0, \mp 1$                         | 0                 | $H'$           |
| $cd'$   | $4 \times (1, 1, \bar{2}, \bar{2})$                          | 0     | 0          | -1       | -1         | $0, \mp 1$                         | 0                 | $H$            |
| $b$  | $1 \times (1, \bar{3}, 1, 1)$                                | 0     | -2         | 0        | 0          | $0, \mp 1$                         | 0                 |                |
| $b$  | $1 \times (1, 1, 1, 1)$                                      | 0     | 2          | 0        | 0          | 0                                  | 0                 |                |
| $c$  | $1 \times (1, 1, \bar{3}, 1)$                                | 0     | 0          | -2       | 0          | $0, \pm 1$                         | 0                 |                |
| $c$  | $1 \times (1, 1, 1, 1)$                                      | 0     | 0          | 2        | 0          | 0                                  | 0                 |                |
| $d$  | $2 \times (1, 1, 1, \bar{3})$                                | 0     | 0          | 0        | -2         | $0, \pm 1$                         | 0                 |                |
| $d$  | $2 \times (1, 1, 1, 1)$                                      | 0     | 0          | 0        | 2          | 0                                  | 0                 |                |
| $bc$  | $8 \times (1, 2, \bar{2}, 1)$                                | 0     | 1          | -1       | 0          | $0, \pm 1$                         | 0                 | $H_u^i, H_d^i$ |
|   | $8 \times (1, \bar{2}, 2, 1)$                                | 0     | -1         | 1        | 0          |                                    |                   |                |

**Table 26.** The chiral spectrum in the open string sector of Model 18 from [50]

| Model 18 [50]   | $SU(4) \times SU(2)_L \times SU(2)_R \times USp(2)^3$ | $Q_4$ | $Q_{2L}$ | $Q_{2R}$ | $Q_{em}$                           | $B-L$             | Field          |
|---|---|-------|----------|----------|------------------------------------|-------------------|----------------|
| $ab$  | $3 \times (4, \bar{2}, 1, 1, 1, 1)$                   | 1     | -1       | 0        | $-\frac{1}{3}, \frac{2}{3}, -1, 0$ | $\frac{1}{3}, -1$ | $Q_L, L_L$     |
| $ac'$   | $3 \times (\bar{4}, 1, \bar{2}, 1, 1, 1)$             | -1    | 0        | -1       | $\frac{1}{3}, -\frac{2}{3}, 1, 0$  | $-\frac{1}{3}, 1$ | $Q_R, L_R$     |
| $bc$  | $3 \times (1, \bar{2}, 2, 1, 1, 1)$                   | 0     | -1       | 1        | $0, \mp 1$                         | 0                 | $H'$           |
| $a2$  | $1 \times (4, 1, 1, \bar{2}, 1, 1)$                   | 1     | 0        | 0        | $\frac{1}{6}, -\frac{1}{2}$        | $\frac{1}{3}, -1$ |                |
| $a4$  | $1 \times (\bar{4}, 1, 1, 1, 1, 2)$                   | -1    | 0        | 0        | $-\frac{1}{6}, \frac{1}{2}$        | $-\frac{1}{3}, 1$ |                |
| $b4$  | $1 \times (1, 2, 1, 1, 1, \bar{2})$                   | 0     | 1        | 0        | $\pm \frac{1}{2}$                  | 0                 |                |
| $c1$  | $3 \times (1, 1, \bar{2}, 2, 1, 1)$                   | 0     | 0        | -1       | $\mp \frac{1}{2}$                  | 0                 |                |
| $c2$  | $2 \times (1, 1, 2, \bar{2}, 1, 1)$                   | 0     | 0        | 1        | $\pm \frac{1}{2}$                  | 0                 |                |
| $b$  | $2 \times (1, 3, 1, 1, 1, 1)$                         | 0     | 2        | 0        | $0, \pm 1$                         | 0                 |                |
| $b$  | $2 \times (1, \bar{1}, 1, 1, 1, 1)$                   | 0     | -2       | 0        | 0                                  | 0                 |                |
| $c$  | $1 \times (1, 1, 3, 1, 1, 1)$                         | 0     | 0        | 2        | $0, \pm 1$                         | 0                 |                |
| $c$  | $1 \times (1, 1, \bar{1}, 1, 1, 1)$                   | 0     | 0        | -2       | 0                                  | 0                 |                |
| $bc'$   | $9 \times (1, 2, 2, 1, 1, 1)$                         | 0     | 1        | 1        | $0, \pm 1$                         | 0                 | $H_u^i, H_d^i$ |
|   | $9 \times (1, \bar{2}, \bar{2}, 1, 1, 1)$             | 0     | -1       | -1       |                                    |                   |                |

Recall that Model 10 share the same gauge coupling ratio with Model 18 from [50] with spectrum shown in Table 26. In Model 18 from [50], there are 9 Higgs doublets arising from the  $\mathcal{N} = 2$  subsector of the intersection of the  $b$ -stack and the  $\mathbb{Z}_2$  image of the  $c$ -stack of D6-branes only, while in Model 10, Higgs multiplets and Higgs-like particles arise from more intersecting origins. Again, similar to the  $d$ -stack of D6-branes introduced into the  $SU(2)_R$  sector, extra  $d$ -stack turns to reduce the number of filler branes. From

the perspective of phenomenology, these two models are considered to be different as the value of gauge couplings  $g_a$  are different from  $\gamma$  in (3.23).

## 5 Landscape of $\mathcal{N} = 1$ supersymmetric Pati-Salam models with extra $d$ -stack of D6-branes

In [50], the standard  $\mathcal{N} = 1$  supersymmetric Pati-Salam models landscape was completed with 202752 number of models that with 33 classes of gauge coupling relations. In each class, the models are symmetrically related, such as by type I/II T-dualities, D6-brane Sign Equivalent Principle (DSEP). With the additional  $d$ -stack of D6-branes introduced, the symmetries of  $\mathcal{N} = 1$  supersymmetric Pati-Salam models get further extended, and therefore we can extend the landscape with an additional  $d$ -stack of D6-branes. Taking Model 1 as an example, we study its dual models and present in the Appendix A.

Firstly, recall that the models are all constructed on  $\mathbb{T}^6 = \mathbb{T}^2 \times \mathbb{T}^2 \times \mathbb{T}^2$  with a two-torus to be tilted. These three tori are all at democratic positions, and thus we have three equal options of the tilted one of three, which accounts for a symmetry factor 3. In model 1, the second torus is chosen to be tilted. We can certainly choose the first or the third torus to be tilted without changing the gauge couplings relation. Model 11 in Appendix A illustrates the model in which the third torus is chosen to be tilted by swapping the wrapping numbers of the second and third torus, since it is obvious that the models connected with the permutation of these three tori are equivalent [17].

We can first learn from the three-generation condition (3.1) that  $I_{ab}$  and  $I_{ab'}$  are in equal positions, which implies that equivalent models can be produced by performing  $b \leftrightarrow b'$ . Applying this transformation with  $R$  in (2.2) for Model 1, Model 12 in Appendix A will be obtained. The second part of (3.1) for Model 1 then reads

$$I_{ac} + I_{ac'} = -1, \text{ and } I_{ad} + I_{ad'} = -2. \quad (5.1)$$

The symmetry transformations  $c \leftrightarrow c'$  and  $d \leftrightarrow d'$  can be derived by following the procedure used for  $b \leftrightarrow b'$ . Performing on Model 1 with  $c \leftrightarrow c'$  and  $d \leftrightarrow d'$ , we then achieve Model 13 and Model 14, respectively. Note that one might overlook the symmetric positions of the  $c$ - and  $d$ -stacks of the D6-branes, thus omitting the corresponding  $c \leftrightarrow d$  transformation. This symmetry is a unique representation of our work, originating from the introduction of the  $d$ -stack. Model 15 can be obtained by applying the  $c \leftrightarrow d$  transformation to Model 1. Based on our analysis, we can derive the symmetry within the three-generation condition which acquires a symmetry factor  $2 \times 2 \times 2 \times 2 = 16$ .

In [50], the symmetry factor was found to be only 4, a result attributed directly to the absence of the  $d$ -stack. Before exploring the dualities of our models in greater depth, let us recall the essential D6-brane Sign Equivalence Principle (DSEP) [17]: two models are considered equivalent if, for any stack of brane, the wrapping numbers on any two tori have opposite signs, while those on the remaining torus are identical. In other words, the transformation  $(n_x^i, l_x^i) \rightarrow (-n_x^i, -l_x^i)$  together with  $(n_x^j, l_x^j) \rightarrow (-n_x^j, -l_x^j)$  leads to an equivalent model, where  $x$  can be any one of  $a, b, c$  and  $d$ , and  $i \neq j$  are chosen from

1, 2 and 3. Here is an example: we choose  $(n_a^1, l_a^1) \rightarrow (-n_a^1, -l_a^1)$  and  $(n_a^2, l_a^2) \rightarrow (-n_a^2, -l_a^2)$  simultaneously for Model 1, and after performing

$$(1, -1) \times (1, 1) \times (1, 0) \xrightarrow{\text{DSEP}} (-1, 1) \times (-1, -1) \times (1, 0) , \quad (5.2)$$

on the  $a$ -stack of branes, we acquire Model 16. We determine the symmetry factor for DSEP to be  $(1 + 3)^4 = 4^4$ . The base  $(1 + 3)$  is derived as follows: “1” represents the case without applying DSEP, while “3” corresponds to the number of combinations for selecting two tori (out of three) to change the wrapping numbers, given by  $C_3^2 = 3$ . The exponent 4 arises because this operation can be applied to any one of the four distinct brane stacks.

Next, we consider the transformation under T-dualities, which establishes a connection between two models that share the same gauge coupling relation via a different operation, specifically the type I T-duality [17]. This type I T-duality as a transformation on the  $i$ -th and the  $j$ -th tori and the wrapping numbers are governed by the transformation rule as below

$$(n_x^i, l_x^i) \rightarrow (-l_x^i, n_x^i) \text{ and } (n_x^j, l_x^j) \rightarrow (l_x^j, -n_x^j) , \quad (5.3)$$

together, where  $x$  runs over all  $a, b, c$  and  $d$  stacks simultaneously, unlike choosing a certain stack in the case of DSEP. For example, we take the first and second torus of Model 1, and apply the following transformation

$$\begin{aligned} (n_a^1, l_a^1) &\rightarrow (-l_a^1, n_a^1) , & (n_b^1, l_b^1) &\rightarrow (-l_b^1, n_b^1) , & (n_c^1, l_c^1) &\rightarrow (-l_c^1, n_c^1) , & (n_d^1, l_d^1) &\rightarrow (-l_d^1, n_d^1) , \\ (n_a^2, l_a^2) &\rightarrow (l_a^2, -n_a^2) , & (n_b^2, l_b^2) &\rightarrow (l_b^2, -n_b^2) , & (n_c^2, l_c^2) &\rightarrow (l_c^2, -n_c^2) , & (n_d^2, l_d^2) &\rightarrow (l_d^2, -n_d^2) . \end{aligned} \quad (5.4)$$

Then Model 17 is constructed. As can be seen,  $\chi_1, \chi_2, \chi_3, x_A, x_B, x_C$ , and  $x_D$  in Models 12-16 are identical, but this is not the case for Model 17. This is because the application of the T-duality transformation in Model 17 results in  $(A, B, C, D) \rightarrow (D, C, B, A)$ , leading to different  $\chi_1, \chi_2, \chi_3, x_A, x_B, x_C$ , and  $x_D$ . That is, the complex structure of such models could change, while the particle spectra will not change, under type I T-duality transformation [17], and the basic gauge coupling relation in (3.23) is invariant. This type I T-duality contributes a symmetry factor  $1 + 3 = 4$ .

Moreover, if we combine DSEP with type I T-duality, it will double the number of such models. This so-called extended type I T-duality as a variation of type II T-duality works on the  $i$ -th and the  $j$ -th tori as transformation by

$$(n_x^i, l_x^i) \rightarrow (l_x^j, -n_x^j) \text{ and } (n_x^j, l_x^j) \rightarrow (-l_x^i, n_x^i) . \quad (5.5)$$

Applying (5.5) to the first and second tori of Model 1, Model 18 is successfully constructed.

In total, considering all the symmetries above, there are

$$3 \times 2 \times 2 \times 2 \times 2 \times 4^4 \times 4 \times 2 = 98304 = 6144 \times 16 \quad (5.6)$$

equivalent models with the same gauge coupling relation for each class of models. It is worth mentioning that when we say two models with the same gauge coupling relation, it

refers to two models with the same value of  $\alpha, \beta$  and  $\gamma$  in (3.23).

Note that models with the same  $\alpha$  and  $\beta$  but different  $\gamma$ , such as Model 4 and Model 10 in [50], are not considered equivalent, since it is impossible to relate these two models via any symmetry and duality discussed above. However, as these models have the same gauge coupling ratio, their RGE rolling to achieve string-scale gauge coupling unification do share similar behavior which we will show in the next section.

## 6 String and GUT scale gauge coupling relation

With an extra  $d$ -stack of D6-branes introduced, we have discussed phenomenologically eight representative  $\mathcal{N} = 1$  supersymmetric Pati-Salam models from their spectrum. In this section, we investigate their string and GUT scale gauge coupling unification with RGE evolution.

In particular, the new models constructed by introducing new  $d$ -stack D6-branes do not have chiral multiplets in the symmetric representation of  $SU(4)_C$  appearing in these models and the exotic particles can be decoupled [52]. In principle, the gauge coupling unification can be performed at the string scale ( $M_{string} \simeq 5 \times 10^{17} \text{GeV}$ ) or the GUT scale ( $M_{GUT} \simeq 2 \times 10^{16} \text{GeV}$ ) as shown in [52]. In which, through the method of two-loop evolution and the addition of vector-like particles, gauge coupling unification can be achieved. These vector-like particles come from  $\mathcal{N} = 2$  subsectors and are chiral multiplets from ajoint representations of  $SU(4)_C$  and  $SU(2)_L$ .

Recall that the gauge coupling relations can be expressed in (3.23), and at the unification scale, we have

$$k_1 g_a^2 = k_2 g_b^2 = k_Y g_Y^2 = g_U^2, \quad (6.1)$$

$$k_1 g_a^2 = k_2 g_L^2 = k_Y g_Y^2 = g_U^2, \quad (6.2)$$

for models with  $SU(2)_{R_1} \times SU(2)_{R_2} \rightarrow SU(2)_R$  and  $SU(2)_{L_1} \times SU(2)_{L_2} \rightarrow SU(2)_L$  respectively. In these two cases, we take  $k_1 = 1$  for convenience, and the constants  $k_2$  and  $k_Y = \frac{5}{3} k_y$  can be obtained from the gauge coupling relations of the models shown in Sections 4 and 4.2. By defining  $\alpha_1 \equiv \frac{k_Y g_Y^2}{4\pi}$ ,  $\alpha_2 \equiv \frac{k_2 g_L^2}{4\pi}$  and  $\alpha_3 \equiv \frac{g_a^2}{4\pi}$ , we represent the gauge coupling relations at the unification scale as [52]

$$\alpha_U^{-1} \equiv \alpha_1^{-1} = \frac{\alpha_2^{-1} + \alpha_3^{-1}}{2}. \quad (6.3)$$

The accuracy is defined by

$$\Delta = \frac{|\alpha_1^{-1} - \alpha_2^{-1}|}{\alpha_1^{-1}}, \quad (6.4)$$

which is usually required to be less than 1%.

Unlike Model 5 in [50] with  $k_2 = 1$  and  $k_Y = \frac{5}{3}$ , the models found in our work cannot naturally achieve unification without introducing additional vector-like particles or chiral multiplets. Thus, in order to obtain the string-scale or GUT scale gauge coupling relation,

two-loop RGEs must be performed [51, 52, 61–64]

$$\frac{dg_i}{d \ln \mu} = \frac{b_i}{(4\pi)^2} g_i^3 + \sum_j \frac{g_i^3}{(4\pi)^4} \left[ \sum_{j=1}^3 B_{ij} g_j^2 - \sum_{\alpha=u,d,e} d_i^\alpha \text{Tr}(h^{\alpha\dagger} h^\alpha) \right], \quad (6.5)$$

where  $g_i (i = 1, 2, 3)$  and  $h^\alpha (\alpha = u, d, e)$  stand for the SM gauge couplings and the Yukawa couplings, respectively. The coefficients for the beta functions in SM [65–69] and supersymmetric models [70–72] are given by

$$b_{\text{SM}} = \left( \frac{41}{6} \frac{1}{k_Y}, -\frac{19}{6} \frac{1}{k_2}, -7 \right), \quad B_{\text{SM}} = \begin{pmatrix} \frac{199}{18} \frac{1}{k_Y} & \frac{27}{6} \frac{1}{k_Y k_2} & \frac{44}{3} \frac{1}{k_Y} \\ \frac{3}{2} \frac{1}{k_Y k_2} & \frac{35}{6} \frac{1}{k_2} & 12 \frac{1}{k_2} \\ \frac{11}{6} \frac{1}{k_Y} & \frac{9}{2} \frac{1}{k_2} & -26 \end{pmatrix}, \quad (6.6)$$

$$d_{\text{SM}}^u = \left( \frac{17}{6} \frac{1}{k_Y}, \frac{3}{2} \frac{1}{k_2}, 2 \right), \quad d_{\text{SM}}^d = 0, \quad d_{\text{SM}}^e = 0, \quad (6.7)$$

$$b_{\text{SUSY}} = \left( 11 \frac{1}{k_Y}, \frac{1}{k_2}, -3 \right), \quad B_{\text{SUSY}} = \begin{pmatrix} \frac{199}{9} \frac{1}{k_Y} & 9 \frac{1}{k_Y k_2} & \frac{88}{3} \frac{1}{k_Y} \\ 3 \frac{1}{k_Y k_2} & 25 \frac{1}{k_2} & 24 \frac{1}{k_2} \\ \frac{11}{3} \frac{1}{k_Y} & 9 \frac{1}{k_2} & 14 \end{pmatrix}, \quad (6.8)$$

$$d_{\text{SUSY}}^u = \left( \frac{26}{3} \frac{1}{k_Y}, 6 \frac{1}{k_2}, 4 \right), \quad d_{\text{SUSY}}^d = 0, \quad d_{\text{SUSY}}^e = 0. \quad (6.9)$$

We numerically solved the two-loop RGEs for the SM gauge couplings. Numerical calculations of one-loop RGEs are performed taking into account the new physics contributions and threshold. In [69], the general one-loop RGEs for Yukawa couplings are given. In the following, we run the gauge couplings from  $M_Z$ , the mass scale of the  $Z$  boson, with the corresponding initial conditions

$$g_1(M_Z) = \sqrt{k_Y} \frac{g_{em}}{\cos \theta_W}, \quad g_2(M_Z) = \sqrt{k_2} \frac{g_{em}}{\sin \theta_W}, \quad g_3(M_Z) = \sqrt{4\pi\alpha_s}, \quad (6.10)$$

in which  $g_{em}$  is the effective coupling strength of the electromagnetic interaction in electroweak theory,  $\theta_W$  is the mixing angle (or the Weinberg angle) and  $\alpha_s$  is the strong coupling constant. Our analysis considers the non-supersymmetric SM spectrum with the top quark pole mass set to  $m_t = 173.34$  GeV, over the range of  $M_Z$  to a supersymmetry breaking scale  $M_S$ . Guided by the experimental lower limits for preserving supersymmetry and the gauge hierarchy, we adopt a supersymmetry breaking scale  $M_S \simeq 3.0$  TeV [52]. In addition, we choose the mass of the  $Z$  boson, the pole mass of the top quark, the Higgs Vacuum Expectation Value (VEV), the strong coupling constant, the fine structure constant and the relation of the mixing angle as follows [73, 74],

$$M_Z = 91.1876 \text{ GeV}, \quad m_t = 173.34 \pm 0.27(\text{stat}) \pm 0.71(\text{syst}) \text{ GeV}, \quad v = 174.10 \text{ GeV}, \\ \alpha_S(M_Z) = 0.1181 \pm 0.0011, \quad \alpha_{em}^{-1}(M_Z) = 128.91 \pm 0.02, \quad \sin^2 \theta_W(M_Z) = 0.23122. \quad (6.11)$$

In addition, in this work we take the usually applied string scale and GUT scale to be  $M_{string} \simeq 5 \times 10^{17} \text{GeV}$  and  $M_{GUT} \simeq 2 \times 10^{16} \text{GeV}$ .

From Model 1 to Model 4, we can achieve the gauge coupling unification at the two-loop level with additionally introduced vector-like particles from the  $\mathcal{N} = 2$  subsector, whose quantum numbers are the same as those of the SM fermions and their Hermitian conjugates. We observe that  $n_v$ , the number of vector-like particles, is determined by the intersections of the D6-branes. The gauge coupling unification can finally be realized by fine-tuning the masses of the additional vector-like particles.

As for Models 7-10, in addition to vector-like particles, we also require chiral multiplets from adjoint representations of  $SU(4)_C$ ,  $SU(2)_{L_1}$  and  $SU(2)_{L_2}$  in addition to vector-like particles. In addition, the chiral multiplet  $XG$  comes from the  $aa$  sector, and the chiral multiplet  $XW$  comes from the  $bb$  and the  $dd$  sectors, as shown in Table 2. Since there are three adjoint chiral multiplets arising from each one of  $aa$ ,  $bb$ ,  $cc$  and  $dd$  sectors, the number of chiral multiplets  $XG$  is restricted to be less than or equal to 3, and the number of chiral multiplets  $XW$  is restricted to be less than or equal to 6. Under  $SU(3)_C \times SU(2)_L \times U(1)_Y$ , we can explicitly write down the quantum numbers of vector-like particles and chiral multiplets [75, 76]

$$(XQ + \overline{XQ}) = (\mathbf{3}, \mathbf{2}, \frac{1}{6}) + (\overline{\mathbf{3}}, \mathbf{2}, -\frac{1}{6}), \quad (6.12)$$

$$(XD + \overline{XD}) = (\mathbf{3}, \mathbf{1}, -\frac{1}{3}) + (\overline{\mathbf{3}}, \mathbf{1}, \frac{1}{3}), \quad (6.13)$$

$$(XU + \overline{XU}) = (\mathbf{3}, \mathbf{1}, \frac{2}{3}) + (\overline{\mathbf{3}}, \mathbf{1}, -\frac{2}{3}), \quad (6.14)$$

$$(XE + \overline{XE}) = (\mathbf{1}, \mathbf{1}, \mathbf{1}) + (\mathbf{1}, \mathbf{1}, -\mathbf{1}), \quad (6.15)$$

$$XG = (\mathbf{8}, \mathbf{1}, \mathbf{0}), \quad (6.16)$$

$$XW = (\mathbf{1}, \mathbf{3}, \mathbf{0}). \quad (6.17)$$

And their contributions to the one-loop beta functions are simply

$$\Delta b^{(XQ+\overline{XQ})} = \left(\frac{1}{5}, 3, 2\right), \quad \Delta b^{(XD+\overline{XD})} = \left(\frac{2}{5}, 0, 1\right), \quad \Delta b^{(XU+\overline{XU})} = \left(\frac{8}{5}, 0, 1\right), \quad (6.18)$$

$$\Delta b^{(XE+\overline{XE})} = \left(\frac{6}{5}, 0, 0\right), \quad \Delta b^{(XG)} = (0, 0, 3), \quad \Delta b^{(XW)} = (0, 2, 0), \quad (6.19)$$

with their contributions to the two-loop beta function to be

$$\Delta B^{(XQ+\overline{XQ})} = \begin{pmatrix} \frac{1}{75} & \frac{3}{5} & \frac{16}{15} \\ \frac{1}{5} & 21 & 16 \\ \frac{2}{15} & 6 & \frac{68}{3} \end{pmatrix}, \quad \Delta B^{(XD+\overline{XD})} = \begin{pmatrix} \frac{8}{75} & 0 & \frac{32}{15} \\ 0 & 0 & 0 \\ \frac{4}{15} & 0 & \frac{34}{3} \end{pmatrix}, \quad \Delta B^{(XU+\overline{XU})} = \begin{pmatrix} \frac{128}{75} & 0 & \frac{128}{15} \\ 0 & 0 & 0 \\ \frac{16}{15} & 0 & \frac{34}{3} \end{pmatrix}, \quad (6.20)$$

$$\Delta B^{(XE+\overline{XE})} = \begin{pmatrix} \frac{72}{25} & 0 & 0 \\ 0 & 0 & 0 \\ 0 & 0 & 0 \end{pmatrix}, \quad \Delta B^{(XG)} = \begin{pmatrix} 0 & 0 & 0 \\ 0 & 0 & 0 \\ 0 & 0 & 54 \end{pmatrix}, \quad \Delta B^{(XW)} = \begin{pmatrix} 0 & 0 & 0 \\ 0 & 24 & 0 \\ 0 & 0 & 0 \end{pmatrix}. \quad (6.21)$$

By introducing additional vector-like particles that come from  $\mathcal{N} = 2$  subsectors, we managed to achieve both string and GUT scale gauge coupling unification via two-loop RGE evolution. The gauge coupling relations achieved for Models 1-4 are summarized in Table 27, while the gauge coupling relations of Models 7-10 are summarized in Table 28.

**Table 27.** Gauge coupling relations for Model 1 to 4 achieved by adding vector-like particles  $XD + \overline{XD}$  and  $XU + \overline{XU}$  from  $\mathcal{N} = 2$  subsector.

| Model No. | $k_y$ | $k_2$ | $n_v$ | $M_{XD}(\text{GeV})$  | $M_{XU}(\text{GeV})$  | $M_U(\text{GeV})$     | $\alpha_U^{-1}$ |
|-----------|-------|-------|-------|-----------------------|-----------------------|-----------------------|-----------------|
| 1         | 5/8   | 1     | 1     |                       | $1.40 \times 10^9$    | $1.50 \times 10^{18}$ | 24.9            |
| 2         | 5/6   | 3     | 4     | $4.00 \times 10^9$    | $3.31 \times 10^{13}$ | $5.00 \times 10^{17}$ | 8.36            |
|           |       |       | 5     | $1.78 \times 10^{11}$ | $2.25 \times 10^{14}$ | $5.00 \times 10^{17}$ | 8.43            |
|           |       |       | 4     | $3.14 \times 10^{11}$ | $8.73 \times 10^9$    | $2.00 \times 10^{16}$ | 8.59            |
|           |       |       | 5     | $3.13 \times 10^{12}$ | $1.61 \times 10^{11}$ | $2.00 \times 10^{16}$ | 8.66            |
| 3         | 5/4   | 6     | 5     | $2.23 \times 10^9$    | $2.18 \times 10^{14}$ | $5.00 \times 10^{17}$ | 4.19            |
|           |       |       | 5     | $3.37 \times 10^{10}$ | $1.59 \times 10^{11}$ | $2.00 \times 10^{16}$ | 4.32            |
| 4         | 1     | 2     | 2     | $5.00 \times 10^3$    | $6.54 \times 10^{12}$ | $3.00 \times 10^{17}$ | 12.8            |
|           |       |       | 3     | $3.71 \times 10^7$    | $1.05 \times 10^{15}$ | $5.00 \times 10^{17}$ | 12.6            |
|           |       |       | 2     | $4.30 \times 10^7$    | $1.11 \times 10^8$    | $2.00 \times 10^{16}$ | 12.9            |
|           |       |       | 3     | $4.30 \times 10^7$    | $1.11 \times 10^8$    | $2.00 \times 10^{16}$ | 13.0            |

**Table 28.** Gauge coupling relations for Model 7 to 10 achieved by adding vector-like particle(s)  $XQ + \overline{XQ}$  from  $\mathcal{N} = 2$  subsector and chiral multiplet(s)  $XG$  or  $XW$  from  $aa$  or  $bb$  ( $dd$ ) sector.

| Model No. | $k_y$ | $k_2$ | $n_v$ | $M_{XQ}(\text{GeV})$  | $n_c$ | $M_{XW}(\text{GeV})$  | $M_U(\text{GeV})$     | $\alpha_U^{-1}$ |
|-----------|-------|-------|-------|-----------------------|-------|-----------------------|-----------------------|-----------------|
| 7         | 1     | 1/2   | 3     | $9.05 \times 10^{14}$ | 1     | $3.20 \times 10^{11}$ | $5.66 \times 10^{17}$ | 21.4            |
|           |       |       | 3     | $9.30 \times 10^{14}$ | 2     | $3.53 \times 10^{14}$ | $5.37 \times 10^{17}$ | 21.5            |
|           |       |       | 3     | $9.65 \times 10^{15}$ | 2     | $3.16 \times 10^8$    | $2.00 \times 10^{16}$ | 25.5            |
| Model No. | $k_y$ | $k_2$ | $n_v$ | $M_{XQ}(\text{GeV})$  | $n_c$ | $M_{XG}(\text{GeV})$  | $M_U(\text{GeV})$     | $\alpha_U^{-1}$ |
| 8         | 5/3   | 3/4   | 4     | $2.00 \times 10^{14}$ | 3     | $3.01 \times 10^{16}$ | $5.00 \times 10^{17}$ | 12.7            |
|           |       |       | 5     | $9.37 \times 10^{14}$ | 3     | $3.16 \times 10^{16}$ | $5.00 \times 10^{17}$ | 12.7            |
|           |       |       | 4     | $1.24 \times 10^{13}$ | 3     | $8.51 \times 10^{15}$ | $2.00 \times 10^{16}$ | 14.8            |
|           |       |       | 5     | $5.64 \times 10^{13}$ | 3     | $8.26 \times 10^{15}$ | $2.00 \times 10^{16}$ | 14.8            |
| 9         | 2     | 3/2   | 5     | $1.31 \times 10^{16}$ | 3     | $5.15 \times 10^{14}$ | $5.00 \times 10^{17}$ | 10.8            |
|           |       |       | 5     | $1.20 \times 10^{15}$ | 2     | $3.91 \times 10^{12}$ | $2.00 \times 10^{16}$ | 12.6            |
| 10        | 10/7  | 1     | 1     | $8.60 \times 10^8$    | 3     | $1.12 \times 10^{16}$ | $5.00 \times 10^{17}$ | 15.0            |
|           |       |       | 2     | $1.71 \times 10^{13}$ | 3     | $1.29 \times 10^{16}$ | $5.00 \times 10^{17}$ | 15.0            |
|           |       |       | 3     | $4.83 \times 10^{14}$ | 3     | $1.45 \times 10^{16}$ | $5.00 \times 10^{17}$ | 15.0            |
|           |       |       | 1     | $9.80 \times 10^8$    | 3     | $3.07 \times 10^{15}$ | $2.00 \times 10^{16}$ | 17.5            |
|           |       |       | 2     | $4.13 \times 10^{12}$ | 3     | $3.17 \times 10^{15}$ | $2.00 \times 10^{16}$ | 17.5            |
|           |       |       | 3     | $7.19 \times 10^{13}$ | 3     | $3.00 \times 10^{15}$ | $2.00 \times 10^{16}$ | 17.5            |

With the two-loop evolution of gauge couplings for Models 1-3 and Models 7-9 presented in the Appendix B, in the following we take Model 4 and Model 10 as examples to

discuss their string and GUT scale gauge coupling unification, in both extra  $SU(2)_L$  and  $SU(2)_R$   $d$ -stack examples.

Firstly, for Model 4, by introducing vector-like particles from  $XD + \overline{XD}$  and  $XU + \overline{XU}$  from the  $\mathcal{N} = 2$  subsector in both cases, we obtain the gauge coupling unification at both string scale and GUT scale in Figure 1 and 2. It can be calculated that in Model 4,  $|I_{ac'}^{(2,3)}| = |(0+1)(-1+0)| = 1$  and  $|I_{ad}^{(1,2)}| = |\frac{1}{2}(1+3)(0+1)| = 2$ . The gauge coupling unification at both string scale and GUT scale can be achieved by adding  $2(XD + \overline{XD}) + 2(XU + \overline{XU})$  or  $3(XD + \overline{XD}) + 3(XU + \overline{XU})$ .

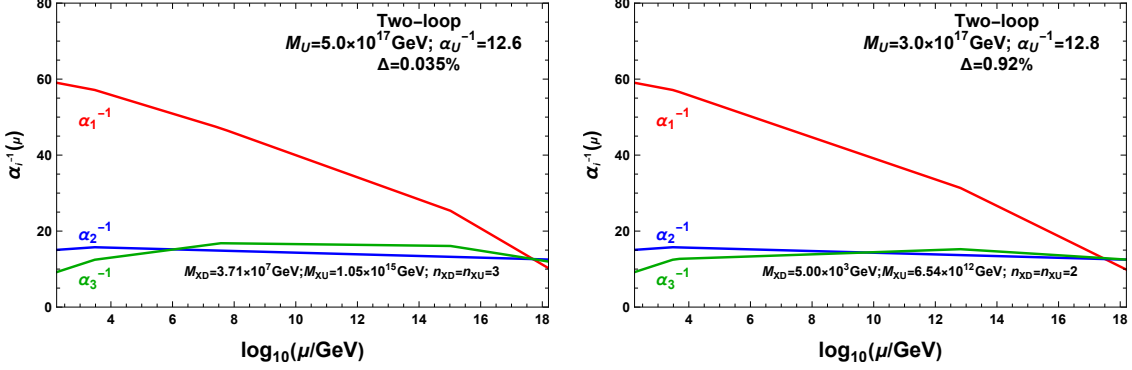


**Figure 1.** Two-loop evolution of gauge couplings for Model 4. The gauge coupling unification can be achieved at string scale by adding  $3(XD + \overline{XD}) + 3(XU + \overline{XU})$  (left panel) and  $2(XD + \overline{XD}) + 2(XU + \overline{XU})$  (right panel).

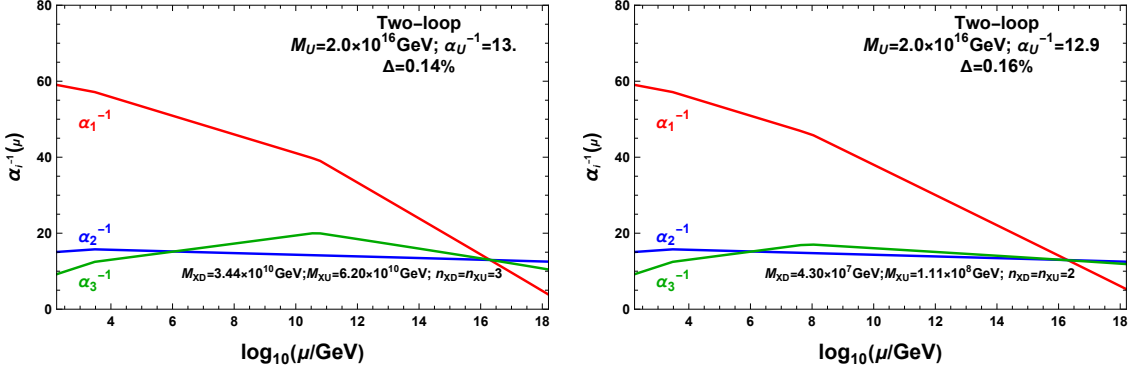


**Figure 2.** Two-loop evolution of gauge couplings for Model 4. The gauge coupling unification can be achieved at GUT scale by adding  $3(XD + \overline{XD}) + 3(XU + \overline{XU})$  (left panel) and  $2(XD + \overline{XD}) + 2(XU + \overline{XU})$  (right panel).

For Model 10 with an extra  $d$ -stack of the  $SU(2)_L$  configuration, we managed to unify the gauge couplings at both string scale (Figure 3) and GUT scale (Figure 4), by introducing vector-like particles  $XQ + \overline{XQ}$  from  $\mathcal{N} = 2$  subsector and  $XG$  from  $aa$  sector in both cases. Here,  $|I_{ab'}^{(2,3)}| = 1$  and  $|I_{ad}^{(1,2)}| = 2$ . With fixed  $n_{XG} = 3$ , we observe that when  $n_{XQ} = |I_{ab'}^{(2,3)}| = 1$ ,  $n_{XQ} = |I_{ad}^{(1,2)}| = 2$  or  $n_{XQ} = |I_{ab'}^{(2,3)}| + |I_{ad}^{(1,2)}| = 3$ , which means that by using  $(XQ + \overline{XQ}) + 3XG$ ,  $2(XQ + \overline{XQ}) + 3XG$  or  $3(XQ + \overline{XQ}) + 3XG$  the gauge

coupling unification can be achieved at both string scale and GUT scale.

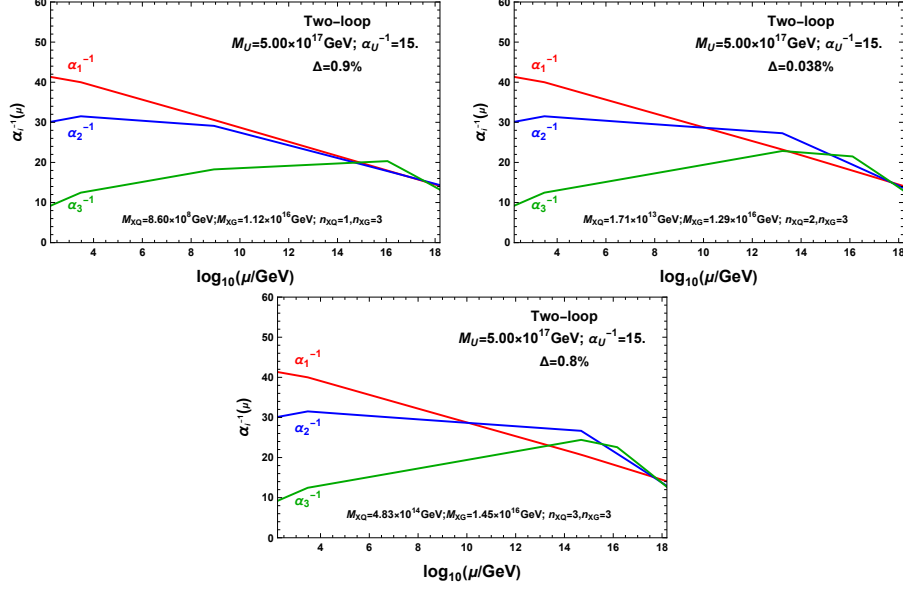


**Figure 3.** Two-loop evolution of gauge couplings for Model 10. The gauge coupling unification can be achieved at string scale by adding  $(XQ + \bar{X}\bar{Q}) + 3XG$  (top left panel),  $2(XQ + \bar{X}\bar{Q}) + 3XG$  (top right panel) and  $3(XQ + \bar{X}\bar{Q}) + 3XG$  (bottom panel).

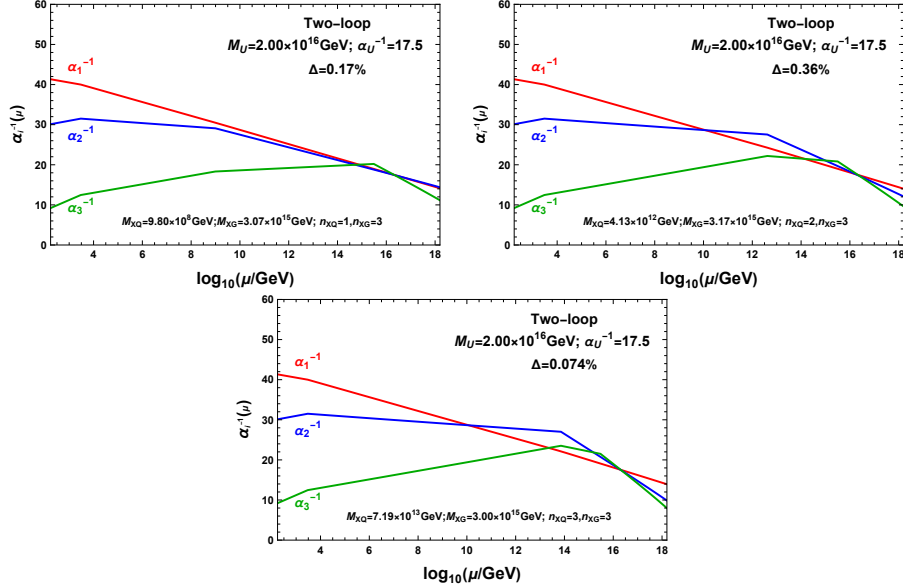


**Figure 4.** Two-loop evolution of gauge couplings for Model 10. The gauge coupling unification can be achieved at GUT scale by adding  $(XQ + \bar{X}\bar{Q}) + 3XG$  (top left panel),  $2(XQ + \bar{X}\bar{Q}) + 3XG$  (top right panel) and  $3(XQ + \bar{X}\bar{Q}) + 3XG$  (bottom panel).

Among all the applicable combinations, it is already known that  $3(XQ + \bar{X}\bar{Q}) + 3XG$  works well, since it has already been presented in Table 4 from [52], which confirms the aforementioned point that different schemes for a certain gauge coupling unification that

implies a possible “degeneracy” of a set of  $k_y$  and  $k_2$  with extra  $d$ -stack of D6-branes introduced. Namely, with the same gauge coupling ratio, there are models that phenomenological independent yet for example, with different values of  $\gamma$  in (3.23) or (4.10).

## 7 Conclusions and outlook

Realizing that the chiral fermion multiplets can arise from various intersection of branes, we introduced extra  $d$ -stack of D6-branes to the  $SU(2)_R$  and  $SU(2)_L$  gauge constructions. The standard Pati-Salam gauge symmetry  $SU(4)_C \times SU(2)_L \times SU(2)_R$  is then extended to  $SU(4)_C \times SU(2)_L \times SU(2)_{R_1} \times SU(2)_{R_2}$  and  $SU(4)_C \times SU(2)_{L_1} \times SU(2)_R \times SU(2)_{L_2}$ , while  $d$ -stack of branes contributing to the symmetries  $SU(2)_{R_2}$  and  $SU(2)_{L_2}$ , respectively. Based on the duality and symmetry of supersymmetric Pati-Salam models, the extra  $d$ -stack of brane introduced an extra factor of 16 to the variation of symmetric transformation comparing to the complete search of landscape in [50].

Based on the model building with extra  $d$ -stack of D6-branes, we successfully constructed four classes of new models with gauge symmetry  $SU(4)_C \times SU(2)_L \times SU(2)_{R_1} \times SU(2)_{R_2}$ , represented by Model 1-4 (see Table 3 to 6) with  $g_a^2 = \alpha g_b^2 = \beta \frac{5}{3} g_Y^2 = \gamma [\pi e^{\phi^4}]$ , and another four classes of models with gauge symmetry  $SU(4)_C \times SU(2)_{L_1} \times SU(2)_R \times SU(2)_{L_2}$ , represented by Model 7-10 (see Table 16 to 19) with  $g_a^2 = \alpha g_L^2 = \beta \frac{5}{3} g_Y^2 = \gamma [\pi e^{\phi^4}]$ . In precise, there are 98304 equivalent models with the same gauge coupling relation for each one of the eight classes of models, and these equivalent models are all related via the permutation of tori, the transformation  $b \leftrightarrow b'$ ,  $c \leftrightarrow c'$ ,  $d \leftrightarrow d'$  and  $c \leftrightarrow d$  ( $b \leftrightarrow d$ ), DSEP and T-duality. This greatly extended the landscape of supersymmetric Pati-Salam models.

From the spectra of these models, we found that introducing extra  $d$ -stack of D6-branes tends to reduce the number of filler branes that carry  $USp(N)$  gauge symmetries. For Model 1, 2, 7 and 8, only two  $USp$  groups are observed in the hidden sector; while no  $USp$  group appears in Model 3, 4, 9 and 10, which is rare compared with all the previous studies of three-family supersymmetric Pati-Salam models. However, as an advantage, it provides more origins to arise Higgs/Higgs-like multiplets that would be interesting phenomenologically. In particular, for Model 1 to 4, Higgs multiplets arise from the intersection of  $b$ - and  $c$ -stacks of branes (or its  $\mathbb{Z}_2$  image) and  $b$ - and  $d$ -stacks of branes (or its  $\mathbb{Z}_2$  image) appear simultaneously; while for Model 7 to 10, Higgs multiplets arise from the intersection of  $b$ - and  $c$ -stacks of branes (or its  $\mathbb{Z}_2$  image) and intersection of  $d$ - and  $c$ -stacks of branes (or its  $\mathbb{Z}_2$  image).

At the string/GUTs gauge unification scale, with  $d$ -stack of D6-branes introduced, the gauge coupling relations become  $g_a^2 = k_2 g_b^2 = k_Y g_Y^2 = g_U^2$ ,  $g_a^2 = k_2 g_L^2 = k_Y g_Y^2 = g_U^2$ , respectively. The coefficients  $k_2$  and  $k_Y$  rely on different models and will be utilized to achieve gauge coupling unification. Among these models, we find that there are newly constructed models that share the same gauge coupling ratio as standard supersymmetric Pati-Salam models in [50] but with a different value of gauge coupling, such as Model 4 and Model 10 in [50]. This shows that a “degeneracy” behavior of gauge coupling ratio exists, which also appears in Model 10 and Model 18 in [50]. It is also inspiring that these

models with different values of  $\gamma$  (such as in (3.23) or (4.10)) but the same gauge coupling ratios can be unified at the target scale with different numbers of additional particles from various origins, as shown in Figures 1 and 2 for string scale and GUT scale unification, respectively.

For future investigation, it would be interesting to further study the “degeneracy” class with the same gauge coupling relation ratio, from both the phenomenology and the model building aspects. As with extra stack of D6-branes introduced, the landscape of supersymmetric Pati-Salam models gets further extended, it could be interesting to study other extensions with more stacks of D6-branes.

## Acknowledgments

TL is supported in part by the National Key Research and Development Program of China Grant No. 2020YFC2201504, by the Projects No. 11875062, No. 11947302, No. 12047503, and No. 12275333 supported by the National Natural Science Foundation of China, by the Key Research Program of the Chinese Academy of Sciences, Grant No. XDPB15, by the Scientific Instrument Developing Project of the Chinese Academy of Sciences, Grant No. YJKYYQ20190049, by the International Partnership Program of Chinese Academy of Sciences for Grand Challenges, Grant No. 112311KYSB20210012, and by the Henan Province Outstanding Foreign Scientist Studio Project, No.GZS2025008. RS is supported by the Fundamental Research Funds for the Central Universities Grant No. E4EQ0102X2. LW is supported by the Natural Science Basic Research Program of Shaanxi, Grant No. 2024JC-YBMS-039.

## References

- [1] M. Berkooz, M. R. Douglas, and R. G. Leigh, *Branes intersecting at angles*, *Nucl. Phys. B* **480** (1996) 265–278, [[hep-th/9606139](#)].
- [2] J. D. Lykken, E. Poppitz, and S. P. Trivedi, *Branes with GUTs and supersymmetry breaking*, *Nucl. Phys. B* **543** (1999) 105–121, [[hep-th/9806080](#)].
- [3] M. Cvetič, M. Plumacher, and J. Wang, *Three family type IIB orientifold string vacua with nonAbelian Wilson lines*, *JHEP* **04** (2000) 004, [[hep-th/9911021](#)].
- [4] G. Aldazabal, A. Font, L. E. Ibanez, and G. Violero,  *$D = 4$ ,  $N=1$ , type IIB orientifolds*, *Nucl. Phys. B* **536** (1998) 29–68, [[hep-th/9804026](#)].
- [5] M. Klein and R. Rabadan,  *$Z(N) \times Z(M)$  orientifolds with and without discrete torsion*, *JHEP* **10** (2000) 049, [[hep-th/0008173](#)].
- [6] G. Aldazabal, L. E. Ibanez, F. Quevedo, and A. M. Uranga,  *$D$ -branes at singularities: A Bottom up approach to the string embedding of the standard model*, *JHEP* **08** (2000) 002, [[hep-th/0005067](#)].
- [7] G. Aldazabal, S. Franco, L. E. Ibanez, R. Rabadan, and A. M. Uranga, *Intersecting brane worlds*, *JHEP* **02** (2001) 047, [[hep-ph/0011132](#)].

- [8] G. Aldazabal, S. Franco, L. E. Ibanez, R. Rabadan, and A. M. Uranga, *D = 4 chiral string compactifications from intersecting branes*, *J. Math. Phys.* **42** (2001) 3103–3126, [[hep-th/0011073](#)].
- [9] L. E. Ibanez, F. Marchesano, and R. Rabadan, *Getting just the standard model at intersecting branes*, *JHEP* **11** (2001) 002, [[hep-th/0105155](#)].
- [10] M. Cvetič, G. Shiu, and A. M. Uranga, *Three family supersymmetric standard - like models from intersecting brane worlds*, *Phys. Rev. Lett.* **87** (2001) 201801, [[hep-th/0107143](#)].
- [11] R. Blumenhagen, L. Gorlich, and T. Ott, *Supersymmetric intersecting branes on the type 2A T6 / Z(4) orientifold*, *JHEP* **01** (2003) 021, [[hep-th/0211059](#)].
- [12] J. R. Ellis, S. Kelley, and D. V. Nanopoulos, *Probing the desert using gauge coupling unification*, *Phys. Lett. B* **260** (1991) 131–137.
- [13] P. Langacker and M.-x. Luo, *Implications of precision electroweak experiments for  $M_t$ ,  $\rho_0$ ,  $\sin^2 \theta_W$  and grand unification*, *Phys. Rev. D* **44** (1991) 817–822.
- [14] U. Amaldi, W. de Boer, and H. Furstenau, *Comparison of grand unified theories with electroweak and strong coupling constants measured at LEP*, *Phys. Lett. B* **260** (1991) 447–455.
- [15] K. R. Dienes, *String theory and the path to unification: A Review of recent developments*, *Phys. Rept.* **287** (1997) 447–525, [[hep-th/9602045](#)].
- [16] V. S. Kaplunovsky, *One loop threshold effects in string unification*, [[hep-th/9205070](#)].
- [17] M. Cvetič, T. Li, and T. Liu, *Supersymmetric Pati-Salam models from intersecting D6-branes: A Road to the standard model*, *Nucl. Phys. B* **698** (2004) 163–201, [[hep-th/0403061](#)].
- [18] M. Cvetič, G. Shiu, and A. M. Uranga, *Chiral four-dimensional N=1 supersymmetric type 2A orientifolds from intersecting D6 branes*, *Nucl. Phys. B* **615** (2001) 3–32, [[hep-th/0107166](#)].
- [19] M. Cvetič, I. Papadimitriou, and G. Shiu, *Supersymmetric three family SU(5) grand unified models from type IIA orientifolds with intersecting D6-branes*, *Nucl. Phys. B* **659** (2003) 193–223, [[hep-th/0212177](#)]. [Erratum: *Nucl.Phys.B* 696, 298–298 (2004)].
- [20] M. Cvetič and I. Papadimitriou, *More supersymmetric standard - like models from intersecting D6-branes on type IIA orientifolds*, *Phys. Rev. D* **67** (2003) 126006, [[hep-th/0303197](#)].
- [21] M. Cvetič, P. Langacker, and G. Shiu, *Phenomenology of a three family standard like string model*, *Phys. Rev. D* **66** (2002) 066004, [[hep-ph/0205252](#)].
- [22] G. Honecker, *Chiral supersymmetric models on an orientifold of Z(4) x Z(2) with intersecting D6-branes*, *Nucl. Phys. B* **666** (2003) 175–196, [[hep-th/0303015](#)].
- [23] T.-j. Li and T. Liu, *Supersymmetric G\*\*3 unification from intersecting D6-branes on type IIA orientifolds*, *Phys. Lett. B* **573** (2003) 193–201, [[hep-th/0304258](#)].
- [24] M. Cvetič, P. Langacker, T.-j. Li, and T. Liu, *D6-brane splitting on type IIA orientifolds*, *Nucl. Phys. B* **709** (2005) 241–266, [[hep-th/0407178](#)].
- [25] R. Blumenhagen, M. Cvetič, P. Langacker, and G. Shiu, *Toward realistic intersecting D-brane models*, *Ann. Rev. Nucl. Part. Sci.* **55** (2005) 71–139, [[hep-th/0502005](#)].

- [26] C. M. Chen, G. V. Kraniotis, V. E. Mayes, D. V. Nanopoulos, and J. W. Walker, *A K-theory anomaly free supersymmetric flipped SU(5) model from intersecting branes*, *Phys. Lett. B* **625** (2005) 96–105, [[hep-th/0507232](#)].
- [27] C.-M. Chen, T. Li, V. E. Mayes, and D. V. Nanopoulos, *Towards realistic supersymmetric spectra and Yukawa textures from intersecting branes*, *Phys. Rev. D* **77** (2008) 125023, [[arXiv:0711.0396](#)].
- [28] C.-M. Chen, T. Li, V. E. Mayes, and D. V. Nanopoulos, *A Realistic world from intersecting D6-branes*, *Phys. Lett. B* **665** (2008) 267–270, [[hep-th/0703280](#)].
- [29] C.-M. Chen, T. Li, and D. V. Nanopoulos, *Standard-like model building on Type II orientifolds*, *Nucl. Phys. B* **732** (2006) 224–242, [[hep-th/0509059](#)].
- [30] C. M. Chen, G. V. Kraniotis, V. E. Mayes, D. V. Nanopoulos, and J. W. Walker, *A Supersymmetric flipped SU(5) intersecting brane world*, *Phys. Lett. B* **611** (2005) 156–166, [[hep-th/0501182](#)].
- [31] C.-M. Chen, T. Li, V. E. Mayes, and D. V. Nanopoulos, *Variations of the hidden sector in a realistic intersecting brane model*, *J. Phys. G* **35** (2008) 095008, [[arXiv:0704.1855](#)].
- [32] C.-M. Chen, T. Li, V. E. Mayes, and D. V. Nanopoulos, *Yukawa Corrections from Four-Point Functions in Intersecting D6-Brane Models*, *Phys. Rev. D* **78** (2008) 105015, [[arXiv:0807.4216](#)].
- [33] T. Li, A. Mansha, and R. Sun, *Revisiting the supersymmetric Pati–Salam models from intersecting D6-branes*, *Eur. Phys. J. C* **81** (2021), no. 1 82, [[arXiv:1910.04530](#)].
- [34] T. Li, A. Mansha, R. Sun, L. Wu, and W. He,  *$N=1$  supersymmetric  $SU(12)_C \times SU(2)_L \times SU(2)_R$  models,  $SU(4)_C \times SU(6)_L \times SU(2)_R$  models, and  $SU(4)_C \times SU(2)_L \times SU(6)_R$  models from intersecting D6-branes*, *Phys. Rev. D* **104** (2021), no. 4 046018.
- [35] J. Halverson, B. Nelson, and F. Ruehle, *Branes with Brains: Exploring String Vacua with Deep Reinforcement Learning*, *JHEP* **06** (2019) 003, [[arXiv:1903.11616](#)].
- [36] G. J. Loges and G. Shiu, *Breeding Realistic D-Brane Models*, *Fortsch. Phys.* **70** (2022), no. 5 2200038, [[arXiv:2112.08391](#)].
- [37] G. Honecker and J. Vanhoof, *Yukawa couplings and masses of non-chiral states for the Standard Model on D6-branes on  $T6/Z6'$* , *JHEP* **04** (2012) 085, [[arXiv:1201.3604](#)].
- [38] P. Anastasopoulos, E. Kiritsis, and A. Lionetto, *On mass hierarchies in orientifold vacua*, *JHEP* **08** (2009) 026, [[arXiv:0905.3044](#)].
- [39] P. Anastasopoulos, G. K. Leontaris, and N. D. Vlachos, *Phenomenological Analysis of D-Brane Pati-Salam Vacua*, *JHEP* **05** (2010) 011, [[arXiv:1002.2937](#)].
- [40] P. Anastasopoulos, G. K. Leontaris, R. Richter, and A. N. Schellekens, *SU(5) D-brane realizations, Yukawa couplings and proton stability*, *JHEP* **12** (2010) 011, [[arXiv:1010.5188](#)].
- [41] P. Anastasopoulos, G. K. Leontaris, R. Richter, and A. N. Schellekens, *Avoiding disastrous couplings in SU(5) orientifolds*, *Fortsch. Phys.* **59** (2011) 1144–1148.
- [42] J. Ecker, G. Honecker, and W. Staessens, *D6-brane model building on  $\mathbb{Z}_2 \times \mathbb{Z}_6$ : MSSM-like and left–right symmetric models*, *Nucl. Phys. B* **901** (2015) 139–215, [[arXiv:1509.00048](#)].
- [43] F. Marchesano, B. Schellekens, and T. Weigand, *D-brane and F-theory Model Building*, 12, 2022. [[arXiv:2212.07443](#)].

- [44] I. Antoniadis and S. Dimopoulos, *Splitting supersymmetry in string theory*, *Nucl. Phys. B* **715** (2005) 120–140, [[hep-th/0411032](#)].
- [45] I. Antoniadis, *Aspects of string phenomenology*, *Int. J. Mod. Phys. A* **25** (2010) 4727–4740.
- [46] E. Kiritsis, *Orientifolds, and the search for the standard model in string theory*, *Les Houches* **87** (2008) 45–123.
- [47] E. Kiritsis, *D-branes in standard model building, gravity and cosmology*, *Phys. Rept.* **421** (2005) 105–190, [[hep-th/0310001](#)]. [Erratum: *Phys.Rept.* 429, 121–122 (2006)].
- [48] M. Sabir, T. Li, A. Mansha, and X.-C. Wang, *The supersymmetry breaking soft terms, and fermion masses and mixings in the supersymmetric Pati-Salam model from intersecting D6-branes*, *JHEP* **04** (2022) 089, [[arXiv:2202.07048](#)].
- [49] M. Sabir, A. Mansha, T. Li, and Z.-W. Wang, *Fermion masses and mixings in the supersymmetric Pati-Salam landscape from Intersecting D6-Branes*, *JHEP* **10** (2024) 252, [[arXiv:2409.09110](#)].
- [50] W. He, T. Li, and R. Sun, *The complete search for the supersymmetric Pati-Salam models from intersecting D6-branes*, *JHEP* **08** (2022) 044, [[arXiv:2112.09632](#)].
- [51] W. He, T. Li, R. Sun, and L. Wu, *The final model building for the supersymmetric Pati-Salam models from intersecting D6-branes*, *Eur. Phys. J. C* **82** (2022), no. 8 710, [[arXiv:2112.09630](#)].
- [52] T. Li, R. Sun, and L. Wu, *String-scale gauge coupling relations in the supersymmetric Pati-Salam models from intersecting D6-branes*, *JHEP* **03** (2023) 210, [[arXiv:2212.05875](#)].
- [53] T. Li, Q. Sun, R. Sun, and L. Wu, *Generalized Three-Family Supersymmetric Pati-Salam Models from Type IIA Intersecting D6-Branes*, [arXiv:2511.16565](#).
- [54] A. Mansha, T. Li, and L. Wu, *The hidden sector variations in the  $\mathcal{N} = 1$  supersymmetric three-family Pati-Salam models from intersecting D6-branes*, *Eur. Phys. J. C* **83** (2023), no. 11 1067, [[arXiv:2303.02864](#)].
- [55] A. Mansha, M. Sabir, T. Li, and L. Wang, *Three-family supersymmetric Pati-Salam models from intersecting D6-branes on rigid cycles*, *Phys. Rev. D* **112** (2025), no. 5 055006, [[arXiv:2505.03664](#)].
- [56] R. Blumenhagen, B. Kors, and D. Lust, *Type I strings with F flux and B flux*, *JHEP* **02** (2001) 030, [[hep-th/0012156](#)].
- [57] M. Cvetič, P. Langacker, and J. Wang, *Dynamical supersymmetry breaking in standard - like models with intersecting D6-branes*, *Phys. Rev. D* **68** (2003) 046002, [[hep-th/0303208](#)].
- [58] T. R. Taylor, *Dilaton, gaugino condensation and supersymmetry breaking*, *Phys. Lett. B* **252** (1990) 59–62.
- [59] R. Brustein and P. J. Steinhardt, *Challenges for superstring cosmology*, *Phys. Lett. B* **302** (1993) 196–201, [[hep-th/9212049](#)].
- [60] B. de Carlos, J. A. Casas, and C. Muñoz, *Supersymmetry breaking and determination of the unification gauge coupling constant in string theories*, *Nucl. Phys. B* **399** (1993) 623–653, [[hep-th/9204012](#)].
- [61] H.-Y. Chen, I. Gogoladze, S. Hu, T. Li, and L. Wu, *The Minimal GUT with Inflaton and Dark Matter Unification*, *Eur. Phys. J. C* **78** (2018), no. 1 26, [[arXiv:1703.07542](#)].

- [62] H.-Y. Chen, I. Gogoladze, S. Hu, T. Li, and L. Wu, *Natural Higgs Inflation, Gauge Coupling Unification, and Neutrino Masses*, *Int. J. Mod. Phys. A* **35** (2020), no. 21 2050117, [[arXiv:1805.00161](#)].
- [63] V. Barger, J. Jiang, P. Langacker, and T. Li, *Non-canonical gauge coupling unification in high-scale supersymmetry breaking*, *Nucl. Phys. B* **726** (2005) 149–170, [[hep-ph/0504093](#)].
- [64] V. Barger, N. G. Deshpande, J. Jiang, P. Langacker, and T. Li, *Implications of Canonical Gauge Coupling Unification in High-Scale Supersymmetry Breaking*, *Nucl. Phys. B* **793** (2008) 307–325, [[hep-ph/0701136](#)].
- [65] M. E. Machacek and M. T. Vaughn, *Two Loop Renormalization Group Equations in a General Quantum Field Theory. 1. Wave Function Renormalization*, *Nucl. Phys. B* **222** (1983) 83–103.
- [66] M. E. Machacek and M. T. Vaughn, *Two Loop Renormalization Group Equations in a General Quantum Field Theory. 2. Yukawa Couplings*, *Nucl. Phys. B* **236** (1984) 221–232.
- [67] M. E. Machacek and M. T. Vaughn, *Two Loop Renormalization Group Equations in a General Quantum Field Theory. 3. Scalar Quartic Couplings*, *Nucl. Phys. B* **249** (1985) 70–92.
- [68] G. Cvetič, C. S. Kim, and S. S. Hwang, *Higgs mediated flavor changing neutral currents in the general framework with two Higgs doublets: An RGE analysis*, *Phys. Rev. D* **58** (1998) 116003, [[hep-ph/9806282](#)].
- [69] I. Gogoladze, B. He, and Q. Shafi, *New Fermions at the LHC and Mass of the Higgs Boson*, *Phys. Lett. B* **690** (2010) 495–500, [[arXiv:1004.4217](#)].
- [70] V. D. Barger, M. S. Berger, and P. Ohmann, *Supersymmetric grand unified theories: Two loop evolution of gauge and Yukawa couplings*, *Phys. Rev. D* **47** (1993) 1093–1113, [[hep-ph/9209232](#)].
- [71] V. D. Barger, M. S. Berger, and P. Ohmann, *The Supersymmetric particle spectrum*, *Phys. Rev. D* **49** (1994) 4908–4930, [[hep-ph/9311269](#)].
- [72] S. P. Martin and M. T. Vaughn, *Two loop renormalization group equations for soft supersymmetry breaking couplings*, *Phys. Rev. D* **50** (1994) 2282, [[hep-ph/9311340](#)]. [Erratum: *Phys.Rev.D* 78, 039903 (2008)].
- [73] **Particle Data Group** Collaboration, M. Tanabashi et al., *Review of Particle Physics*, *Phys. Rev. D* **98** (2018), no. 3 030001.
- [74] **Particle Data Group** Collaboration, P. A. Zyla et al., *Review of Particle Physics*, *PTEP* **2020** (2020), no. 8 083C01.
- [75] J. Jiang, T. Li, and D. V. Nanopoulos, *Testable Flipped  $SU(5) \times U(1)(X)$  Models*, *Nucl. Phys. B* **772** (2007) 49–66, [[hep-ph/0610054](#)].
- [76] J. Jiang, T. Li, D. V. Nanopoulos, and D. Xie, *F-SU(5)*, *Phys. Lett. B* **677** (2009) 322–325, [[arXiv:0811.2807](#)].

## A Representative dual supersymmetric Pati-Salam models of Model 1

In this section, we representatively present dual supersymmetric Pati-Salam models of Model 1 under the equivalent symmetric transformation, with the same gauge coupling relation  $g_a^2 = g_b^2 = \frac{1}{2}g_R^2 = \frac{5}{8}(\frac{5}{3}g_Y^2) = 2\sqrt{2} 3^{1/4} \pi e^{\phi_4}$ .

**Table 29.** D6-brane configurations and intersection numbers of Model 11, and its MSSM gauge coupling relation is  $g_a^2 = g_b^2 = \frac{1}{2}g_R^2 = \frac{5}{8}(\frac{5}{3}g_Y^2) = 2\sqrt{2} 3^{1/4} \pi e^{\phi_4}$ , for which the third torus is tilted.

| Model 11 |     | $U(4) \times U(2)_L \times U(2)_{R_1} \times U(2)_{R_2} \times USp(2)^2$ |  |               |     |      |     |      |     |      |    |    |
|----------|-----|--|--|---------------|-----|------|-----|------|-----|------|----|----|
| stack    | $N$ | $(n^1, l^1) \times (n^2, l^2) \times (n^3, l^3)$                         | $n_{\square\square}$   | $n_{\square}$ | $b$ | $b'$ | $c$ | $c'$ | $d$ | $d'$ | 1  | 3  |
| $a$      | 8   | $(1, -1) \times (1, 0) \times (1, 1)$                                    | 0  | 0             | 3   | 0    | -1  | 0    | -2  | 0    | 0  | 0  |
| $b$      | 4   | $(0, -1) \times (-1, 3) \times (1, -1)$                                  | 2  | -2            | -   | -    | 0   | -2   | 2   | 1    | -3 | 0  |
| $c$      | 4   | $(-1, 0) \times (1, 1) \times (-1, 1)$                                   | 0  | 0             | -   | -    | -   | -    | -2  | 1    | 0  | 1  |
| $d$      | 4   | $(-1, -1) \times (0, -1) \times (-1, -3)$                                | -2   | 2             | -   | -    | -   | -    | -   | -    | 3  | -1 |
| 1        | 2   | $(1, 0) \times (1, 0) \times (2, 0)$                                     | $x_A = \frac{1}{3}x_B = \frac{1}{3}x_C = \frac{1}{3}x_D$<br>$\beta_1^g = 0, \beta_3^g = -4$<br>$\chi_1 = \frac{1}{\sqrt{3}}, \chi_2 = \frac{1}{\sqrt{3}}, \chi_3 = \frac{2}{\sqrt{3}}$ |               |     |      |     |      |     |      |    |    |
| 3        | 2   | $(0, -1) \times (1, 0) \times (0, 2)$                                    |  |               |     |      |     |      |     |      |    |    |

**Table 30.** D6-brane configurations and intersection numbers of Model 12, and its MSSM gauge coupling relation is  $g_a^2 = g_b^2 = \frac{1}{2}g_R^2 = \frac{5}{8}(\frac{5}{3}g_Y^2) = 2\sqrt{2} 3^{1/4} \pi e^{\phi_4}$ , for which the second torus is tilted.

| Model 12 |     | $U(4) \times U(2)_L \times U(2)_{R_1} \times U(2)_{R_2} \times USp(2)^2$ |  |               |     |      |     |      |     |      |   |    |
|----------|-----|--|--|---------------|-----|------|-----|------|-----|------|---|----|
| stack    | $N$ | $(n^1, l^1) \times (n^2, l^2) \times (n^3, l^3)$                         | $n_{\square\square}$   | $n_{\square}$ | $b$ | $b'$ | $c$ | $c'$ | $d$ | $d'$ | 1 | 4  |
| $a$      | 8   | $(1, -1) \times (1, 1) \times (1, 0)$                                    | 0  | 0             | 0   | 3    | -1  | 0    | -2  | 0    | 0 | 0  |
| $b$      | 4   | $(0, 1) \times (1, 1) \times (-1, -3)$                                   | -2   | 2             | -   | -    | 2   | 0    | -1  | -2   | 3 | 0  |
| $c$      | 4   | $(-1, 0) \times (-1, 1) \times (1, 1)$                                   | 0  | 0             | -   | -    | -   | -    | -2  | 1    | 0 | 1  |
| $d$      | 4   | $(-1, -1) \times (-1, -3) \times (0, -1)$                                | -2   | 2             | -   | -    | -   | -    | -   | -    | 3 | -1 |
| 1        | 2   | $(1, 0) \times (2, 0) \times (1, 0)$                                     | $x_A = \frac{1}{3}x_B = \frac{1}{3}x_C = \frac{1}{3}x_D$<br>$\beta_1^g = 0, \beta_4^g = -4$<br>$\chi_1 = \frac{1}{\sqrt{3}}, \chi_2 = \frac{2}{\sqrt{3}}, \chi_3 = \frac{1}{\sqrt{3}}$ |               |     |      |     |      |     |      |   |    |
| 4        | 2   | $(0, -1) \times (0, 2) \times (1, 0)$                                    |  |               |     |      |     |      |     |      |   |    |

**Table 31.** D6-brane configurations and intersection numbers of Model 13, and its MSSM gauge coupling relation is  $g_a^2 = g_b^2 = \frac{1}{2}g_R^2 = \frac{5}{8}(\frac{5}{3}g_Y^2) = 2\sqrt{2} 3^{1/4} \pi e^{\phi_4}$ , for which the second torus is tilted.

| Model 13 |     | $U(4) \times U(2)_L \times U(2)_{R_1} \times U(2)_{R_2} \times USp(2)^2$ |  |               |     |      |     |      |     |      |    |    |
|----------|-----|--|--|---------------|-----|------|-----|------|-----|------|----|----|
| stack    | $N$ | $(n^1, l^1) \times (n^2, l^2) \times (n^3, l^3)$                         | $n_{\square\square}$   | $n_{\square}$ | $b$ | $b'$ | $c$ | $c'$ | $d$ | $d'$ | 1  | 4  |
| $a$      | 8   | $(1, -1) \times (1, 1) \times (1, 0)$                                    | 0  | 0             | 3   | 0    | 0   | -1   | -2  | 0    | 0  | 0  |
| $b$      | 4   | $(0, -1) \times (1, -1) \times (-1, 3)$                                  | 2  | -2            | -   | -    | -2  | 0    | 2   | 1    | -3 | 0  |
| $c$      | 4   | $(-1, 0) \times (-1, -1) \times (1, -1)$                                 | 0  | 0             | -   | -    | -   | -    | -1  | 2    | 0  | -1 |
| $d$      | 4   | $(-1, -1) \times (-1, -3) \times (0, -1)$                                | -2   | 2             | -   | -    | -   | -    | -   | -    | 3  | -1 |
| 1        | 2   | $(1, 0) \times (2, 0) \times (1, 0)$                                     | $x_A = \frac{1}{3}x_B = \frac{1}{3}x_C = \frac{1}{3}x_D$<br>$\beta_1^g = 0, \beta_4^g = -4$<br>$\chi_1 = \frac{1}{\sqrt{3}}, \chi_2 = \frac{2}{\sqrt{3}}, \chi_3 = \frac{1}{\sqrt{3}}$ |               |     |      |     |      |     |      |    |    |
| 4        | 2   | $(0, -1) \times (0, 2) \times (1, 0)$                                    |  |               |     |      |     |      |     |      |    |    |

**Table 32.** D6-brane configurations and intersection numbers of Model 14, and its MSSM gauge coupling relation is  $g_a^2 = g_b^2 = \frac{1}{2}g_R^2 = \frac{5}{8}(\frac{5}{3}g_Y^2) = 2\sqrt{2} 3^{1/4} \pi e^{\phi_4}$ , for which the second torus is tilted.

| Model 14 |     | $U(4) \times U(2)_L \times U(2)_{R_1} \times U(2)_{R_2} \times USp(2)^2$ |  |               |     |      |     |      |     |      |    |   |
|----------|-----|--|--|---------------|-----|------|-----|------|-----|------|----|---|
| stack    | $N$ | $(n^1, l^1) \times (n^2, l^2) \times (n^3, l^3)$                         | $n_{\square\square}$   | $n_{\square}$ | $b$ | $b'$ | $c$ | $c'$ | $d$ | $d'$ | 1  | 4 |
| $a$      | 8   | $(1, -1) \times (1, 1) \times (1, 0)$                                    | 0  | 0             | 3   | 0    | -1  | 0    | 0   | -2   | 0  | 0 |
| $b$      | 4   | $(0, -1) \times (1, -1) \times (-1, 3)$                                  | 2  | -2            | -   | -    | 0   | -2   | 1   | 2    | -3 | 0 |
| $c$      | 4   | $(-1, 0) \times (-1, 1) \times (1, 1)$                                   | 0  | 0             | -   | -    | -   | -    | 1   | -2   | 0  | 1 |
| $d$      | 4   | $(-1, 1) \times (-1, 3) \times (0, 1)$                                   | 2  | -2            | -   | -    | -   | -    | -   | -    | -3 | 1 |
| 1        | 2   | $(1, 0) \times (2, 0) \times (1, 0)$                                     | $x_A = \frac{1}{3}x_B = \frac{1}{3}x_C = \frac{1}{3}x_D$<br>$\beta_1^g = 0, \quad \beta_4^g = -4$<br>$\chi_1 = \frac{1}{\sqrt{3}}, \chi_2 = \frac{2}{\sqrt{3}}, \chi_3 = \frac{1}{\sqrt{3}}$ |               |     |      |     |      |     |      |    |   |
| 4        | 2   | $(0, -1) \times (0, 2) \times (1, 0)$                                    |  |               |     |      |     |      |     |      |    |   |

**Table 33.** D6-brane configurations and intersection numbers of Model 15, and its MSSM gauge coupling relation is  $g_a^2 = g_b^2 = \frac{1}{2}g_R^2 = \frac{5}{8}(\frac{5}{3}g_Y^2) = 2\sqrt{2} 3^{1/4} \pi e^{\phi_4}$ , for which the second torus is tilted.

| Model 15 |     | $U(4) \times U(2)_L \times U(2)_{R_1} \times U(2)_{R_2} \times USp(2)^2$ |  |               |     |      |     |      |     |      |    |    |
|----------|-----|--|--|---------------|-----|------|-----|------|-----|------|----|----|
| stack    | $N$ | $(n^1, l^1) \times (n^2, l^2) \times (n^3, l^3)$                         | $n_{\square\square}$   | $n_{\square}$ | $b$ | $b'$ | $c$ | $c'$ | $d$ | $d'$ | 1  | 4  |
| $a$      | 8   | $(1, -1) \times (1, 1) \times (1, 0)$                                    | 0  | 0             | 3   | 0    | -2  | 0    | -1  | 0    | 0  | 0  |
| $b$      | 4   | $(0, -1) \times (1, -1) \times (-1, 3)$                                  | 2  | -2            | -   | -    | 2   | 1    | 0   | -2   | -3 | 0  |
| $c$      | 4   | $(-1, -1) \times (-1, -3) \times (0, -1)$                                | -2   | 2             | -   | -    | -   | -    | 2   | 1    | 3  | -1 |
| $d$      | 4   | $(-1, 0) \times (-1, 1) \times (1, 1)$                                   | 0  | 0             | -   | -    | -   | -    | -   | -    | 0  | 1  |
| 1        | 2   | $(1, 0) \times (2, 0) \times (1, 0)$                                     | $x_A = \frac{1}{3}x_B = \frac{1}{3}x_C = \frac{1}{3}x_D$<br>$\beta_1^g = 0, \quad \beta_4^g = -4$<br>$\chi_1 = \frac{1}{\sqrt{3}}, \chi_2 = \frac{2}{\sqrt{3}}, \chi_3 = \frac{1}{\sqrt{3}}$ |               |     |      |     |      |     |      |    |    |
| 4        | 2   | $(0, -1) \times (0, 2) \times (1, 0)$                                    |  |               |     |      |     |      |     |      |    |    |

**Table 34.** D6-brane configurations and intersection numbers of Model 16, and its MSSM gauge coupling relation is  $g_a^2 = g_b^2 = \frac{1}{2}g_R^2 = \frac{5}{8}(\frac{5}{3}g_Y^2) = 2\sqrt{2} 3^{1/4} \pi e^{\phi_4}$ , for which the second torus is tilted.

| Model 16 |     | $U(4) \times U(2)_L \times U(2)_{R_1} \times U(2)_{R_2} \times USp(2)^2$ |  |               |     |      |     |      |     |      |    |    |
|----------|-----|--|--|---------------|-----|------|-----|------|-----|------|----|----|
| stack    | $N$ | $(n^1, l^1) \times (n^2, l^2) \times (n^3, l^3)$                         | $n_{\square\square}$   | $n_{\square}$ | $b$ | $b'$ | $c$ | $c'$ | $d$ | $d'$ | 1  | 4  |
| $a$      | 8   | $(-1, 1) \times (-1, -1) \times (1, 0)$                                  | 0  | 0             | 3   | 0    | -1  | 0    | -2  | 0    | 0  | 0  |
| $b$      | 4   | $(0, -1) \times (1, -1) \times (-1, 3)$                                  | 2  | -2            | -   | -    | 0   | -2   | 2   | 1    | -3 | 0  |
| $c$      | 4   | $(-1, 0) \times (-1, 1) \times (1, 1)$                                   | 0  | 0             | -   | -    | -   | -    | -2  | 1    | 0  | 1  |
| $d$      | 4   | $(-1, -1) \times (-1, -3) \times (0, -1)$                                | -2   | 2             | -   | -    | -   | -    | -   | -    | 3  | -1 |
| 1        | 2   | $(1, 0) \times (2, 0) \times (1, 0)$                                     | $x_A = \frac{1}{3}x_B = \frac{1}{3}x_C = \frac{1}{3}x_D$<br>$\beta_1^g = 0, \quad \beta_4^g = -4$<br>$\chi_1 = \frac{1}{\sqrt{3}}, \chi_2 = \frac{2}{\sqrt{3}}, \chi_3 = \frac{1}{\sqrt{3}}$ |               |     |      |     |      |     |      |    |    |
| 4        | 2   | $(0, -1) \times (0, 2) \times (1, 0)$                                    |  |               |     |      |     |      |     |      |    |    |

**Table 35.** D6-brane configurations and intersection numbers of Model 17, and its MSSM gauge coupling relation is  $g_a^2 = g_b^2 = \frac{1}{2}g_R^2 = \frac{5}{8}(\frac{5}{3}g_Y^2) = 2\sqrt{2} 3^{1/4} \pi e^{\phi_4}$ , for which the second torus is tilted.

| Model 17 |     | $U(4) \times U(2)_L \times U(2)_{R_1} \times U(2)_{R_2} \times USp(2)^2$ |   |               |     |      |     |      |     |      |    |    |
|----------|-----|--|---|---------------|-----|------|-----|------|-----|------|----|----|
| stack    | $N$ | $(n^1, l^1) \times (n^2, l^2) \times (n^3, l^3)$                         | $n_{\square\square}$  | $n_{\square}$ | $b$ | $b'$ | $c$ | $c'$ | $d$ | $d'$ | 1  | 4  |
| $a$      | 8   | $(1, 1) \times (1, -1) \times (1, 0)$                                    | 0   | 0             | 3   | 0    | -1  | 0    | -2  | 0    | 0  | 0  |
| $b$      | 4   | $(1, 0) \times (-1, -1) \times (-1, 3)$                                  | 2   | -2            | -   | -    | 0   | -2   | 2   | 1    | -3 | 0  |
| $c$      | 4   | $(0, -1) \times (1, 1) \times (1, 1)$                                    | 0   | 0             | -   | -    | -   | -    | -2  | 1    | 0  | 1  |
| $d$      | 4   | $(1, -1) \times (-3, 1) \times (0, -1)$                                  | -2  | 2             | -   | -    | -   | -    | -   | -    | 3  | -1 |
| 1        | 2   | $(1, 0) \times (2, 0) \times (1, 0)$                                     | $x_A = x_B = x_C = 3x_D$<br>$\beta_1^g = -4, \beta_4^g = 0$<br>$\chi_1 = \sqrt{3}, \chi_2 = 2\sqrt{3}, \chi_3 = \frac{1}{\sqrt{3}}$ |               |     |      |     |      |     |      |    |    |
| 4        | 2   | $(0, -1) \times (0, 2) \times (1, 0)$                                    |   |               |     |      |     |      |     |      |    |    |

**Table 36.** D6-brane configurations and intersection numbers of Model 18, and its MSSM gauge coupling relation is  $g_a^2 = g_b^2 = \frac{1}{2}g_R^2 = \frac{5}{8}(\frac{5}{3}g_Y^2) = 2\sqrt{2} 3^{1/4} \pi e^{\phi_4}$ , for which the first torus is tilted.

| Model 18 |     | $U(4) \times U(2)_L \times U(2)_{R_1} \times U(2)_{R_2} \times USp(2)^2$ |   |               |     |      |     |      |     |      |    |    |
|----------|-----|--|---|---------------|-----|------|-----|------|-----|------|----|----|
| stack    | $N$ | $(n^1, l^1) \times (n^2, l^2) \times (n^3, l^3)$                         | $n_{\square\square}$  | $n_{\square}$ | $b$ | $b'$ | $c$ | $c'$ | $d$ | $d'$ | 1  | 4  |
| $a$      | 8   | $(1, -1) \times (1, 1) \times (1, 0)$                                    | 0   | 0             | 3   | 0    | -1  | 0    | -2  | 0    | 0  | 0  |
| $b$      | 4   | $(-1, -1) \times (1, 0) \times (-1, 3)$                                  | 2   | -2            | -   | -    | 0   | -2   | 2   | 1    | 0  | -3 |
| $c$      | 4   | $(1, 1) \times (0, -1) \times (1, 1)$                                    | 0   | 0             | -   | -    | -   | -    | -2  | 1    | 1  | 0  |
| $d$      | 4   | $(-3, 1) \times (1, -1) \times (0, -1)$                                  | -2  | 2             | -   | -    | -   | -    | -   | -    | -1 | 3  |
| 1        | 2   | $(2, 0) \times (1, 0) \times (1, 0)$                                     | $x_A = x_B = x_C = 3x_D$<br>$\beta_1^g = -4, \beta_4^g = 0$<br>$\chi_1 = 2\sqrt{3}, \chi_2 = \sqrt{3}, \chi_3 = \frac{1}{\sqrt{3}}$ |               |     |      |     |      |     |      |    |    |
| 4        | 2   | $(0, -2) \times (0, 1) \times (1, 0)$                                    |   |               |     |      |     |      |     |      |    |    |

## B RGE evolution for Model 1,2,3,7,8,9

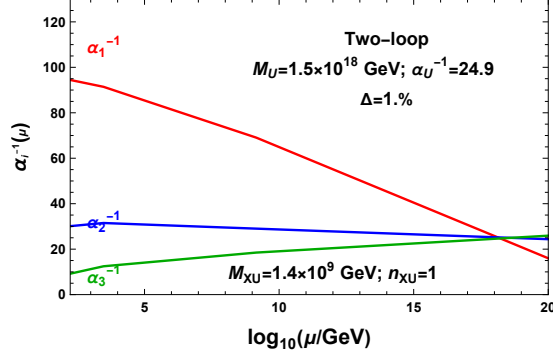


**Figure 5.** Two-loop evolution of gauge couplings for Model 1. The gauge coupling unification can be achieved at around string scale by adding  $(XU + \overline{XU})$ .

For Model 1, the gauge coupling unification is achieved at  $M_U = 1.5 \times 10^8 \text{ GeV} \simeq 3M_{string}$  as shown in Figure 5. We can still obtain the gauge coupling unification of Model 1, by introducing an extra vector-like particle  $XU + \overline{XU}$  from the  $\mathcal{N} = 2$  subsector. The number of this vector-like particle  $XU + \overline{XU}$  is determined by  $|I_{ac}^{(1,3)}| = |-1 \times 1| = 1$  on the first and third tori. This is equivalent to observing  $|I_{ac}^{(1,3)}| = 1$  in Model 13, which is the dual situation ( $c \leftrightarrow c'$ ) of Model 1.

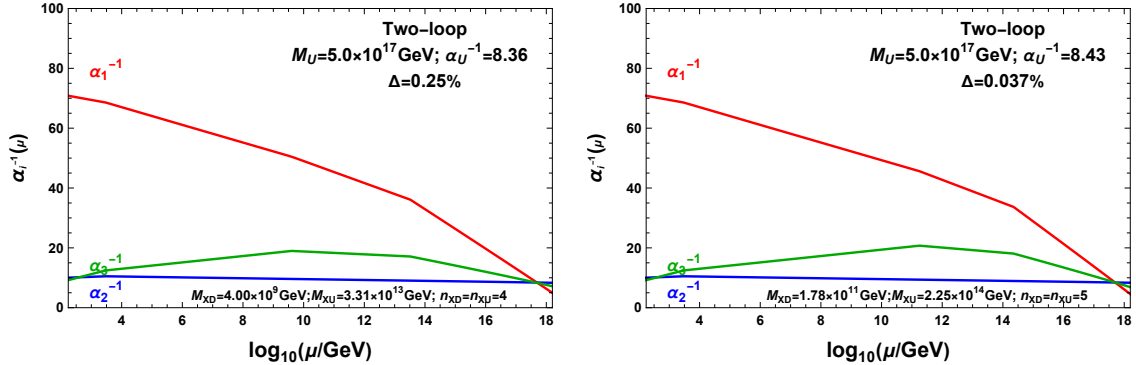


**Figure 6.** Two-loop evolution of gauge couplings for Model 2. The gauge coupling unification can be achieved at string scale by adding  $4(XD + \overline{XD}) + 4(XU + \overline{XU})$  (left panel) and  $5(XD + \overline{XD}) + 5(XU + \overline{XU})$  (right panel).

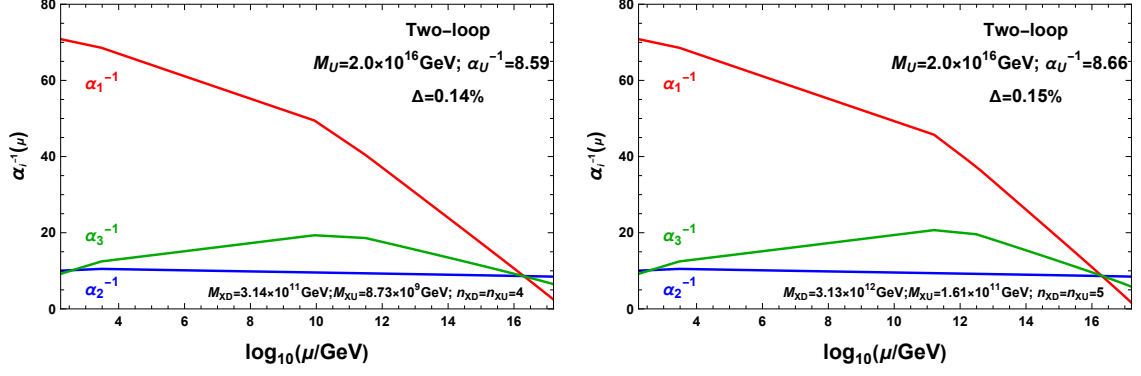


**Figure 7.** Two-loop evolution of gauge couplings for Model 2. The gauge coupling unification can be achieved at GUT scale by adding  $4(XD + \overline{XD}) + 4(XU + \overline{XU})$  (left panel) and  $5(XD + \overline{XD}) + 5(XU + \overline{XU})$  (right panel).

For Model 2, we can successfully unify the gauge couplings at both the string scale (Figure 6) and the GUT scale (Figure 7), introducing vector-like particles  $XD + \overline{XD}$  and  $XU + \overline{XU}$  from the  $\mathcal{N} = 2$  subsector in both cases. It can be calculated that in Model 2,  $|I_{ac'}^{(1,2)}| = 1$  and  $|I_{ad}^{(1,2)}| = 4$ . We observe that when applying  $n_v = |I_{ad}^{(1,2)}| = 4$  or  $n_v = |I_{ad}^{(1,2)}| + |I_{ac'}^{(1,2)}| = 5$ , *i.e.* adding  $4(XD + \overline{XD}) + 4(XU + \overline{XU})$  or  $5(XD + \overline{XD}) + 5(XU + \overline{XU})$ , the gauge coupling unification can be smoothly achieved.

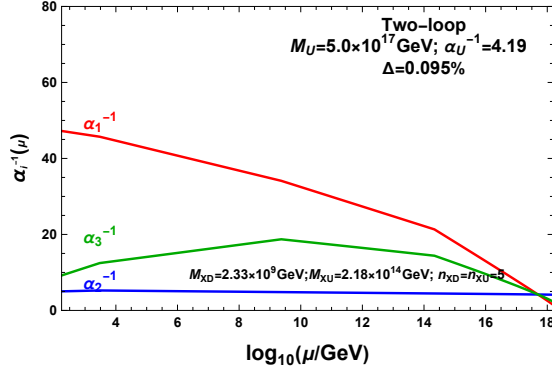


**Figure 8.** Two-loop evolution of gauge couplings for Model 3. The gauge coupling unification can be achieved at string scale by adding  $5(XD + \overline{XD}) + 5(XU + \overline{XU})$ .

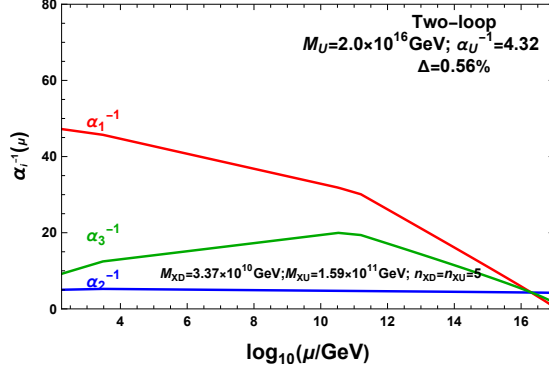


**Figure 9.** Two-loop evolution of gauge couplings for Model 3. The gauge coupling unification can be achieved at GUT scale by adding  $5(XD + \overline{XD}) + 5(XU + \overline{XU})$ .

The unification of gauge couplings of Model 3 is realized at both string scale and GUT scale, as shown in Figure 8 and Figure 9. The intersection numbers are calculated as  $|I_{ac}^{(2,3)}| = 1$  and  $|I_{ad}^{(2,3)}| = 4$ . The gauge coupling unification can be obtained at both string scale and GUT scale by choosing  $n_v = |I_{ac}^{(2,3)}| + |I_{ad}^{(2,3)}| = 5$ , which means introducing vector-like particles  $5(XD + \overline{XD}) + 5(XU + \overline{XU})$ .

With the assistance of additional vector-like particles  $XQ + \overline{XQ}$  and chiral multiplets  $XG$  and  $XW$ , we successfully achieve their gauge coupling unification at both string scale and GUT scale.

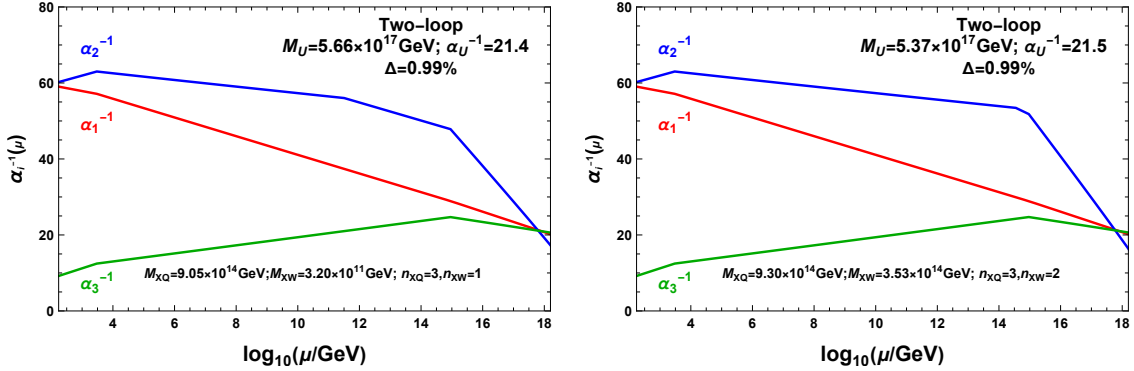


**Figure 10.** Two-loop evolution of gauge couplings for Model 7. The gauge coupling unification can be achieved at string scale by adding  $3(XQ + \overline{XQ}) + XW$  (left panel) and  $3(XQ + \overline{XQ}) + 2XW$  (right panel).

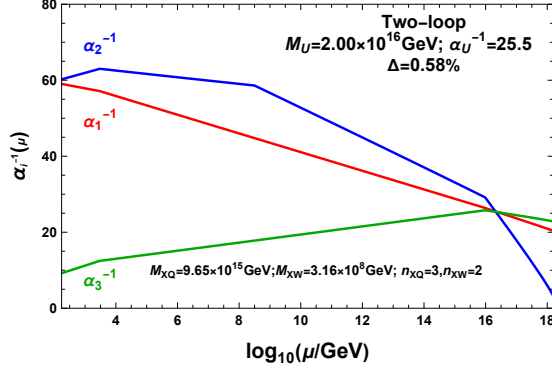


**Figure 11.** Two-loop evolution of gauge couplings for Model 7. The gauge coupling unification can be achieved at GUT scale by adding  $3(XQ + \overline{XQ}) + 2XW$ .

For Model 7, we can successfully unify the gauge couplings at both string scale (Figure 10) and GUT scale (Figure 11), introducing vector-like particles  $XQ + \overline{XQ}$  from  $\mathcal{N} = 2$  subsector and  $XW$  from  $bb$  sector in both cases. It can be calculated that in Model 7,  $|I_{ab'}^{(2,3)}| = 1$  and  $|I_{ad}^{(1,2)}| = 2$ . We observe that when applying  $n_{XQ} = |I_{ab'}^{(2,3)}| + |I_{ad}^{(1,2)}| = 3$  and  $n_{XW} = 2$  or  $3$ , *i.e.*, adding  $3(XQ + \overline{XQ}) + 2XW$  or  $3(XQ + \overline{XQ}) + 3XW$ , the gauge coupling unification can be achieved at string scale. Besides, gauge couplings in Model 7 can also be unified at GUT scale by introducing  $3(XQ + \overline{XQ}) + 2XW$ .

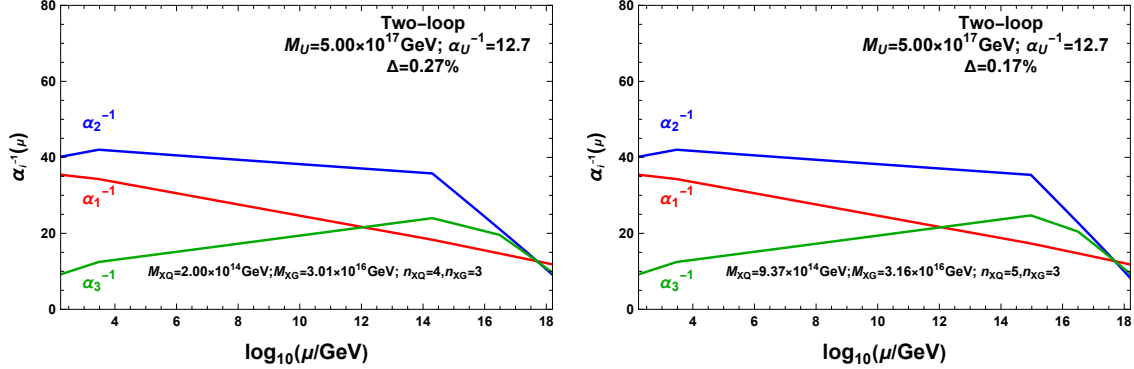


**Figure 12.** Two-loop evolution of gauge couplings for Model 8. The gauge coupling unification can be achieved at string scale by adding  $4(XQ + \overline{XQ}) + 3XG$  (left panel) and  $5(XQ + \overline{XQ}) + 3XG$  (right panel).

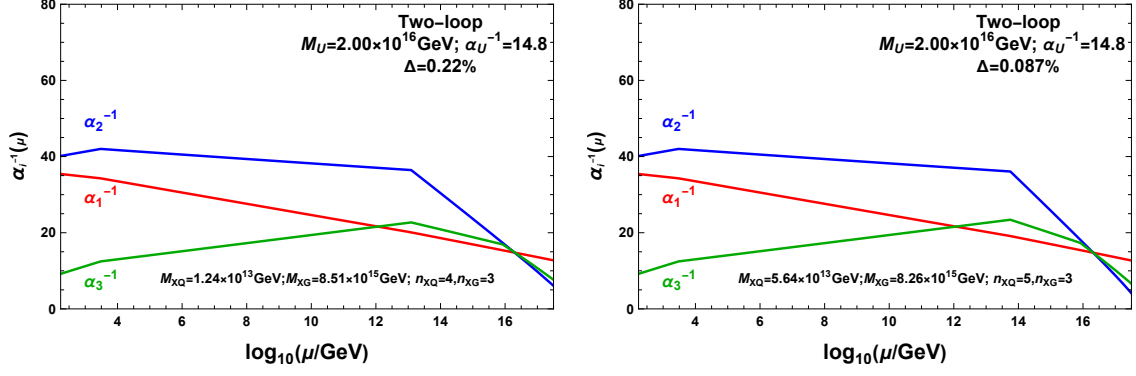


**Figure 13.** Two-loop evolution of gauge couplings for Model 8. The gauge coupling unification can be achieved at GUT scale by adding  $4(XQ + \bar{X}\bar{Q}) + 3XG$  (left panel) and  $5(XQ + \bar{X}\bar{Q}) + 3XG$  (right panel).

For Model 8, we can successfully unify the gauge couplings at both string scale (Figure 12) and GUT scale (Figure 13), introducing vector-like particles  $XQ + \bar{X}\bar{Q}$  from the  $\mathcal{N} = 2$  subsector and  $XG$  from the  $aa$  sector in both cases. We calculate that in Model 8,  $|I_{ab'}^{(2,3)}| = 1$  and  $|I_{ad'}^{(2,3)}| = 4$ . Fixing  $n_{XG} = 3$ , we observe that when adding  $n_{XQ} = |I_{ad'}^{(2,3)}| = 4$ , or  $n_{XQ} = |I_{ab'}^{(2,3)}| + |I_{ad'}^{(2,3)}| = 5$ , namely introducing  $4(XQ + \bar{X}\bar{Q}) + 3XG$  or  $5(XQ + \bar{X}\bar{Q}) + 3XG$ , the gauge coupling unification can be smoothly achieved at both string scale and GUT scale.

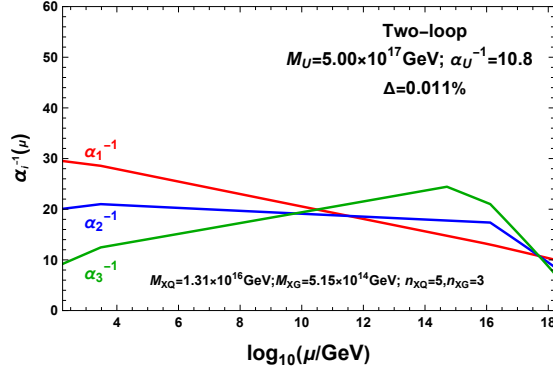


**Figure 14.** Two-loop evolution of gauge couplings for Model 9. The gauge coupling unification can be achieved at string scale by adding  $5(XQ + \bar{X}\bar{Q}) + 3XG$ .

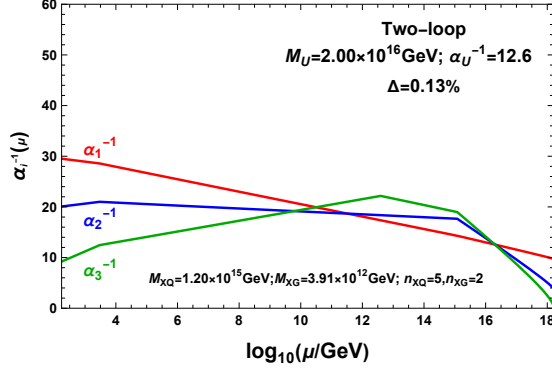


**Figure 15.** Two-loop evolution of gauge couplings for Model 9. The gauge coupling unification can be achieved at GUT scale by adding  $5(XQ + \overline{XQ}) + 2XG$ .

For Model 9, we can successfully unify the gauge couplings at both string scale (Figure 14) and GUT scale (Figure 15), introducing vector-like particles  $XQ + \overline{XQ}$  from the  $\mathcal{N} = 2$  subsector and  $XG$  from the  $aa$  sector in both cases. Recall that in Model 9,  $|I_{ab'}^{(2,3)}| = 1$  and  $|I_{ad'}^{(2,3)}| = 4$ , when we take  $n_{XG} = 3$ , we observe that when adding  $n_{XQ} = |I_{ab'}^{(2,3)}| + |I_{ad'}^{(2,3)}| = 5$ , *i.e.* utilizing  $5(XQ + \overline{XQ}) + 3XG$ , the gauge coupling unification can be smoothly achieved at string scale. Similarly, with  $N_{XG} = 2$ , namely with the combination  $5(XQ + \overline{XQ}) + 2XG$ , the gauge coupling unification can be realized at GUT scale.